

**THE REGENERATION OF HIGH TEMPERATURE SULFUR DIOXIDE SORBENTS:  
THE CO REDUCTION OF SUPPORTED ALKALI SULFATES**

Thesis by

Theresa Ann Weston

In Partial Fulfillment of the Requirements

for the Degree of

Doctor of Philosophy

California Institute of Technology

Pasadena, California

1985

(Submitted May 6, 1985)

© 1985

Theresa Ann Weston

All Rights Reserved

*To my family, George, Joyce, Lisa and Chris Weston,  
and Gatsby and Natasha*

*May 1985*

"Messe ocus Pangur ban,  
cehtar nathar fria saindan;  
bith a menma-sam fri seilgg,  
mu menma cein im saincheirdd."

-Anonymous

### **Acknowledgments**

I would like to thank my advisor, George R. Gavalas, for his guidance throughout this project. I would also like to thank Miretta Stephanopoulos who provided guidance, especially in the early stages of the project.

This project would have been impossible without working experimental equipment and I wish to express gratitude to everyone at Caltech who helped me put together the experimental system, especially George Griffith, who seemed to be a never-ending source of advice and help.

Atomic Absorption Analysis and some early experimental work was done at the Jet Propulsion Laboratory, La Canada-Flintridge, CA. I would like to thank JPL for their cooperation and support. Surface area measurements were done on an experimental system built by Scott Northrop. I would like to thank him for the use of his system and his aid in using it.

Thermodynamic calculations were performed using STANJAN developed by Dr. W. C. Reynolds of Stanford University. I would like to thank Sergio Edelstein for getting STANJAN "on to the computer". I'd also like to thank Sergio for all his help with the experimental equipment.

Thanks to Kathy Lewis for typing, Valerie Purvis for making the illustrations and Donna Johnson for typing the tables.

My time at Caltech would not have been nearly so rewarding without my many friends, and associates here. I would like to acknowledge the Gavalas group in general. In particular, I would like to acknowledge Dave Allen, Brian Davison, Murray and Dinah Gray, Puvin Pichaichanarong, Eliana Makhoulouf and Dave Strand.

Finally, I wish to thank my family for their emotional support throughout my years at Caltech. Special thanks to my sister Lisa who also proofread this thesis.

**Abstract**

The chemical reactions involved in the regeneration step of a high temperature  $\text{SO}_2$  removal process have been investigated. In particular, the CO reduction of supported alkali sulfates has been studied. Thermogravimetric measurements have yielded the time-resolved composition of sorbent and gaseous products during reduction with 10% CO at 700 and 800°C. FTIR was used to identify reaction intermediates. A flow microreactor was used to compare gaseous product selectivity between  $\text{SO}_2$ , COS and elemental sulfur of sorbents reduced with 1 and 10% CO at 700 and 800°C.

The experimental results show regeneration; i.e., sulfur removal is greatly increased by the presence of lithium in the sorbent material. Reaction between the support and the alkali material greatly influences the degree of regeneration. Support materials are apparently active in the catalysis of the reduction of  $\text{SO}_2$  to elemental sulfur and the reaction between elemental sulfur and CO to form COS, and therefore, influences the product selectivity. A reaction scheme which qualitatively explains the experimental results is proposed.

**Table of Contents**

	<u>Page</u>
Dedication	i
Acknowledgments	i i
Abstract	i v
Table of Contents	v
List of Figures	x
List of Tables	xv
1. Introduction	1
References	4
2. Background Chemistry and Thermodynamics	5
2.1 Sulfation	6
2.1.1 Kinetics of Sulfation	6
2.1.2 Thermodynamics of Sulfation	7
2.2 Sorbent Regeneration	7
2.2.1 General Concerns	7
2.2.2 Reduction of Alkali Sulfates	10
2.3 Reactions of the Support Materials	15
2.3.1 Direct Support Interaction	15
2.3.2 Catalysis of Secondary Reactions by the Support Material	15
2.4 Thermodynamics of Regeneration	18
2.4.1 Reduction Reactions	18

	<u>Page</u>
2.4.2 Gas Phase Reactions	24
References	29
3. Sorbent Materials	33
3.1 Physical Structure of Sorbents	34
3.1.1 Phase Behavior of Alkali Sulfates and Their Reduction Products	34
3.2 Sorbent Preparation	37
3.2.1 Excess Solution Impregnation	37
3.2.2 Incipient Wetness Impregnation	38
3.3 Sorbent Analysis	38
3.3.1 Sulfate Loading	38
3.3.2 Surface Area	40
References	42
4. Thermogravimetric Analysis of Supported Sulfate Reduction by CO	43
4.1 Introduction	44
4.2 Experimental System	44
4.3 Experimental Conditions and Procedures	46
4.3.1 Gravimetric Analysis	46
4.3.2 Measurement of Sorbent Composition	47
4.4 Results	52
4.4.1 Gravimetric Results	52
4.4.1a Sulfate Decomposition in N <sub>2</sub>	52

	<u>Page</u>
4.4.1b Reduction	54
4.4.1c Product Selectivity	67
4.4.1d Carbonate Decomposition in N <sub>2</sub>	70
4.4.2 Sorbent Composition Changes During Reduction	72
4.5 Discussion	78
4.5.1 Effect of the Nature of the Alkali Material	78
4.5.1a Effect of the Presence of Lithium in the Alkali Material	78
4.5.1b Effect of the Phase Behavior of the Alkali Material	80
4.5.2 Effect of the Support	80
4.5.3 Interpretation of the Sorbent Composition Changes During Reduction	82
References	87
5. Fourier Transform Infrared Spectroscopy	88
5.1 Introduction	89
5.1.1 Inorganic Infrared Spectroscopy	89
5.1.2 Fourier Transform Infrared Spectroscopy	89
5.2 Experimental Conditions and Sample Preparation	91
5.2.1 Sample Preparation	91
5.2.2 Spectrometry	91
5.3 Results and Discussion	92
5.3.1 Sulfated Samples	92

	<u>Page</u>
5.3.2 Reduction at 800°C	92
5.3.3 Reduction at 700°C	95
References	97
6. Microreactor Experiments	98
6.1 Introduction	99
6.2 Experimental System	99
6.3 Experimental Conditions	103
6.3.1 Sorbent Reduction	103
6.3.2 Support Catalysis	104
6.4 Reduction Results and Discussion	104
6.4.1 Results	104
6.4.1a $\alpha$ -Alumina Supported Sorbents	104
6.4.1b Silica and Zirconia Supported Sorbents	112
6.4.2 Discussion	116
6.4.2a Effect of the Nature of the Alkali Material	116
6.4.2b Effect of Support	118
6.4.2c Effect of CO Concentration	119
6.4.2d Effect of Temperature	120
6.5 Support Catalysis Results and Discussion	120
References	129
7. Conclusions and Recommendations	130
7.1 Comparison of TGA and FTIR Results	131

	<u>Page</u>
7.2 Comparison of TGA and Microreactor Results	131
7.3 Possible Reaction Mechanism	132
7.4 Conclusions	134
7.5 Recommendations	135

### List of Figures

	<u>Page</u>
Figure 2.1: Decomposition of Alkali Sulfates in Air	8
Figure 2.2: Decomposition of Alkali Sulfates in N <sub>2</sub>	9
Figure 2.3: Vapor Pressure of Sulfur over Na <sub>2</sub> S <sub>x</sub>	14
Figure 2.4: Standard Free Energy Changes for Alkali Aluminate Formation Reactions	16
Figure 2.5: Standard Free Energy Changes for Reduction Reactions of Sodium Sulfate	20
Figure 2.6: Standard Free Energy Changes for Reduction Reactions of Lithium Sulfate	21
Figure 2.7: Standard Free Energy Changes for Reactions Involving the Conversion of Sulfide to Oxide	22
Figure 2.8: Equilibrium Sulfide Fraction as a Function of Temperature	23
Figure 2.9: Equilibrium Sulfide Fraction for the Sodium Sulfide-Sodium Aluminate System as a Function of CO <sub>2</sub> /S <sup>2-</sup> Ratio	25
Figure 2.10: Equilibrium Composition in the SO <sub>2</sub> -CO-S <sub>2</sub> System as a Function of CO/SO <sub>2</sub> Ratio	26
Figure 2.11: The Effect of Temperature on the SO <sub>2</sub> -COS-S <sub>2</sub> Equilibrium Composition	27
Figure 2.12: The Effect of N <sub>2</sub> Dilution on the SO <sub>2</sub> -COS-S <sub>2</sub> Equilibrium Composition	28
Figure 4.1: Thermogravimetric Analyzer System	45
Figure 4.2: Experiments to Determine Sorbent Composition	48

Figure 4.3: Variation Due to Carbonate/Aluminate Ratio in Calculated Sorbent Composition of $\text{Na}_2\text{SO}_4/\alpha\text{-Al}_2\text{O}_3$ Sorbents Reduced at 800°C	51
Figure 4.4: Variation Due to Carbonate/Aluminate Ratio in Calculated Sorbent Composition of $\text{Na}_2\text{SO}_4/\alpha\text{-Al}_2\text{O}_3$ Sorbents Reduced at 700°C	53
Figure 4.5: Sulfate Decomposition of $\gamma\text{-Al}_2\text{O}_3$ Sorbents During Nitrogen Heating	55
Figure 4.6: Reduction of $\text{Na}_2\text{SO}_4/\alpha\text{-Al}_2\text{O}_3$ (.11 mmole/g) at 700°C and 800°C with 10% CO Using the TGA System	56
Figure 4.7: Reduction of $\text{Na}_2\text{SO}_4/\alpha\text{-Al}_2\text{O}_3$ (.68 mmole/g) at 700°C and 800°C with 10% CO Using the TGA System	57
Figure 4.8: Reduction of $\text{NaLiSO}_4/\alpha\text{-Al}_2\text{O}_3$ at 700°C and 800°C with 10% CO Using the TGA System	58
Figure 4.9: Reduction of $\text{Li}_2\text{SO}_4/\alpha\text{-Al}_2\text{O}_3$ at 700°C and 800°C with 10% CO Using the TGA System	59
Figure 4.10: Reduction of $\text{Na}_2\text{SO}_4/\gamma\text{-Al}_2\text{O}_3$ at 700°C and 800°C with 10% CO Using the TGA System	60
Figure 4.11: Reduction of $\text{NaLiSO}_4/\gamma\text{-Al}_2\text{O}_3$ at 700°C and 800°C with 10% CO Using the TGA System	61
Figure 4.12: Reduction of $\text{NaLiSO}_4/\gamma\text{-Al}_2\text{O}_3$ at 700°C and 800°C with 1% CO Using the TGA System	63
Figure 4.13: Reduction of $\text{NaLiSO}_4/\gamma\text{-Al}_2\text{O}_3$ at 700°C and 800°C with 10% CO and 5.5% $\text{CO}_2$ Using the TGA System	64
Figure 4.14: $\text{SO}_2$ Production Per Surface Area During Reduction at 800°C Using the TGA System	65
Figure 4.15: Initial Weight Loss of $\text{Na}_2\text{SO}_4/\alpha\text{-Al}_2\text{O}_3$ Sorbents During Reduction	

	<u>Page</u>
at 800°C.	66
Figure 4.16: SO <sub>2</sub> Production Per Surface Area During Reduction at 700°C using the TGA System	68
Figure 4.17: Alkali Carbonate Decomposition.	71
Figure 4.18: Sorbent Composition During Reduction of Na <sub>2</sub> SO <sub>4</sub> /α-Al <sub>2</sub> O <sub>3</sub> at 800°C.	73
Figure 4.19: Sorbent Composition During Reduction of Na <sub>2</sub> SO <sub>4</sub> /α-Al <sub>2</sub> O <sub>3</sub> at 700°C.	74
Figure 4.20: Sorbent Composition During Reduction of NaLiSO <sub>4</sub> /α-Al <sub>2</sub> O <sub>3</sub> at 800°C.	75
Figure 4.21: Sorbent Composition During Reduction of NaLiSO <sub>4</sub> /α-Al <sub>2</sub> O <sub>3</sub> at 750°C.	76
Figure 4.22: Sorbent Composition During Reduction of NaLiSO <sub>4</sub> /α-Al <sub>2</sub> O <sub>3</sub> at 700°C.	77
Figure 4.23: Sulfate-Sulfite-Sulfide-Aluminate Contents During Reduction of Na <sub>2</sub> SO <sub>4</sub> /α-Al <sub>2</sub> O <sub>3</sub> .	84
Figure 4.24: Sulfate-Sulfite-Sulfide-Aluminate Contents During Reduction of NaLiSO <sub>4</sub> /α-Al <sub>2</sub> O <sub>3</sub> .	85
Figure 5.1: Characteristic Wavelengths of Absorption	90
Figure 5.2: Spectra of Sulfated Samples	93
Figure 5.3: Spectra of Samples Reduced and Partially Reduced at 800°C	94
Figure 5.4: Spectra of Samples Reduced and Partially Reduced at 700°C	96
Figure 6.1: Microreactor System	100

	<u>Page</u>
Figure 6.2: Detail of Microreactor	101
Figure 6.3: Temperature Profile of Reactor Bed	102
Figure 6.4: Reduction of $\text{Na}_2\text{SO}_4/\alpha\text{-Al}_2\text{O}_3$ with 10% CO and 800°C using the Microreactor System	105
Figure 6.5: Reduction of $\text{Na}_2\text{SO}_4/\alpha\text{-Al}_2\text{O}_3$ with 1% CO and 800°C using the Microreactor System	106
Figure 6.6: Reduction of $\text{NaLiSO}_4/\alpha\text{-Al}_2\text{O}_3$ with 10% CO and 800°C using the Microreactor System	107
Figure 6.7: Reduction of $\text{NaLiSO}_4/\alpha\text{-Al}_2\text{O}_3$ with 1% CO and 800°C using the Microreactor System	108
Figure 6.8: Reduction of $\text{NaLiSO}_4/\alpha\text{-Al}_2\text{O}_3$ with 10% CO and 700°C using the Microreactor System	109
Figure 6.9: Reduction of $\text{NaLiSO}_4/\alpha\text{-Al}_2\text{O}_3$ with 1% CO and 700°C using the Microreactor System	110
Figure 6.10: Reduction of $\text{NaLiSO}_4/\text{SiO}_2$ with 10% CO and 800°C using the Microreactor System	113
Figure 6.11: Reduction of $\text{NaLiSO}_4/\text{ZrO}_2$ with 10% CO and 800°C using the Microreactor System	114
Figure 6.12: Reduction of $\text{NaLiSO}_4/\text{ZrO}_2$ with 10% CO and 700°C using the Microreactor System	115
Figure 6.13: $\text{SO}_2$ Production Per Surface Area During Reduction at 800°C using the Microreactor System	117
Figure 6.14: $\text{SO}_2$ Absorption by $\alpha$ -Alumina	121

	<u>Page</u>
Figure 6.15: Conversion of 1% CO/2000 ppm SO <sub>2</sub> at 800° C	123
Figure 6.16: Conversion of 12% CO/2000 ppm SO <sub>2</sub> at 800° C	124
Figure 6.17: Conversion of 1% CO/2000 ppm SO <sub>2</sub> at 700° C	125
Figure 6.18: Conversion of 12% CO/2000 ppm SO <sub>2</sub> at 700° C	126
Figure 7.1: Possible Reaction Mechanism	133

**List of Tables**

	<u>Page</u>
Table 3.1: Supports Used in Sorbent Preparation	35
Table 3.2: Eutectic Points of Mixtures of Alkali Sulfates and Their Reduction Products	36
Table 3.3: Analysis of Prepared Sorbents for Sulfate Loading	39
Table 3.4: Surface Area of Sorbents	41
Table 4.1: Product Selectivity of Sorbents Reduced at 700°C and 800°C, with 10% CO on the Thermogravimetric Analyzer System	69
Table 6.1: Product Selectivity of Sorbents Reduced Using the Microreactor System	111
Table 6.2: Steady State Conversion of SO <sub>2</sub> and CO Over Support Materials	127

1.

## CHAPTER 1

### INTRODUCTION

Sulfur dioxide in the flue gas of coal burning power plants and the exhaust of sulfide mineral smelters poses serious environmental and health problems. Sulfur oxide removal is therefore an important operation in connection with coal combustion, and other industrial processes.

Several processes for sulfur dioxide removal have been commercialized and many others are at various stages of research and development (Pfeiffer, 1975). These processes utilize various sorbents in solution, slurry or solid form and vary widely in their operating temperature. Some processes involve sorbent regeneration, converting the removed sulfur to a useful form, usually either sulfuric acid or elemental sulfur. Regenerable processes have the advantage of not requiring sorbent disposal, but they tend to be more complex than non-regenerable processes.

This work studies the chemistry involved in a high temperature, regenerable process of  $\text{SO}_2$  removal. Such a process could be used to scrub either concentrated  $\text{SO}_2$  streams, such as smelter exhausts, or dilute  $\text{SO}_2$  streams such as flue gas from coal combustion. The sorbent considered consists of an alkali oxide distributed on a porous, solid support. Absorption and regeneration may both be conducted at temperatures of 700 to 800°C. Operating in this temperature range, the sorbent is potentially interesting for *in situ* sulfur removal in fluidized coal combustion.

Several types of sorbent have been investigated previously for *in situ* sulfur removal. The most commonly used sorbent is limestone, which upon absorption of  $\text{SO}_2$  produces calcium sulfate. Although sulfated limestone sorbents have been found to be regenerable under certain conditions (Yang and Shen, 1979), alternate sorbent materials are also being sought. This search for alternate regenerable sorbents has centered around various

metal oxides and supported metal oxides. Vogel et al. (1974) as well as Ruth and Varga (1979) found alkali oxides and supported alkali oxides to be active sorbents. Alkali aluminates and titanates have also been found to be active (Ruth and Varga, 1979; Schlesinger and Illig, 1971).

The use of bulk alkali sorbents for sulfur oxide removal has been investigated. Oldenkamp and Margolin (1969) report  $\text{SO}_2$  removal in a molten bath of alkali carbonate. The alkali sulfate formed remains in solution in the molten carbonate and regeneration is performed by reduction with  $\text{CO}$  or  $\text{H}_2$ . The use of the melt in this fashion presents relatively large mass transfer resistance and entails severe corrosion problems. Dispersing the alkali sorbent on a porous support eliminates corrosion and greatly enhances mass transfer. A material of this type is the U.S. Bureau of Mines alkalized alumina sorbent, a sodium deficient bulk sodium aluminate (Schlesinger and Illig, 1971). A related material is alumina impregnated with alkali oxide. The active sorbent is dispersed on the pore surface of the support and provides a relatively large surface area for reaction. The rate of  $\text{SO}_2$  absorption and the available capacity for  $\text{SO}_2$  (per sodium atom) are higher for alumina impregnated with sodium oxide than for alkalized alumina (Vogel et al., 1974).

The goals of this research were to demonstrate the ability to use supported alkali oxide in regenerable sulfur dioxide sorbents, and to elucidate the chemical mechanisms which occur during regeneration by reduction with carbon monoxide. In particular, we investigated the effect of different alkali oxides and supports on the reaction activity and product selectivity.

**References**

1. Oldenkamp, R. D. and E. D. Margolin, "The Molten Carbonate Process for Sulfur Oxide Emissions," *Chem. Eng. Prog.*, **65**(11), 73 (1969).
2. Pfeiffer, John B., Ed., *Sulfur Removal and Recovery from Industrial Processes*, Advances in Chemistry Series, 139, American Chemical Society (1975).
3. Ruth, L. A. and G. M. Varga, Jr., "New Regenerable Sorbent for Fluidized Bed Coal Combustion," *Env. Sci. Tech.*, **13**(6), 715 (1979).
4. Schlesinger, M. D. and E. G. Illig, "The Regeneration of Alkalized Alumina," *Chem. Eng. Prog. Symposium Series*, **67**(115), 46 (1971).
5. Vogel, R. F., B. R. Mitchell and F. E. Massoth, "Reactivity of SO<sub>2</sub> with Supported Metal Oxide-Alumina Supports," *Env. Sci. Tech.*, **8**(5), 432 (1974).
6. Yang, R. T. and Shen, M., "A Regenerative Process for Fluidized Bed Combustion of Coal with Lime Additives," *Ind. Eng. Chem. Proc. Des. Dev.* **18**(2), 312 (1979).

CHAPTER 2

BACKGROUND CHEMISTRY AND THERMODYNAMICS

## 2.1 Sulfation

The sulfation of alkali metal oxide can be written in general form



where M = Li, Na, etc.

The process takes place through a series of elementary steps. At lower temperatures (<200°C) or when low O<sub>2</sub> concentrations are used, sulfite may also form (Schlesinger and Illig, 1971).



where M = Na, Li, etc.

At higher temperatures (>600°C), sulfite will disproportionate to sulfate and sulfide (Foerster and Kubel, 1924).



This disproportionation occurs through an as yet unknown series of steps. Any sulfide formed will, under the oxidative conditions present during sulfation, react to form sulfate.

Oxide formed during the reduction of supported alkali sulfates will react with the alumina support to form aluminate. Vogel et al. (1974) showed that even in this case sulfation produces alkali sulfate and alumina from SO<sub>2</sub>, O<sub>2</sub> and aluminate. Formation of a layer of sulfate through which SO<sub>2</sub> and O<sub>2</sub> must diffuse to react with aluminate may slow the rate of sulfation.

### 2.1.1. Kinetics of Sulfation

Vogel et al. (1974) found sulfation to be first order in SO<sub>2</sub> for both sodium-oxide supported on alumina and for the alkalized alumina sorbent produced

by the Bureau of Mines. Alkalized alumina was found to react more slowly than alumina-supported  $\text{Na}_2\text{O}$  indicating that conversion from aluminate to sulfate is slower than from oxide to sulfate. The oxide/alumina sorbent, however, may also have been present as a surface aluminate, because it was calcinated at  $538^\circ\text{C}$  for ten hours. The difference in sulfation rate is more likely due to diffusional differences between the bulk and the supported material.

### 2.1.2. Thermodynamics of Sulfation

The sulfation of both alkali oxides and alkali aluminates is very favorable thermodynamically in the temperature range of interest. The equilibrium vapor pressure of  $\text{SO}_2$  in air above  $\text{Na}_2\text{O}$ ,  $\text{Li}_2\text{O}$ ,  $\text{NaAlO}_2$  and  $\text{LiAlO}_2$  is shown in Fig. 2.1. Even for the least favorable lithium sulfate-lithium aluminate reaction, the equilibrium  $\text{SO}_2$  level is very low, approximately one ppm at  $800^\circ\text{C}$ .

The alkali sulfates show good stability in nitrogen as well as in air, Fig. 2.2. The level of  $\text{SO}_2$  for all systems is below 100 ppm at  $800^\circ\text{C}$ .

## 2.2. Sorbent Regeneration

### 2.2.1. General Concerns

Regeneration of sulfated sorbents requires reduction of the sulfate to the oxide. The reduction of sulfate may be accomplished using CO as a reducing agent in the following reaction sequence.



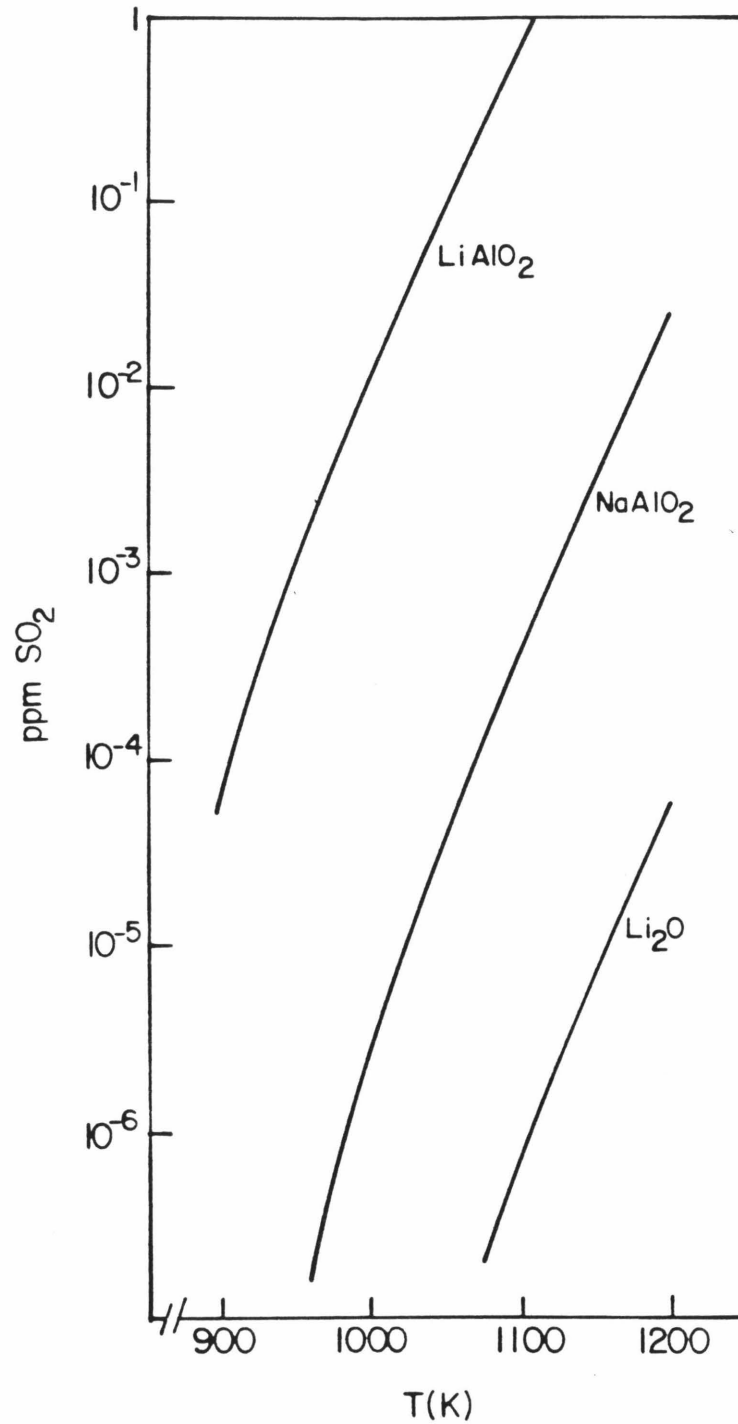


Figure 2.1: Decomposition of Alkali Sulfates in Air  
(Data from JANAF, 1971 and Barin and Knacke, 1973)

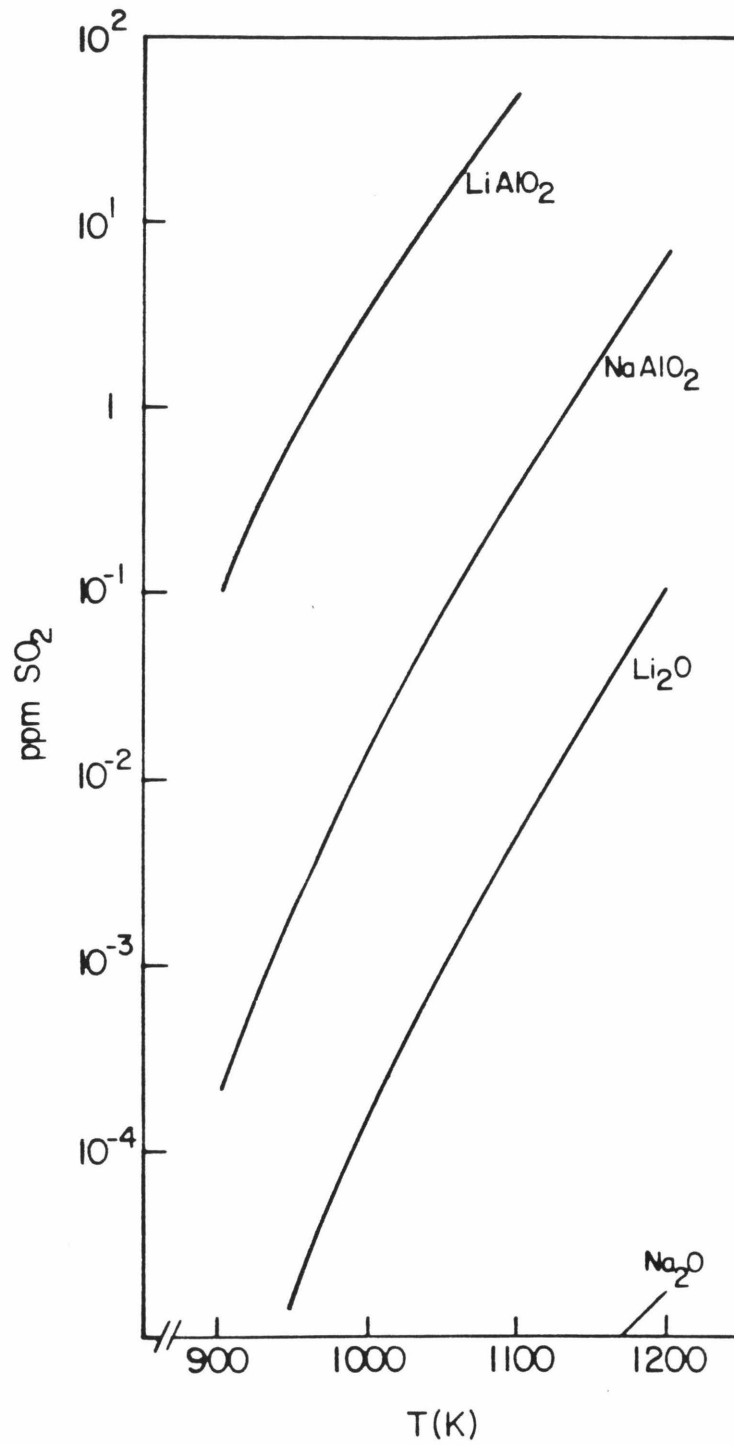


Figure 2.2: Decomposition of Alkali Sulfates in  $N_2$   
(Data from JANAF, 1971 and Barin and Knacke, 1973)

where M = Na, Li, etc.

Reduction produces both oxide and sulfide. Sulfide formation decreases the ability of the reduced sorbent to reabsorb  $\text{SO}_2$ , and is detrimental to the overall regeneration process. Sulfur dioxide produced during reduction can be reduced further to produce elemental sulfur and COS. Elemental sulfur is the product of choice. The reduction reactions have not been fully characterized. Several possible side reactions exist.

### **2.2.2. Reduction of Alkali Sulfates**

The reduction of alkali sulfates and allied materials has been studied by several investigators, under various reaction conditions and using various reducing media. The reduction of sulfated alkalized alumina with pure CO and pure  $\text{H}_2$  was studied at temperatures between 620 and 680°C (Schlesinger and Illig, 1971). Reduction with CO was found to produce a mixture of sulfide and aluminate. The aluminate produced was 30% or less; the only gaseous product reported was COS. Reduction with  $\text{H}_2$  caused a higher fraction of aluminate in the product than reduction with CO. The fraction of aluminate increased with increasing temperature and was 0.8 at 680°C. Hydrogen sulfide was the gaseous product. Iron was found to catalyze the reduction with  $\text{H}_2$ . Schlesinger and Illig also investigated the reduction of pure sodium sulfate in  $\text{H}_2$  or CO, and temperatures of 750°C or higher were required for reaction to take place. This indicates that alumina or alkalized alumina present in the sample may catalyze for the reduction reaction.

The reduction of unsupported sulfates has been studied by other investigators. Ahlgren et al. (1967) investigated the reduction of bulk molten sodium sulfate with CO and  $\text{H}_2$ . At 900°C, reduction of sodium sulfate with CO for 60 minutes produced sodium oxide, which reacted with  $\text{CO}_2$  present as

a reaction product, to form sodium carbonate. Sodium sulfide and sodium polysulfides were also produced. Thirty minutes of reduction under the same conditions produced sodium sulfide only. The reactions appeared to be autocatalytic. Reduction of sulfate with hydrogen produced only sulfide.

Sulfate dissolved in molten mixed alkali carbonate has been reduced with CO and H<sub>2</sub> at 600°C (Oldenkamp and Margolin, 1969). Dissolved sulfide is cited as the primary product in both cases. Birk et al. (1971) investigated the same dissolved sulfate system using H<sub>2</sub> as the reductant at temperatures from 600 to 900°C. Sulfide was again the major product. These investigators found that the reaction was autocatalytic with respect to sulfide. The autocatalysis was attributed to a reaction between sulfide and sulfate. Several metals were found to catalyze the reaction, iron being the most active.

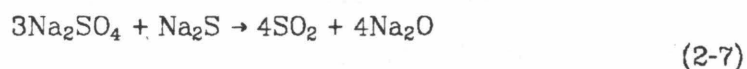
The reduction of sodium sulfate, both alone and dissolved in molten carbonate has been studied with coal as the reductant (Budnikov, 1934; Cameron and Grace, 1983). In both cases, the loss of sulfate was found to be autocatalytic.

The electrochemical reduction of molten mixed alkali sulfates has been investigated. The product selectivity depended on the exact reducing conditions, and the duration of reduction. At 550°C the products consisted of a small amount of sulfite with larger amounts of dissolved sulfur and oxide (Johnson and Laitenen, 1963). At 625°C, a mixture of sulfite and sulfide with a small amount of sulfur was found after reduction, while sulfur, oxide and SO<sub>2</sub> were found after prolonged reduction at this temperature (Lui, 1962; Burrows and Hills, 1970).

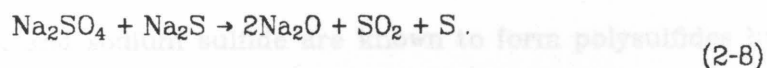
These studies show a wide range of product variation with reaction conditions. Aside from the desired oxide, reactions produce sulfide and possibly

sulfite and polysulfides. Reactions in the molten phase appear to be autocatalytic. The exact nature of the reactions is not clear.

Some of the aspects of the reduction become clearer when reactions that contribute to the overall reduction are treated separately. Such reactions are those which may occur between sulfate and sulfide ions in a molten phase. These types of reactions have been invoked as a cause of the reduction's autocatalysis (Budnikov, 1934; Birk et al., 1971). As early as 1924, Foerster and Kubel had observed the reaction of sulfate and sulfide to form oxide and sulfur dioxide at temperatures above 800°C.



This reaction is the reverse of the sulfite disproportionation reaction (Eq. 2-3), combined with the dissociation of sulfite to oxide and  $\text{SO}_2$ . The reaction will not take place in a single step, but will be the sum of a series of ion-ion reactions, driven by the ultimate evolution of sulfur dioxide. Manring et al. (1967) found a more general set of reactions ranging from Eq. (2-7) to



Manring et al. (1967), Kohlmeyer and Lohrke (1955) and Dearnaley et al. (1983) observed that these reactions were facilitated by the presence of silica and other refractory oxides which can combine with the  $\text{Na}_2\text{O}$  and drive the reaction.



The presence of a support may then act to promote overall sulfur removal. If  $\text{CO}_2$  is present, these reactions might also be driven by the formation of carbonate from the oxide.



Aside from forming carbonate by direct reaction with oxide, the  $\text{CO}_2$  produced during the reduction may contribute greatly to the overall reaction scheme through secondary reactions, such as that converting sulfide to oxide.



This reaction has been observed to proceed at low temperatures ( $435^\circ\text{C}$ ) and is exploited as a separate step in the regeneration of sulfide produced during the molten carbonate process (Oldenkamp and Margolin, 1969). Ahlgren et al. (1967) observed the reaction of  $\text{CO}_2$  and  $\text{Na}_2\text{S}$  at  $900^\circ\text{C}$  to form carbonate and polysulfide. The presence of a solid support such as silica or alumina, or the presence of excess  $\text{CO}_2$ , may once again drive the reaction by the formation of stable compounds from the oxide.

Polysulfides have been mentioned as possible reaction products by several investigators (Ahlgren et al., 1967; Dearnaley et al., 1983; Birk et al., 1971). Both lithium sulfide and sodium sulfide are known to form polysulfides by reaction with elemental sulfur (Letoffe et al., 1976)



Lithium has only one known polysulfide,  $\text{Li}_2\text{S}_2$ , while sodium has several which have been characterized (Oei, 1973). Under various reaction conditions, polysulfides may form as intermediates. The decomposition pressure of sulfur above sodium polysulfide-sulfide mixtures of composition  $\text{Na}_2\text{S}_x$  are shown in Fig. 2.3.

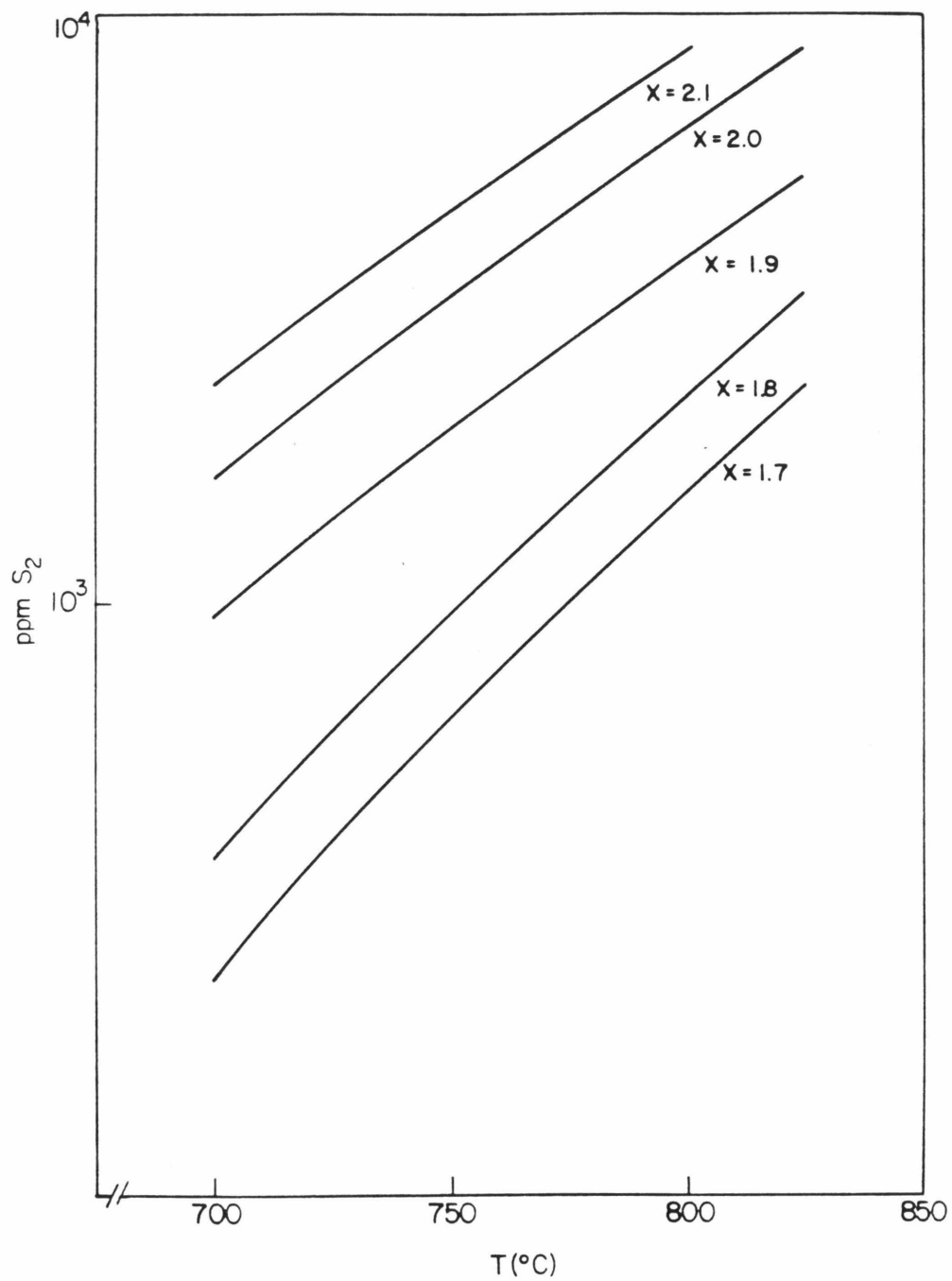


Figure 2.3: Vapor Pressure of Sulfur Over Na<sub>2</sub>S<sub>x</sub>  
(Data from Janz, et al., 1979)

## 2.3. Reactions of the Support Materials

### 2.3.1. Direct Support Interaction

The reaction of oxide with a support such as alumina or silica has been cited as a possible driving force away from sulfide in the overall reaction scheme. As early as 1910, Cobb studied the reaction of oxide with silica (Eq. 2-9) or alumina,



to form stable compounds. He found sodium carbonate decomposed in the presence of either silica or alumina at temperatures around 700°C. The aluminate formed decomposed when exposed to an oxidative atmosphere containing sulfur oxides. Kovalenko and Bukin (1978) discovered that the reaction between carbonate and alumina was dependent upon the defect structure of the alumina present.  $\gamma$ -alumina was more reactive than  $\alpha$ -alumina.  $\gamma$ -alumina reacted at 570-580°C while  $\alpha$ -alumina did not react until the temperature reached 620°C. Christie et al. (1978) found the rate of the  $\text{Na}_2\text{CO}_3$ /alumina reaction limited by the formation of a layer of sodium aluminate through which cations and anions had to diffuse.

The alkali anion present affects significantly the formation of aluminate. Lithium aluminate is more stable than sodium aluminate in comparison with their respective carbonates (Fig. 2-4).

### 2.3.2. Catalysis of Secondary Reactions by the Support

In addition to reacting directly with alkali material, the support may act as a catalyst for the further reduction of  $\text{SO}_2$  by CO (Eq. 2-5), the reaction of sulfur with CO to form COS (Eq. 2-6), or the reduction of  $\text{SO}_2$  with COS,

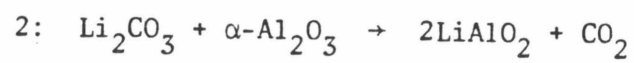
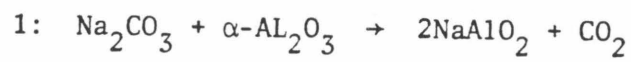
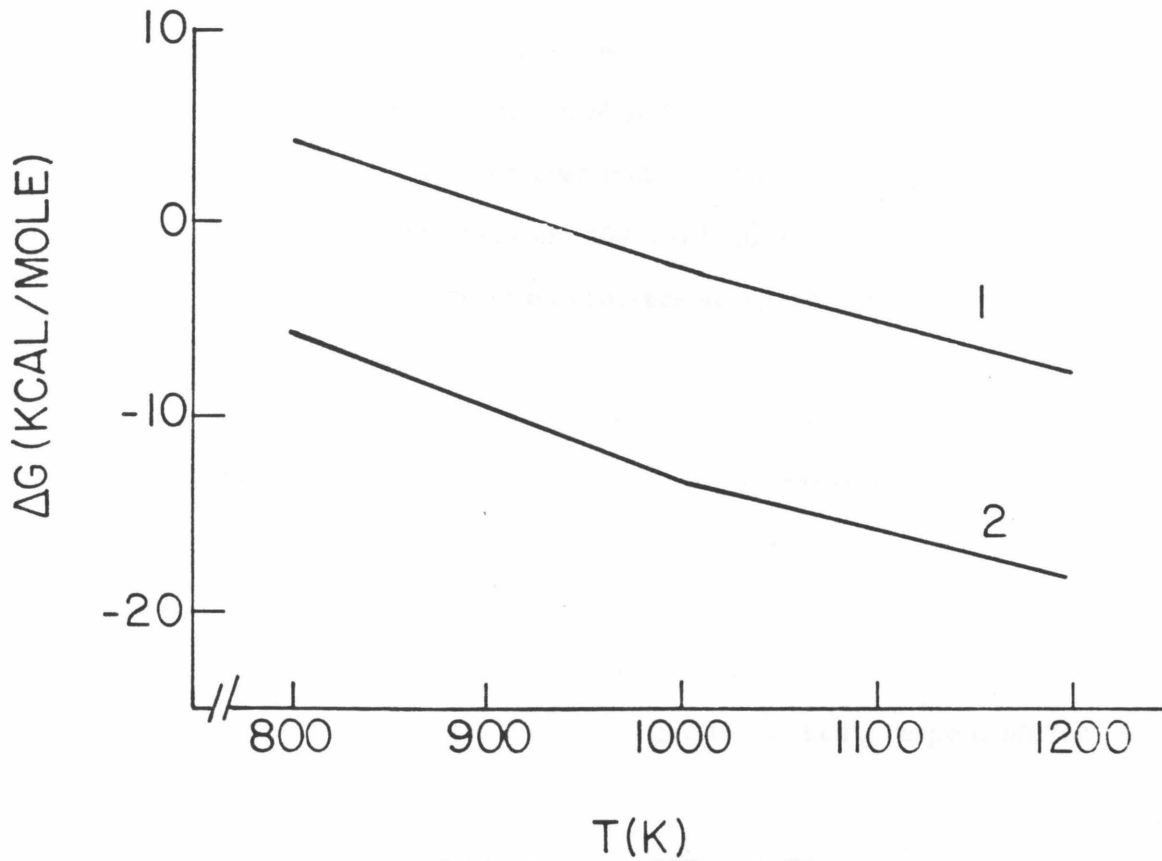
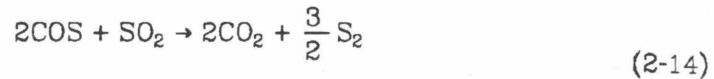


Figure 2.4: Standard Free Energy Changes for Alkali Aluminate Formation Reactions  
(Data from Barin and Knacke, 1973)



These reactions and their catalysis by various materials have been the subject of much study. The reduction of sulfur dioxide with carbon monoxide (Eq. 2-5) is known to proceed over metal, copper or iron, and alumina catalysts at moderate temperatures, 400-500°C (Querido and Short 1973; Khalafalla et al., 1971). This reaction proceeds at higher temperatures when the gases are in contact with alumina or other surfaces. Lepsoe (1940) observed that although this reaction proceeded slowly at 800°C in the absence of catalyst, almost any kind of surface was capable of catalysis at this temperature. Alumina (boehmite) was an efficient catalyst at temperatures above 300°C. Khalafalla and Haas (1972) found  $\gamma$ -alumina active at temperatures above 450°C, while  $\alpha$ -alumina was not active until 650-700°C. The basic function of a Brönsted site was suggested as being responsible for  $\text{SO}_2$  absorption.

The Claus reaction (Eq. 2-14) between COS and  $\text{SO}_2$  is also known to proceed over various surfaces. Lepsoe (1940) found that the reaction proceeded over almost any hot surface, and was approximately four times as fast as the CO- $\text{SO}_2$  reaction. Studying the catalysis of the COS- $\text{SO}_2$  reaction at temperatures of 500-800°, Haas and Khalafalla (1973) found that the presence of transition metals on an alumina catalyst decreased the conversion. Transition metals had been found to increase catalytic activity towards the CO- $\text{SO}_2$  reaction.

Catalysis of the CO- $\text{SO}_2$  and COS- $\text{SO}_2$  reactions may be influenced by the alkali phase present during reduction. Catalysis may also be affected by reduction products or intermediates. Sodium oxide, sodium sulfide and sodium carbonate have been cited as catalysts for the COS- $\text{SO}_2$  reaction

(Ferm, 1957). The addition of alkali hydroxides to either silica or alumina was found to increase the activity of the material as a Claus reaction catalyst (Dudzick and George, 1980; George, 1975). In both cases the rate went through a maximum with increasing alkali hydroxide loading. The nature of the cation,  $\text{Na}^+$ ,  $\text{Li}^+$  or  $\text{K}^+$ , had an effect on the rate enhancement by alkali hydroxide (George, 1975). He observed strong correlation between catalyst activity and the polarizing power of the cation:  $\text{Li}^+ > \text{Na}^+ > \text{K}^+$ .

Elemental sulfur formed during reaction has been found to activate alumina catalysts for the  $\text{CO-SO}_2$  reaction (Khalafalla and Haas, 1972). Sulfate, on the other hand, has been found to be a poison for alumina Claus catalysts (Pearson, 1973).

The decomposition of  $\text{COS}$  to sulfur and  $\text{CO}$  and its reverse reaction (Eq. 2-6) is also catalyzed by common support surfaces. Akimoto et al. (1984) found catalysis of the decomposition of  $\text{COS}$  by  $\text{Al}_2\text{O}_3$  ( $400^\circ\text{C}$ ),  $\text{MgO}$  ( $440^\circ\text{C}$ ),  $\text{TiO}_2$  ( $450^\circ\text{C}$ ) and  $\text{SiO}_2$  ( $550^\circ\text{C}$ ). Haas and Khalafalla (1973) found the  $\text{COS}$  decomposition reaction proceeded at temperatures above  $500^\circ\text{C}$  over  $\alpha$ -alumina,  $\chi$ -alumina and silica gel. They found all these surfaces had the same activity at temperatures above  $500^\circ\text{C}$ .

At reaction temperatures, all of the aforementioned secondary reactions may take place. The  $\text{CO-SO}_2$  and  $\text{COS-SO}_2$  (Claus) reaction activity will probably depend on the support and on the nature of the alkali component of the sorbent. The  $\text{COS-S}_2\text{-CO}$  reaction will likely proceed with any support.

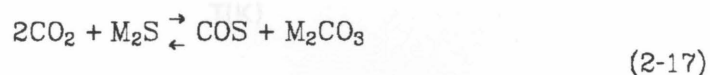
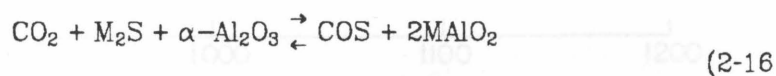
## **2.4. Thermodynamics of Regeneration**

### **2.4.1. Reduction Reactions**

The standard free energy changes for the various reactions involved in

alkali sulfate reduction are shown for the sodium system in Fig. 2.5 and for the lithium system in Fig. 2.6. The reduction to form sulfide is the most thermodynamically favored in both systems. The reaction to form oxide is the least favored thermodynamically. Reactions which form carbonate or aluminate are significantly more favorable than those which form oxide. In the sodium system the carbonate and aluminate formation reactions are equally favorable, while in the lithium system the aluminate formation reaction is more favorable than that which forms carbonate. All the reactions may be driven to completion by an excess of CO.

The partition between sulfide and oxide, including carbonate and aluminate, is important since it determines the degree of regeneration of the sorbent. To determine the thermodynamic limits on this partition, the following reactions can be considered.



where M = Li, Na. The standard free energy changes are shown as a function of temperature in Fig. 2-7. In an excess of CO all sulfate will be completely reduced to sulfide or oxide (aluminate, carbonate). Also in excess CO it can be assumed that sulfur gases produced during the formation of oxides will be primarily present as COS. Using these assumptions and the equilibrium expressions for reactions (2-15) through (2-17) limitations on the sulfide oxide partition were found. The equilibrium sulfide mole fraction under excess CO is shown as a function of temperature in Fig. 2.8. At equilibrium, the product is entirely sulfide if no compound forms with oxide. Carbonate

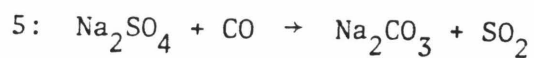
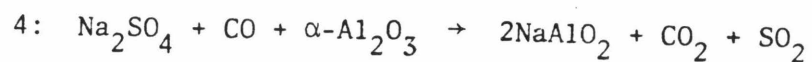
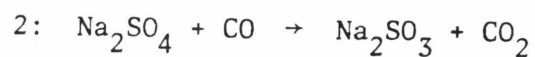
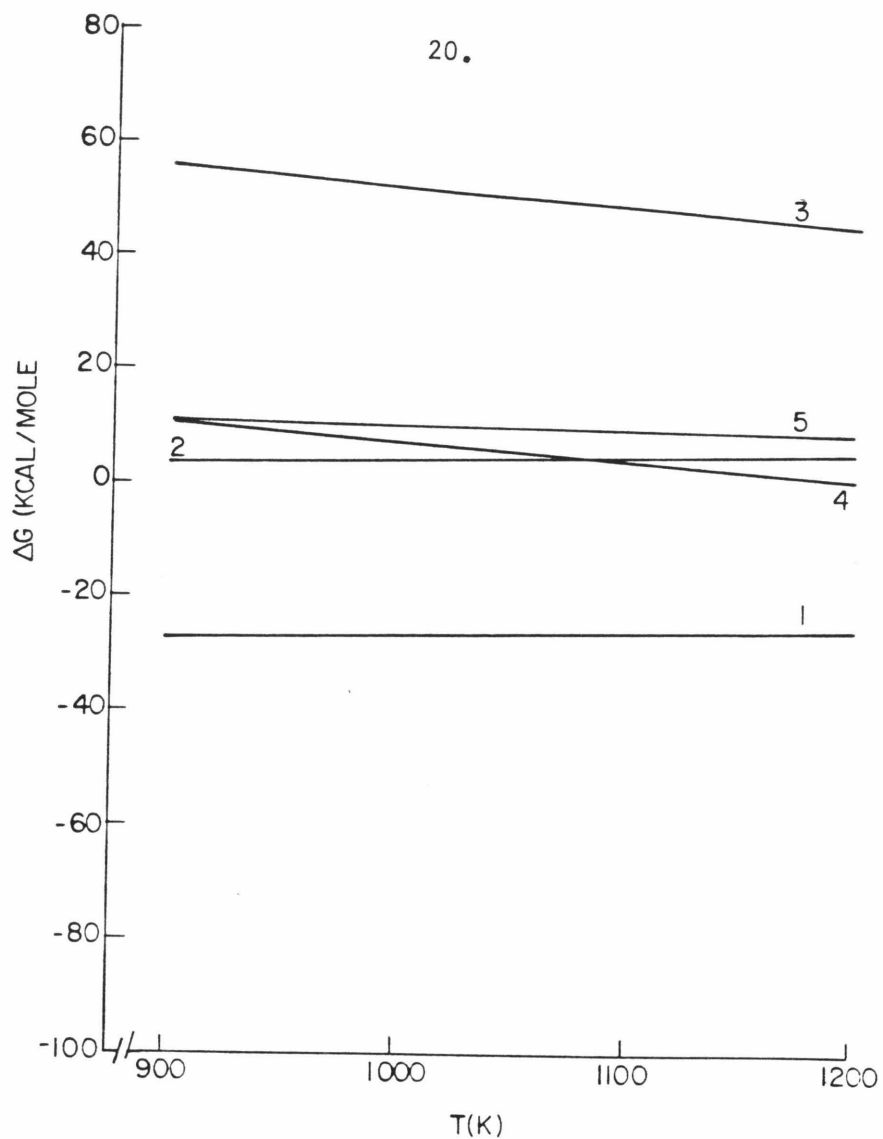


Figure 2.5: Standard Free Energy Changes for the Reduction Reactions of Sodium Sulfate  
(Data from JANAF, 1971, and Barin and Knacke, 1973)

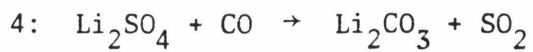
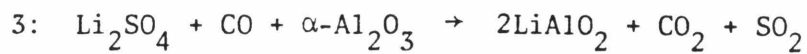
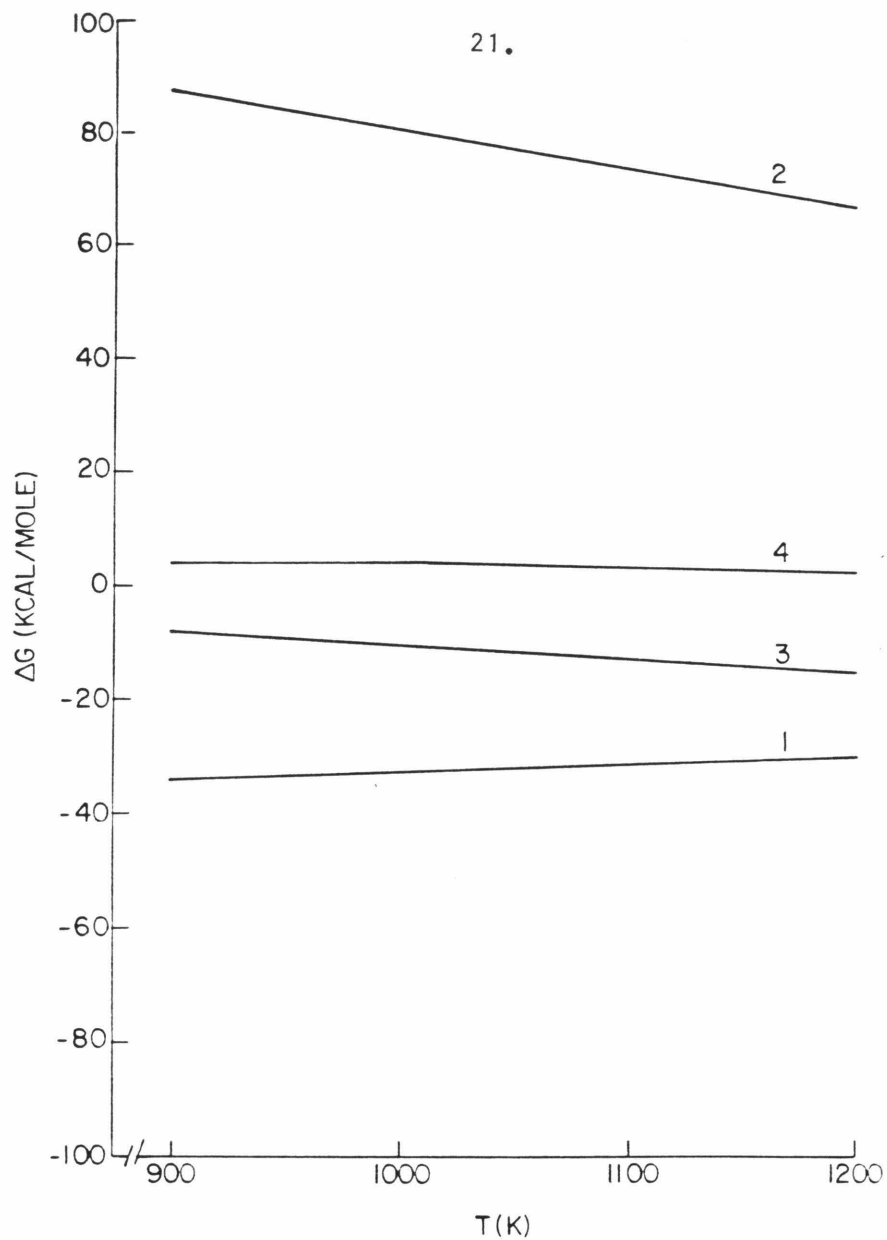


Figure 2.6: Standard Free Energy Changes for the Reduction Reactions of Lithium Sulfate  
(Data from Barin and Knacke, 1973)

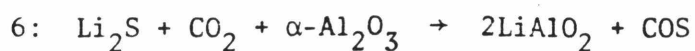
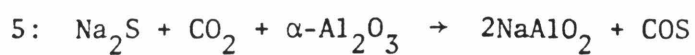
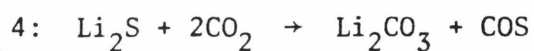
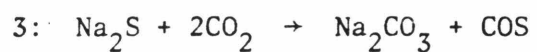
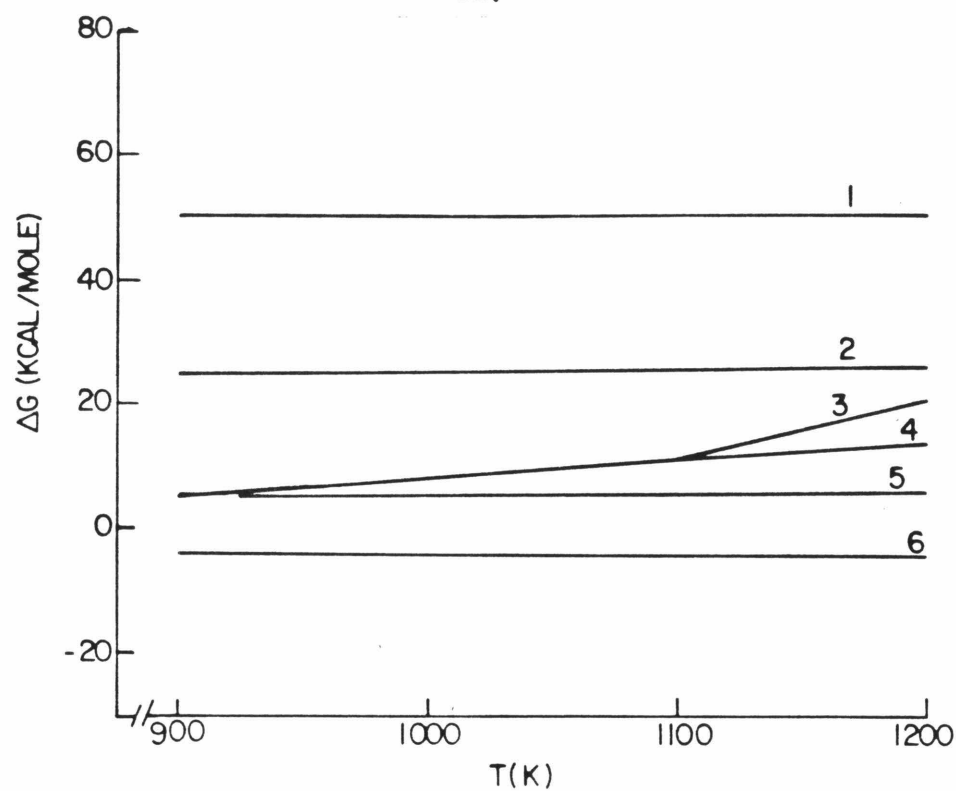


Figure 2.7: Standard Free Energy Changes for Reactions Involving the Conversion of Sulfide to Oxide  
(Data from JANAF, 1971, and Barin and Knacke, 1973)

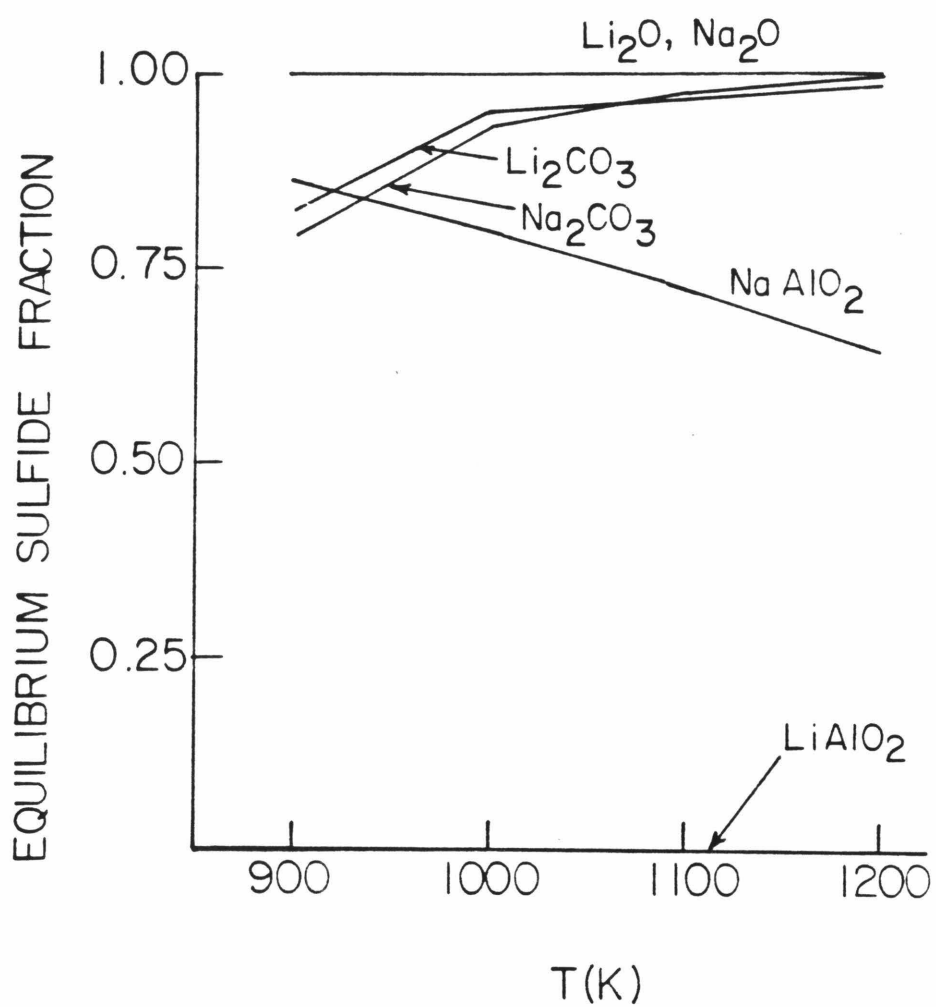


Figure 2.8: Equilibrium Sulfide Fraction as a Function of Temperature (Calculated assuming initially an excess of CO with sulfate, no added CO<sub>2</sub>, and all the sulfur in the gas phase is present as COS.)

and aluminate both increase the equilibrium sulfur removal. Aluminate, however, is much more effective at reducing the sulfide fraction. When lithium aluminate was allowed to form the sulfide is completely removed at equilibrium. Increasing the temperature increases the sulfur removal for the sodium aluminate material and decreases the removal for the carbonate system. If  $\text{CO}_2$  in excess of that formed during reduction is added, the sulfur removal will be increased. Figure 2-9 shows the dependence of the equilibrium sulfide fraction for the sodium sulfide-sodium aluminate system at 1100 K as a function of the carbon dioxide-sulfide ratio. A ratio of 4 corresponds to excess CO, as 4 moles of  $\text{CO}_2$  are formed for each mole of sulfide.

#### 2.4.2. Gas Phase Reactions

The equilibrium of the gaseous species present during reduction: CO,  $\text{SO}_2$ ,  $\text{S}_2$ , COS and  $\text{CO}_2$  was examined using STANJAN, a program for calculating equilibrium based on the minimization of free energy. This program was developed by W. C. Reynolds at Stanford University. The distribution of sulfur between  $\text{SO}_2$ , COS and  $\text{S}_2$  was determined for varying temperature, CO/ $\text{SO}_2$  ratio and gas dilution (amount of diluent  $\text{N}_2$  added). The results are shown in Figs. 2-10 through 2-12. Sulfur is the major product in a certain range of CO/ $\text{SO}_2$  ratios. Lower ratios give  $\text{SO}_2$  as the major product, and higher ratios give COS. Raising the temperature enlarges the range where sulfur is the major product, as does increasing the dilution.

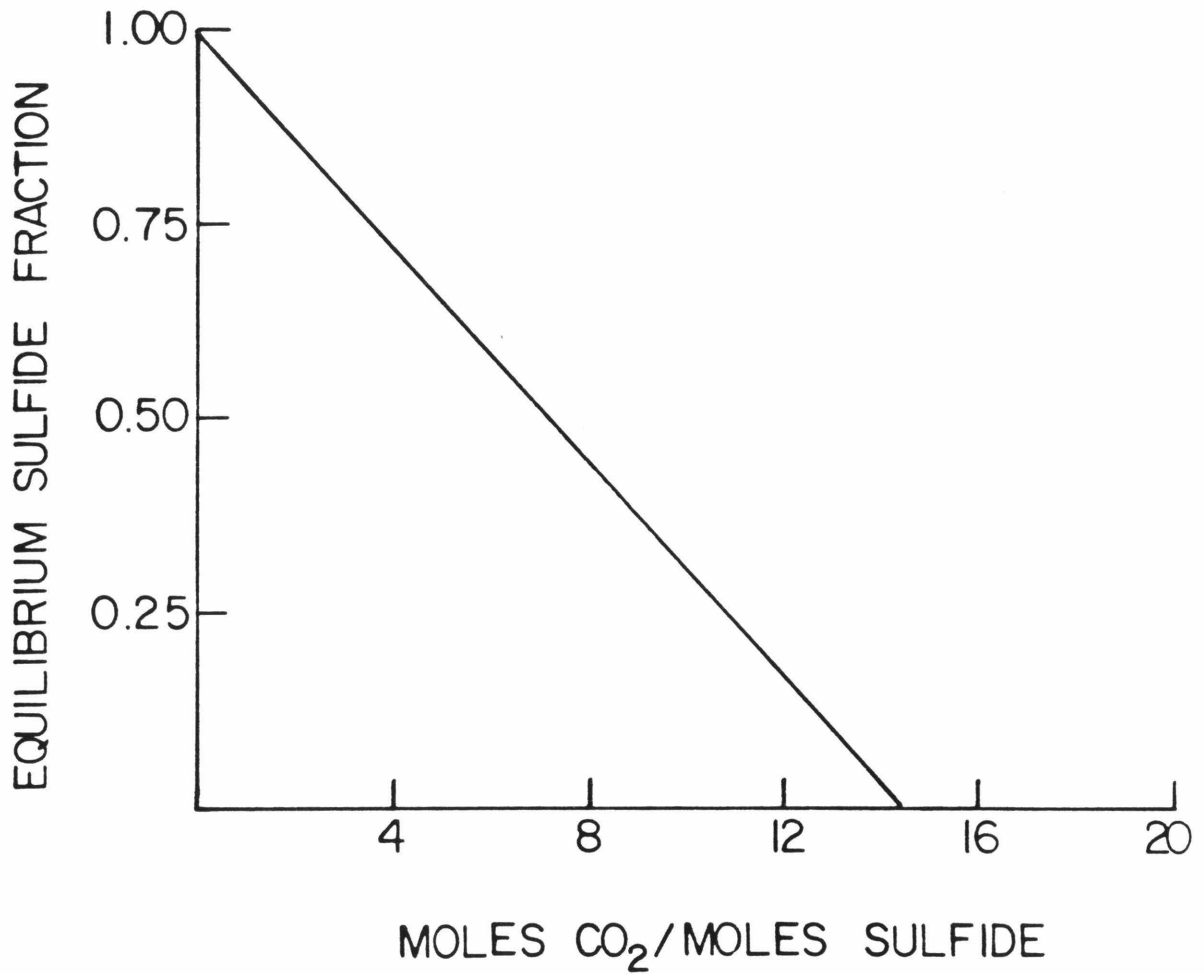


Figure 2.9: Equilibrium Sulfide Fraction for the Sodium Sulfide-Sodium Aluminate System as a Function of CO<sub>2</sub>/S Ratio ( T=1100 K)

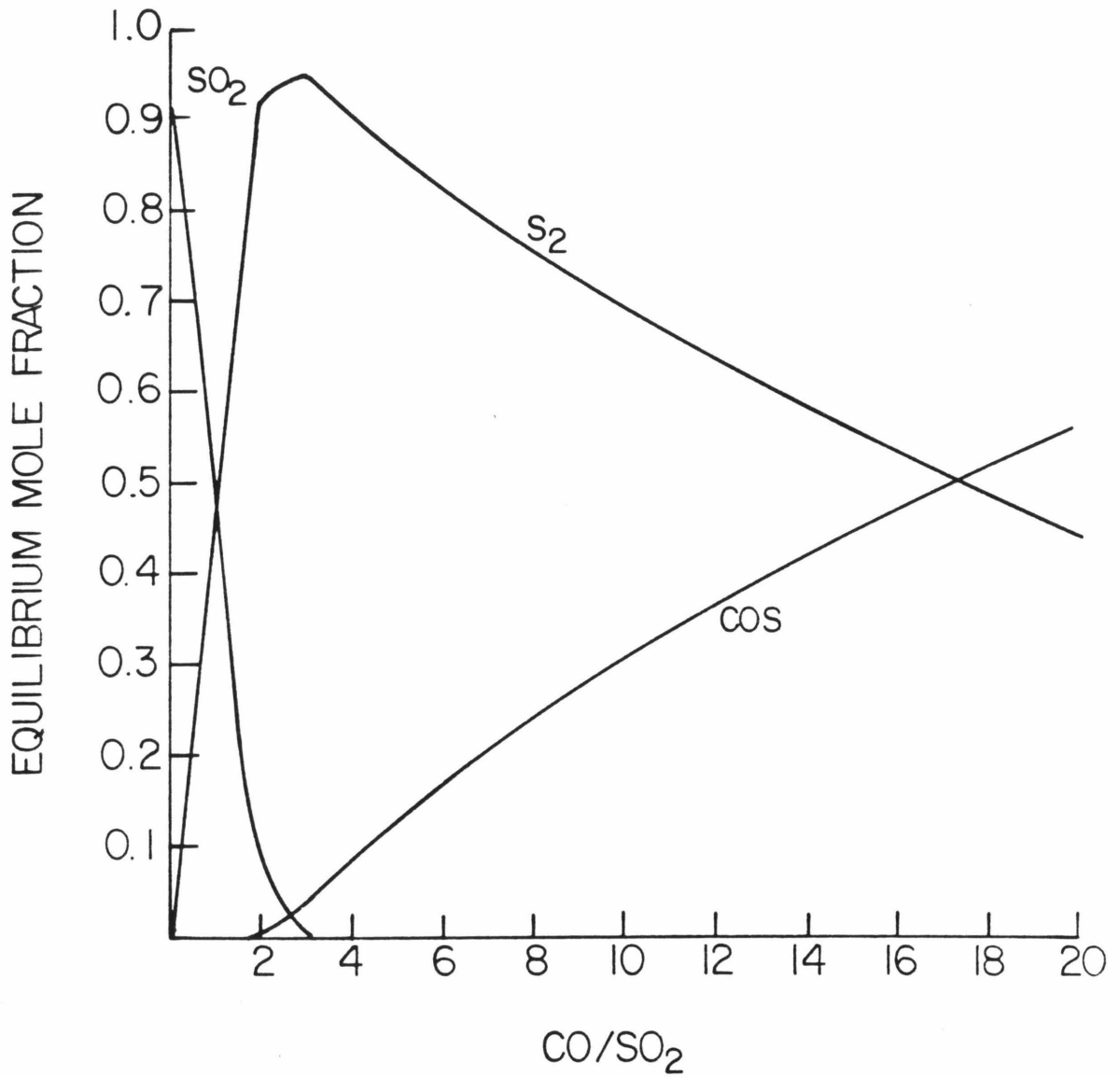


Figure 2.10: Equilibrium Composition in the SO<sub>2</sub>-COS-S<sub>2</sub> System as a Function of CO/SO<sub>2</sub> Ratio (1000 ppm total sulfur, 800 °C)

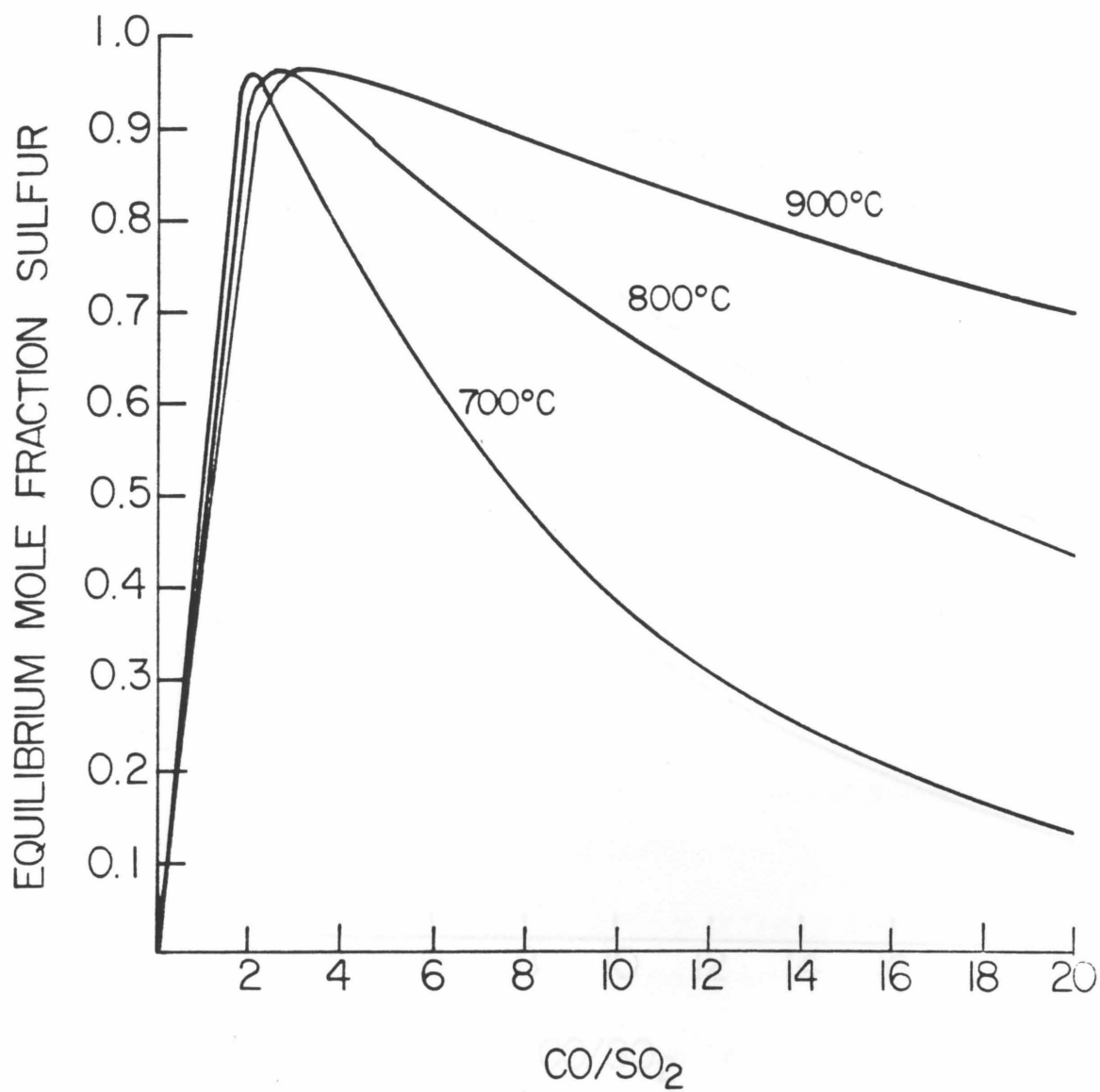


Figure 2.11: The Effect of Temperature on the SO<sub>2</sub>-CO-S<sub>2</sub> Equilibrium Composition (1000 ppm total sulfur)

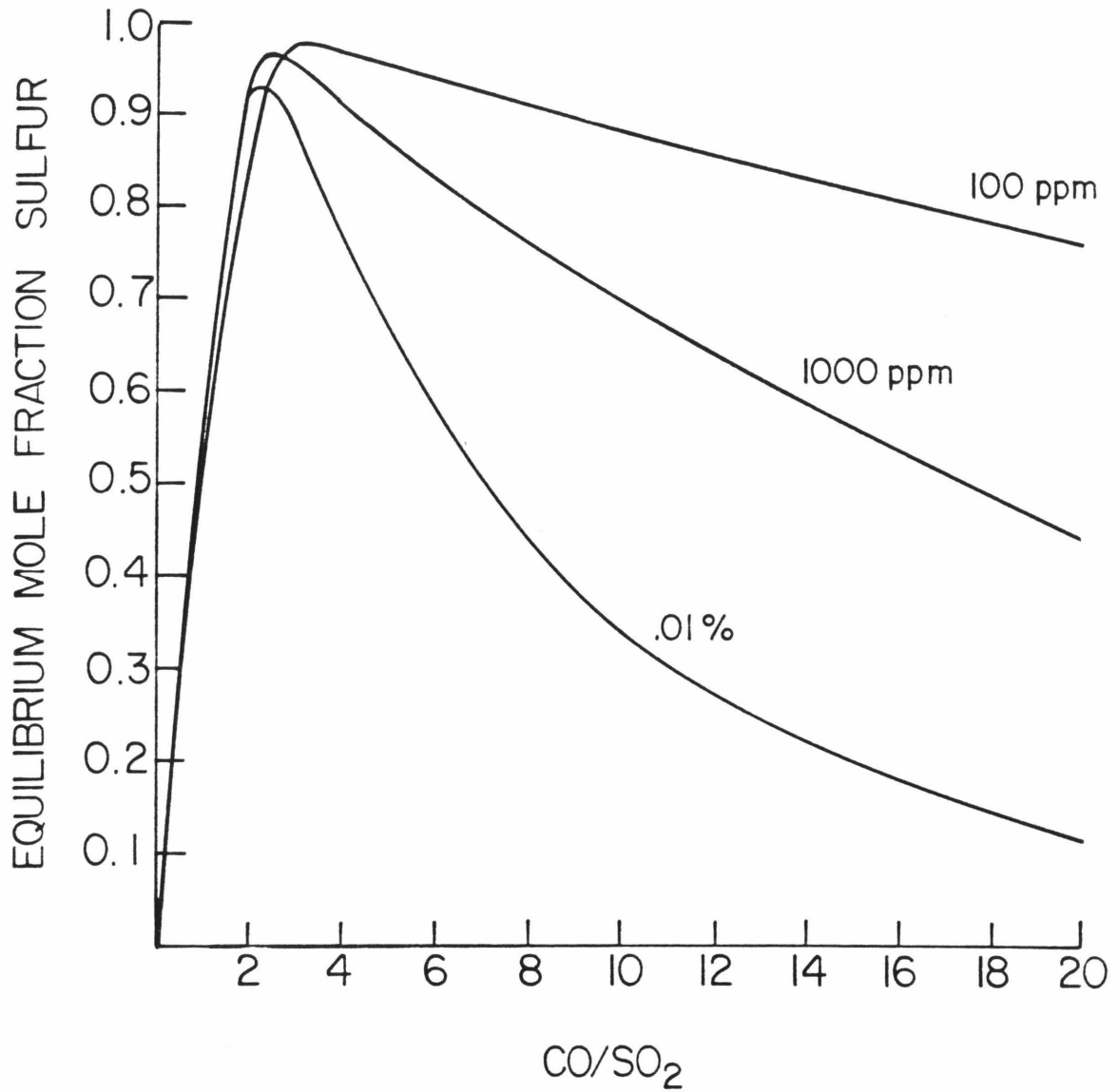


Figure 2.12: The Effect of N<sub>2</sub> Dilution on the SO<sub>2</sub>-COS-S<sub>2</sub> Equilibrium Composition (800 °C)  
(Concentration levels refer to total sulfur gas concentration)

**References**

1. Ahlgren, P., S. Lemmon and A. Leder, "Preparation of Sodium Polysulfides by Solid and Molten State Reactions," *Acta. Chem. Scand.*, **21**, 1119 (1967).
2. Akimoto, M., K. Yamagami and E. Echigoya, "A Mechanistic Study on Vapor-Phase Catalytic Oxidative Dehydrogenation of Ethylbenzene with Carbonyl Sulfide," *J. Catal.*, **86**, 205 (1984).
3. Barin, I. and O. Knacke, *Thermochemical Properties of Inorganic Substances*, Springer-Verlag, Berlin (1973).
4. Birk, J. R., C. M. Larsen, W. G. Vaux and R. D. Oldenkamp, "Hydrogen Reduction of Alkali Sulfate," *Ind. Eng. Chem., Process Des. Develop.*, **10**(1), 7 (1971).
5. Budnikov, P., "On the Reaction of the Reduction of Sodium Sulfate to Sodium Sulfide," *Comptes Rendus*, **1**, 334 (1934).
6. Burrows, B. W. and G. J. Hills, "Electrochemical Studies of Molten Alkali Sulfates," *Electrochemical Acta*, **15**, 445 (1970).
7. Cameron, J. H. and T. M. Grace, "Kinetic Study of Sulfate Reduction with Carbon," *Ind. Eng. Chem. Fund.*, **15**(4), 486 (1983).
8. Christie, J. R., A. J. Darnell and D. F. Dustin, "Reaction of Molten Carbonate with Aluminum Oxide," *J. Phys. Chem.*, **82**(1), 33 (1978).
9. Cobb, J. W., "The Synthesis of a Glaze, Glass or Other Complex Silicate," *J. Soc. Chem. Ind.*, **29**, 399 (1910).
10. Dearnaley, R. I., D. H. Kerridge and D. J. Rogers, "Molten Lithium Sulfate-Sodium Sulfate-Potassium Sulfate Eutectic: Reactions of Some Sulfur Compounds," *Inorg. Chem.*, **22**, 3242 (1983).

11. Dudzik, Z. and Z. M. George, "Electron Donor Properties of Claus Catalysts," *J. Catal.*, **63**, 72 (1980).
12. Ferm, R. J., "The Chemistry of Carbonyl Sulfide," *Chem. Rev.*, **57**, 621 (1957).
13. Foerster, V. F. and K. Kubel, "Über die Zersetzung der Schwefligsauren Salze in der Glühhitze," *Z. Anorg. Allge. Chem.*, **139**, 261 (1924).
14. George, Z. M., "Effect of Basicity of the Catalyst on Claus Reaction," *Adv. in Chemistry Ser.*, **139**, 75 (1975).
15. Haas, L. A. and S. E. Khalafalla, "Catalytic Thermal Decomposition of Carbonyl Sulfide and Its Reactions with Sulfur Dioxide," *J. Catal.*, **30**, 451 (1973).
16. *JANAF Thermochemical Tables*, 2nd ed., NSRDS-NS-37 (1971).
17. Janz, G. J., C. B. Allen, N. P. Bansal, R. M. Murphy and R. P. Tomkins, *Physical Properties Data Compilations Relevant to Energy Storage II: Molten Salts: Data on Single and Multi-Component Salt Systems*, U.S. NSRDS-NBS 61, Part II (1979).
18. Johnson, K. E. and H. A. Laitinen, "Electrochemistry and Reactions in Molten  $\text{Li}_2\text{SO}_4\text{-Na}_2\text{SO}_4\text{-K}_2\text{SO}_4$ ," *J. Electrochem. Soc.*, **110**(4), 314 (1963).
19. Khalafalla, S. E., E. F. Foerster and L. A. Haas, "Catalytic Reduction of Sulfur Dioxide on Iron-Alumina Bifunctional Catalysts," *Ind. Eng. Chem. Prod. Res. Develop.*, **10**(2), 133 (1971).
20. Khalafalla, S. E. and L. A. Haas, "Active Sites for Catalytic Reduction of  $\text{SO}_4$  with CO on Alumina," *J. Cat.*, **24**, 115 (1972).
21. Khalafalla, S. E. and L. A. Haas, "The Role of Metallic Component in the Iron-Alumina Bifunctional Catalyst for Reduction of  $\text{SO}_2$  with CO," *J.*

- Catal.*, **24**, 121 (1972).
22. Kohlmeyer, V. E. J. and G. Lohrke, "Über die Thermischen Verhältnisse im System Natrium-Schwefel-Sauerstoff," *Z. Anorg. Allge. Chem.*, **289**, 54 (1955).
23. Kovalenko, V. I. and H. G. Bukin, "Reaction of Sodium Carbonate with Different Forms of Aluminum Oxide," *Russ. J. Inorg. Chem.*, **23**(2), 158 (1978).
24. Lepsoe, R., "Chemistry of Sulfur Dioxide Reduction," *Ind. Eng. Chem.*, **32**(7), 910 (1940).
25. Letoffe, I. M., J. M. Blanchard and J. Bousquet, "Preparation et Etude du Comportement Thermique des Polysulfures de Lithium et de Sodium," *Bull. Soc. Chim. France*, **3**, 395 (1976).
26. Lui, C. H., "Electrode Potentials in Molten Lithium Sulfate-Potassium Sulfate Eutectic," *J. Am. Chem. Soc.*, **66**, 164 (1962).
27. Manring, W. H., D. D. Billings, A. R. Conroy and W. C. Bauer, "Reduced Sulfur Compounds as Melting and Refining Aids for Flint Soda-Lime Glasses," *The Glass Ind.*, **48**(7), 374 (1967).
28. Oei, D., "The Sodium-Sulfur System. II. Polysulfides of Sodium," *Inorg. Chem.*, **12**(2), 438 (1973).
29. Oldenkamp, R. D. and E. D. Margolin, "The Molten Carbonate Process for Sulfur Oxide Emissions," *Chem. Eng. Prog.*, **65**(11), 73 (1969).
30. Pearson, M. J., "Developments in Claus Catalysts," *Hydrocarbon Processing*, 81 (1973).
31. Querido, R. and W. L. Short, "Removal of Sulfur Dioxide from Stack Gases by Catalytic Reduction to Elemental Sulfur with Carbon Monoxide," *Ind.*

- Eng. Chem. Proc. Des. Develop.*, **12**(1), 10 (1973).
32. Schlesinger, M. D. and E. G. Illig, "The Regeneration of Alkalized Alumina,"  
*Chem. Eng. Prog. Symposium Series*, **67**(115), 46 (1971).
33. Vogel, R. F., B. R. Mitchell and F. E. Massoth, "Reactivity of SO<sub>2</sub> with Supported Metal Oxide-Alumina Sorbents," *Env. Sci. Tech.*, **8**(5), 432 (1974).

CHAPTER 3

SORBENT MATERIALS

### 3.1. Physical Structure of Sorbents

Supported alkali sulfates were chosen for investigation of the regeneration of SO<sub>2</sub> sorbents. These materials were constructed in a manner similar to that of a typical supported catalyst. They consisted of a layer of alkali sulfate deposited on the pore surface of a support.

Sorbents were prepared with different alkali sulfates, and with different supports. Depending on the alkali sulfate used, the reaction conditions and the extent of reaction, the supported material may be a solid, a melt or a mixture of a solid and a melt. The sulfates chosen were sodium sulfate, lithium sulfate and a 40/60 mixture of lithium and sodium sulfates. Several commercial catalyst supports, with varying surface areas, were used as sorbent supports (Table 3.1).

#### 3.1.1. Phase Behavior of Alkali Sulfates and Their Reduction Products

The three sulfates chosen for study differ in their phase behavior at reaction temperatures of 700-800°C. Sodium sulfate and lithium sulfate, when alone, are solid until 884°C and 845°C, respectively. The 40/60 mixture of lithium and sodium sulfate melts at 630°C. The physical behavior of the sulfates is complicated by the formation of eutectic melts with their reduction products, sulfide and oxide (Kohlmeyer and Lohrke, 1955). The eutectic points of mixtures of alkali sulfates and their reduction products are shown in Table 3.2. Examination of the eutectic behavior shows that the supported material of the sodium or lithium sorbent, although initially solid, may melt completely or partially during reduction. The sodium lithium is initially molten and should remain molten throughout reduction.

The fate of oxide during reduction influences the physical behavior of the sorbents. If oxide reacts with carbon dioxide and forms carbonate, melt

Table 3.1: Supports Used in Sorbent Preparation

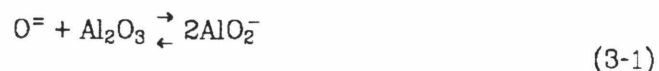
<u>Support</u>	<u>Supplier</u>	<u>Surface Area (m<sup>2</sup>/g)</u>
$\alpha$ -Al <sub>2</sub> O <sub>3</sub>	Harshaw (A1-3980)	4
$\gamma$ -Al <sub>2</sub> O <sub>3</sub>	United Catalysts (T-2432)	89
ZrO <sub>2</sub>	Alfa (#11852)	20
SiO <sub>2</sub>	Davison (#646)	288

Table 3.2: Eutectic Points of Mixtures of Alkali Sulfates and Their Reduction Products\*

	<u>Molar Composition</u>	<u>Eutectic Temperature</u>
Mixed Alkali Systems	.60 Na <sub>2</sub> SO <sub>4</sub> , .40 Li <sub>2</sub> SO <sub>4</sub>	630°C
	.76 Na <sub>2</sub> O, .24 Li <sub>2</sub> O	770°C
	.58 Na <sub>2</sub> CO <sub>3</sub> , .42 Li <sub>2</sub> CO <sub>3</sub>	510°C
Sodium Sulfate and Its Reduction Products	.72 Na <sub>2</sub> SO <sub>4</sub> , .28 Na <sub>2</sub> S	740°C
	.15 Na <sub>2</sub> SO <sub>4</sub> , .85 Na <sub>2</sub> O	550°C
	.28 Na <sub>2</sub> SO <sub>4</sub> , .17 Na <sub>2</sub> S, .55 Na <sub>2</sub> O	620°C
	.40 Na <sub>2</sub> S, .60 Na <sub>2</sub> O	682°C
	.38 Na <sub>2</sub> S, .62 Na <sub>2</sub> CO <sub>3</sub>	756°C
Lithium Sulfate and Its Reduction Products	.39 Li <sub>2</sub> SO <sub>4</sub> , .61 Li <sub>2</sub> CO <sub>3</sub>	520°C

\*Data from Papin, 1973; Kohlmeyer and Lohrke, 1955; Levin et al., 1964; Tammann and Oelson, 1930.

formation would be facilitated, as carbonate forms eutectic melts with sulfates and sulfides. On the other hand, if oxide reacts with the support material, as in the alumina/aluminate reaction



it will form a material which does not participate in the eutectic melt behavior. This reaction, therefore, would effectively remove oxide from the melt behavior, leaving only the sulfate and sulfide. If polysulfides are formed during reduction, melting should be facilitated as these compounds form eutectics with sulfide (Janz et al., 1979).

### 3.2. Sorbent Preparation

The sorbents were all prepared in their sulfated form from the alkali sulfate and the required support material. Two impregnation techniques were used, excess solution and incipient wetness; a brief description of each of these techniques follows.

#### 3.2.1. Excess Solution Impregnation

Support particles which had been ground to -30+60 mesh were stirred gently in a solution of alkali sulfate. The volume of solution used was greatly in excess of that needed to fill the pore volume of the particles. The particles were then filtered from the solution, and dried. After drying, the particles were rinsed with distilled water to remove sulfate on the exterior surface of the support, which might have caused the particles to stick together or caused corrosion of the reaction vessel in later experiments. The amount of sulfate in the final material was calculated by the following equation, based on complete pore filling and no outside layer formation.

$$\frac{\text{moles SO}_4^-}{\text{g sorbent}} = \frac{(\text{conc of solution})(\text{pore volume of support})}{1 + (\text{mol wt of sulfate})(\text{conc solution})(\text{pore vol})} \quad (3-2)$$

The total loading of sulfate is limited by the solubility of the sulfate, and the pore volume of the support.

### 3.2.2. Incipient Wetness Impregnation

The impregnation was again conducted on -30+60 particles of support. A solution of sulfate was dripped on support particles with intermittent shaking. The amount of solution added was just enough to fill the pores of the support. This amount was determined by observing the onset of "clumping" of the particles. The particles were then dried. The pore-filling and drying were then repeated until the desired sulfate level was reached. A final addition of distilled water was used to wash any sulfate which may have been on the exterior of the particles into the interior pore volume. The sulfate addition was monitored by weighing the particles before impregnation, and after each drying. The incipient wetness technique has the advantage that sorbent loading is not limited by sulfate solubility, as the impregnation/drying process can be repeated an indefinite number of times.

## 3.3. Sorbent Analysis

### 3.3.1. Sulfate Loading

Some of the sorbent materials were analyzed for sulfate content using a barium sulfate precipitation method (Skoog and West, 1976). All sorbent materials were analyzed for sodium and lithium by atomic absorption spectroscopy. Table 3.3 compares the results of these analyses to the sulfate loadings measured by the change of weight from impregnation. Good agreement between the analyses and the loadings measured weighing during impregnation was achieved with sorbents impregnated on  $\alpha$ -alumina.

Table 3.3: Analysis of Prepared Sorbents

Sorbent	Composition	Method Impregnation	Sulfate Loading by Weight During Impregnation	AA Analysis		BaSO <sub>4</sub> Precipitation
			$\left(\frac{\text{m mol SO}_4^{=}}{\text{g}}\right)$	$\left(\frac{\text{m mol M}^+}{\text{g}}\right)$		$\left(\frac{\text{m mol SO}_4^{=}}{\text{g}}\right)$
				Na	Li	
Nα1	Na <sub>2</sub> SO <sub>4</sub> /α-Al <sub>2</sub> O <sub>3</sub>	Excess Solution*		1.18	0	.51
Nα2	Na <sub>2</sub> SO <sub>4</sub> /α-Al <sub>2</sub> O <sub>3</sub>	Excess Solution*		2.38	0	1.61
Nα3	Na <sub>2</sub> SO <sub>4</sub> /α-Al <sub>2</sub> O <sub>3</sub>	Incipient Wetness	.64	1.37	0	-
Nα4	Na <sub>2</sub> SO <sub>4</sub> /α-Al <sub>2</sub> O <sub>3</sub>	Incipient Wetness	.22		0	-
Nγ	Na <sub>2</sub> SO <sub>4</sub> /γ-Al <sub>2</sub> O <sub>3</sub>	Incipient Wetness	1.37	3.31	0	-
NLα	NaLiSO <sub>4</sub> /α-Al <sub>2</sub> O <sub>3</sub>	Incipient Wetness	.83	1.04	.68	.86
NLY	NaLiSO <sub>4</sub> /γ-Al <sub>2</sub> O <sub>3</sub>	Incipient Wetness	.73	1.00	.66	-
NLZ	NaLiSO <sub>4</sub> /ZrO <sub>2</sub>	Incipient Wetness	.73	1.05	.72	-
NLS	NaLiSO <sub>4</sub> /SiO <sub>2</sub>	Incipient Wetness	.78	1.45	.91	-
Lα	Li <sub>2</sub> SO <sub>4</sub> /α-Al <sub>2</sub> O <sub>3</sub>	Incipient Wetness	.74	0	1.49	-

\*Excess solution samples were prepared to have  $.73 \left(\frac{\text{m mol SO}_4^{=}}{\text{g}}\right)$ , as calculated by Eqn. 3-2.

Analysis of sorbents impregnated on  $\gamma\text{-Al}_2\text{O}_3$  showed higher loadings than those expected from the weight change during impregnation. Water initially adsorbed on the support may have been lost during the drying step of the impregnation. This would have decreased the observed impregnation weight gain and, therefore, caused the sulfate loading to be underestimated.

Sorbents made using excess solution impregnation were expected to have a sulfate loading of .73 mmol/g, as calculated by Eq. (3-2). Analysis of these samples showed considerable sample variability, and poor predictability of sulfate loading.

### 3.3.2. Surface Area

The surface areas of the sorbents were measured using a B-E-T apparatus. Surface areas of the supports did not exhibit any appreciable change upon impregnation, except for that of the  $\text{NaLiSO}_4/\text{ZrO}_2$  sorbent which showed a slight decrease (Table 3.4).

Table 3.4: Surface Area of Sorbents

<u>Sorbent</u>	<u>Surface Area (m<sup>2</sup>/g)</u>	<u>Surface Area of Support (m<sup>2</sup>/g)</u>
Na <sub>2</sub> SO <sub>4</sub> /α+Al <sub>2</sub> O <sub>3</sub> *	5.0	4.1
NaLiSO <sub>4</sub> /α-Al <sub>2</sub> O <sub>3</sub> **	3.4	4.1
NaLiSO <sub>4</sub> /γ-Al <sub>2</sub> O <sub>3</sub> **	90.3	89.4
NaLiSO <sub>4</sub> /ZrO <sub>2</sub> **	15.8	20.0

\* Prepared by excess solution impregnation

\*\* Prepared by incipient wetness impregnation

**References**

1. Janz, G. J., C. B. Allen, N. P. Bansal, R. M. Murphy and R. P. Tomkins, *Physical Properties Data Compilations Relevant to Energy Storage II: Molten Salts: Data On Single and Multi-Component Salt Systems*, U.S. NSRDS-NBS 61, Part II (1979).
2. Kohlemeyer, V. E. J. and B. Lohrke, "Über die Thermischen Verhältnisse in System Natrium-Schwefel-Sauerstoff," *Z. Anorg. Chem.*, **281**, 54 (1955).
3. Levin, E. M., C. R. Robbins and H. F. McMurdie, *Phase Diagrams for Ceramists*, The American Ceramic Society, Columbus, OH (1964).
4. Papin, G., "Le Systeme Binare Oxyde de Sodium-Oxyde de Lithium," *C. R. Acad. Sc. Paris, Series C*, **277**, 497 (1973).
5. Skoog, D. A. and D. M. West, *Fundamentals of Analytical Chemistry*, Holt, Rinehart, and Winston, New York (1976).
6. Tammann, Von G., and W. Oelson, "Die Reaktionen beim Zusammenschmelzen von Glassätzen," *Z. Anorg. Allg. Chim.* **193**, 245 (1930).

CHAPTER 4

THERMOGRAVIMETRIC ANALYSIS OF THE SUPPORTED SULFATE REDUCTION BY CO

#### 4.1. Introduction

Thermogravimetric analysis is a common technique for studying decomposition, and other reactions which involve weight loss. Most common procedures involve heating at a constant rate and, therefore, follow the reaction as a function of temperature. In our experiments the gravimetric analysis of the reduction of sulfated sorbents was carried out under isothermal conditions, so the reactions were followed as a function of time.

#### 4.2 Experimental System

The thermogravimetric system shown in Fig. 4.1 consists of a du Pont 951 thermogravimetric analyzer and a Varian series 3700 gas chromatograph equipped with a flame photometric detector, which is specific for sulfur compounds. A sample of 30 to 50 milligrams of sorbent was used for each experiment. Gaseous reactants were introduced through a side arm directly into the TGA reaction chamber. A switching valve enabled switching between inert, reducing and sulfating gases. A nitrogen diluent flowed through the bulb housing the balance mechanism of the thermogravimetric analyzer at all times. This diluent stream insured that no corrosive gases would contact the balance mechanism. The flow rates of the reactant gas and the N<sub>2</sub> diluent were measured using calibrated gas flow meters.

Because of the small sample size, the amount of elemental sulfur produced was too small to be measured directly. Any sulfur that was formed, however, was trapped by glass wool in the exit line of the thermogravimetric analyzer to prevent it from depositing in the sample valve of the gas chromatograph. During reduction, the concentration of SO<sub>2</sub> and COS were measured by the gas chromatograph. The two compounds were separated isothermally at 60°C using a Supelco 6 ft. x 1/8 in. Chromosil 310 column with a carrier

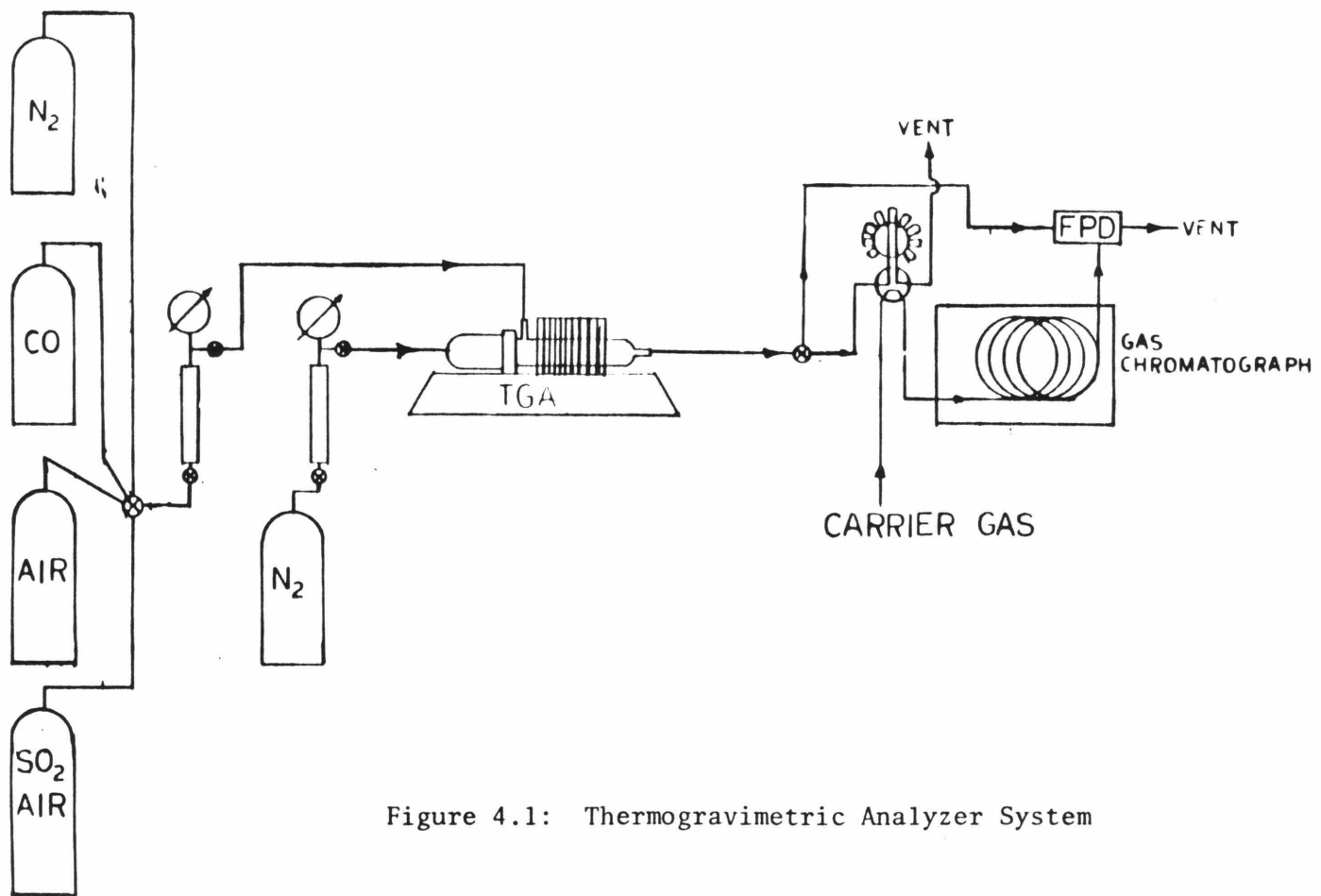


Figure 4.1: Thermogravimetric Analyzer System

gas (He) flow rate of 30 ml/min. Under these conditions the analysis of each sample required approximately four minutes. At the beginning of the reduction period, the gas concentrations in the product gas were found to change rapidly within the four-minute time span of a gas chromatogram. Therefore, a multiport valve which allowed the collection of up to nine samples was installed. At the beginning of the reduction period, samples were collected every 15 to 30 seconds, using this multiport valve. During the remainder of the period, samples were injected on-line. The collected samples were analyzed at the conclusion of the reduction period.

The response of the flame photometric detector is not linear, although it is very sensitive to any sulfur species. Calibrations over a wide range of concentrations were necessary. This was accomplished by using a stirred vessel of known volume. The vessel was initially filled with a known concentration of SO<sub>2</sub> or COS. N<sub>2</sub> was then passed through the vessel at a known flow rate. Samples from the exit stream were injected into the gas chromatograph. The calibration of the gas chromatograph was checked using gas mixtures of known concentration. The volumes of each of the ten sample loops on the multiport valve were calibrated for size using a known standard gas mixture, 197.9 ppm SO<sub>2</sub> in N<sub>2</sub>.

### **4.3. Experimental Conditions and Procedures**

#### **4.3.1. Gravimetric Analysis**

Gravimetric experiments were conducted at 700 and 800°C, and at atmospheric pressure. Samples were heated to the desired temperature in N<sub>2</sub> to prevent reaction during the heat-up period. Weight loss during the heating in inert was monitored to observe any sulfate decomposition.

The flows of the reducing gas and the N<sub>2</sub> diluent stream were adjusted to obtain a reducing atmosphere which consisted of 10% CO and .5% CO<sub>2</sub> in nitrogen. The CO<sub>2</sub> was added to prevent carbon deposition by means of the reaction



The reduction was monitored by the weight loss using the TGA, and on-line gas chromatograms.

Reduction was studied using both fresh sorbents and sorbents previously reduced and resulfated. Resulfation was accomplished by exposing the reduced sorbent to 1% SO<sub>2</sub> in air at 800°C.

#### 4.3.2. Measurement of Sorbent Composition

The sulfated sorbent when reduced undergoes a complicated series of reactions which produce both sulfide and oxide, present as aluminate or carbonate. To measure the removal of sulfur and oxygen from the sorbent independently, a second measurement other than weight loss is needed. In our experiments, the sulfur and oxygen contents at the end of a reduction period were determined by measuring the weight gain when the reduced sorbent was exposed to oxygen (Fig. 4.2). All oxygen deficient species present after reduction were thus oxidized to sulfate. The sorbent may then be fully regenerated by exposure to SO<sub>2</sub> and air, and another experiment with the same or with a different reduction interval performed. Results presented in terms of fractions of sulfur and oxygen remaining in the sorbent depend on knowing the initial sulfate loading of the sample. Errors in the measurement of this loading will effect the absolute values but not the relative values of sulfur and oxygen loss.

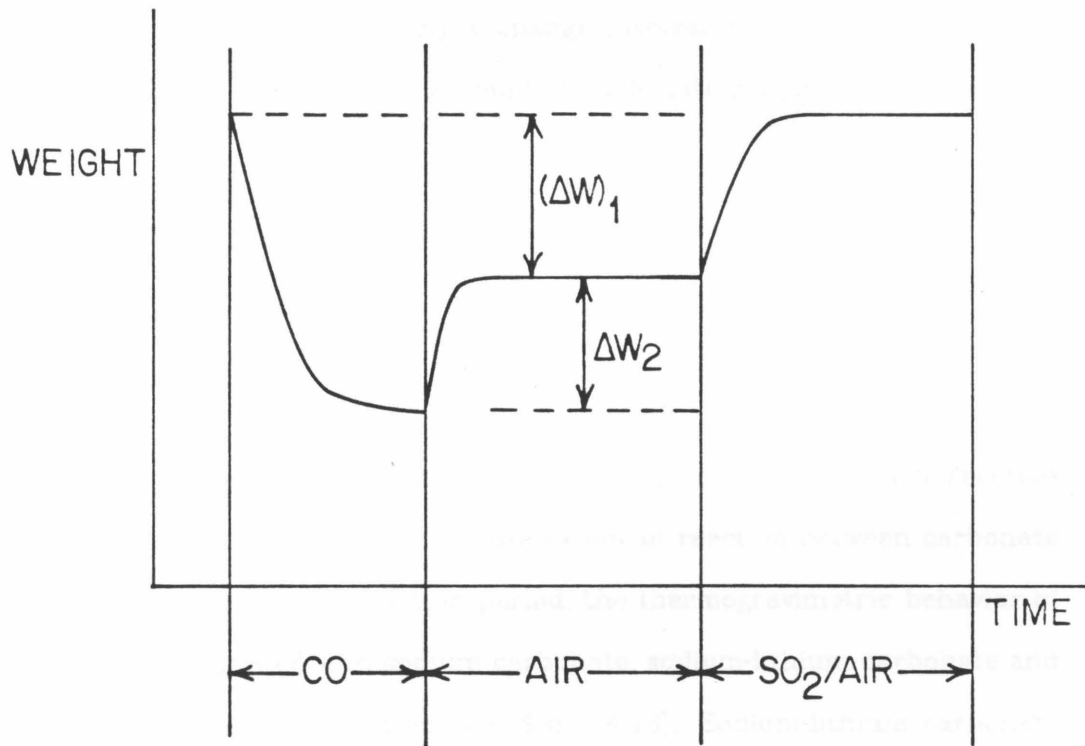


Figure 4.2: Experiments to Determine Sorbent Composition

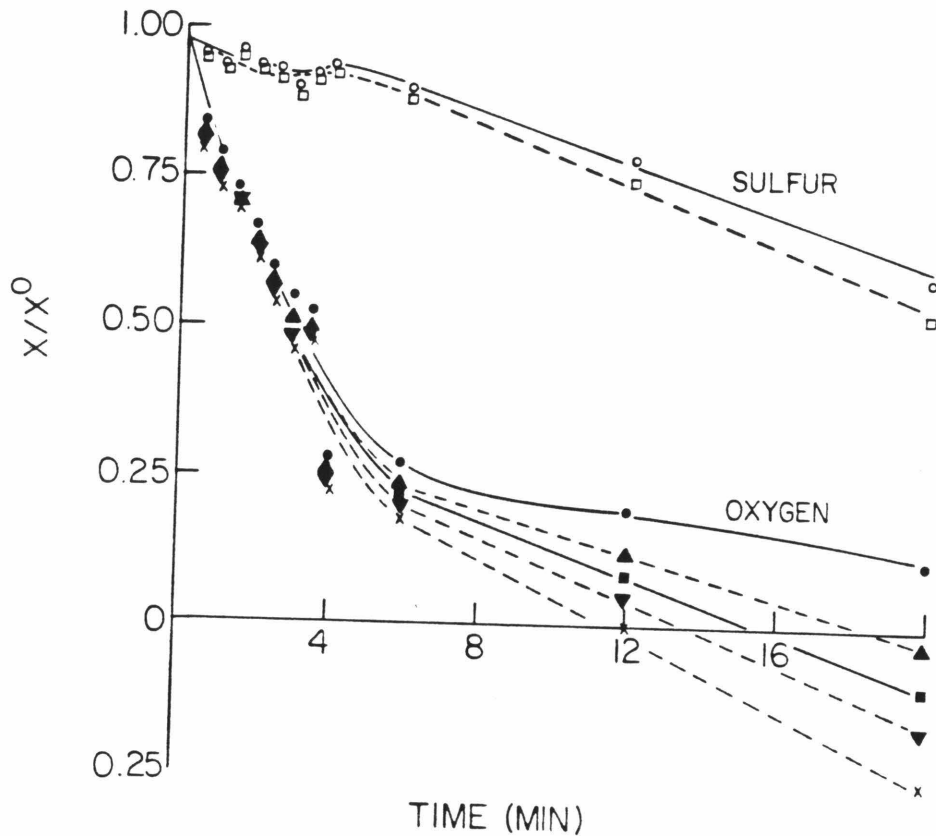
Analysis of the results from these experiments requires assumptions about the nature of the compounds not containing sulfur. Oxide is unstable in the presence of either alumina or carbon dioxide; therefore, during reduction it is converted either to aluminate or to carbonate. For the analysis of total oxygen and sulfur, it is unnecessary to distinguish between oxide and aluminate, as there is no weight change involved in aluminate formation from oxide and alumina. The amount of carbonate present must be known, however.

The fraction of sulfur and oxygen remaining after a period of reduction can be calculated assuming a value for the ratio of carbonate to aluminate. The amount of carbonate and aluminate present depends on the extent and rate of reaction between carbonate and alumina to form aluminate. Equilibrium calculations predict complete conversion to aluminate under reaction conditions (Fig. 2.4). To estimate the extent of reaction between carbonate and alumina during the reaction period, the thermogravimetric behavior of alumina impregnated with sodium carbonate, sodium-lithium carbonate and lithium carbonate was studied (see Sec. 4.4.1d). Sodium-lithium carbonate and lithium carbonate were completely converted at 700°C. Sodium lithium carbonate and lithium carbonate reacted with alumina to form aluminate at a rate comparable to the rate at which carbonate would be formed during reduction.

Sodium carbonate begins reaction with alumina between 650 and 700°C. Although the reaction rate of the sodium material was slower than that of its sodium-lithium counterpart, it was significant at temperatures at or above 700°C. Christie et al. (1978) studied the reaction of sodium carbonate and alumina at temperatures of 900°C and above. Their results indicate that the rate of reaction is dependent on diffusion through an aluminate layer which

increases in size with the extent of reaction. The differences in the rates of reaction of sodium and the sodium lithium carbonates is most likely due to differences in the diffusivity of the cation and the anions through the different aluminates formed during reaction.

As the sodium lithium carbonate was found to react with alumina to form aluminate at a rate comparable to the rate at which any carbonate would be formed, at both 700 and 800°C, sorbent materials containing lithium were analyzed assuming complete conversion to aluminate. When a sorbent material contained only sodium, the carbonate might not have been converted completely to aluminate by the end of the reduction period, but any carbonate present after the reduction period should have been converted during exposure to oxygen. The results of the sodium sorbent reduction experiments at 800°C were analyzed using several different assumptions about the carbonate content during reduction: no carbonate was present at the end of the reduction period, no carbonate was present at the end of the oxidation period but 50% of the aluminate was formed during this period, no carbonate was present at the end of the oxidation period but all of the aluminate was formed during this period, 25% carbonate was present at the end of the oxidation period but 50% of the aluminate present was formed during this period, and 25% carbonate was present at the end of the oxidation period but all the aluminate was formed during this period (Fig. 4.3). The observed sulfur content is only affected by the assumptions of carbonate contents at the end of the oxidation period. The observed oxygen content at short reduction times is only slightly affected by varying the assumptions. At longer times, however, the assumption made is much more crucial. The assumption of carbonate presence at these late times will produce negative mole fractions from the calculations, indicating that no carbonate is



○ no carbonate at the end of oxidation } sulfur  
 ◻ 25% carbonate at the end of oxidation }

● no carbonate at the end of reduction  
 ▲ no carbonate at the end of oxidation, 50% of aluminate formed during oxidation  
 ▼ no carbonate at the end of oxidation, all of aluminate formed during oxidation  
 ■ 25% carbonate at the end of oxidation, 50% of aluminate formed during oxidation  
 x 25% carbonate at the end of oxidation, all aluminate formed during oxidation } oxygen

Figure 4.3: Variation Due to Carbonate/Aluminate Ratio in Calculated Sorbent Composition of  $\text{Na}_2\text{SO}_4/\alpha\text{-Al}_2\text{O}_3$  Sorbents Reduced at  $800^\circ\text{C}$  (Sorbent No1)

present. Thus, in comparing the sodium sorbent's reduction at 800°C to that of the sodium-lithium it is best to use the assumption that all carbonate decomposes during the reduction period. When the sodium sorbent was reduced at 700°C, significant amounts of carbonate may be present at the end of the reduction period, or at the end of the period of air exposure. Sulfur and oxygen content was calculated assuming the same assumptions as in the 800°C case (Fig. 4.4).

The measurement of sorbent composition provides the amount of sulfur, in any form, removed from the sorbent during reduction. Comparison of the total sulfur removed with the total amounts of SO<sub>2</sub> and COS produced, found by integration of gas sampling data, yields the amount of elemental sulfur produced during a reduction period.

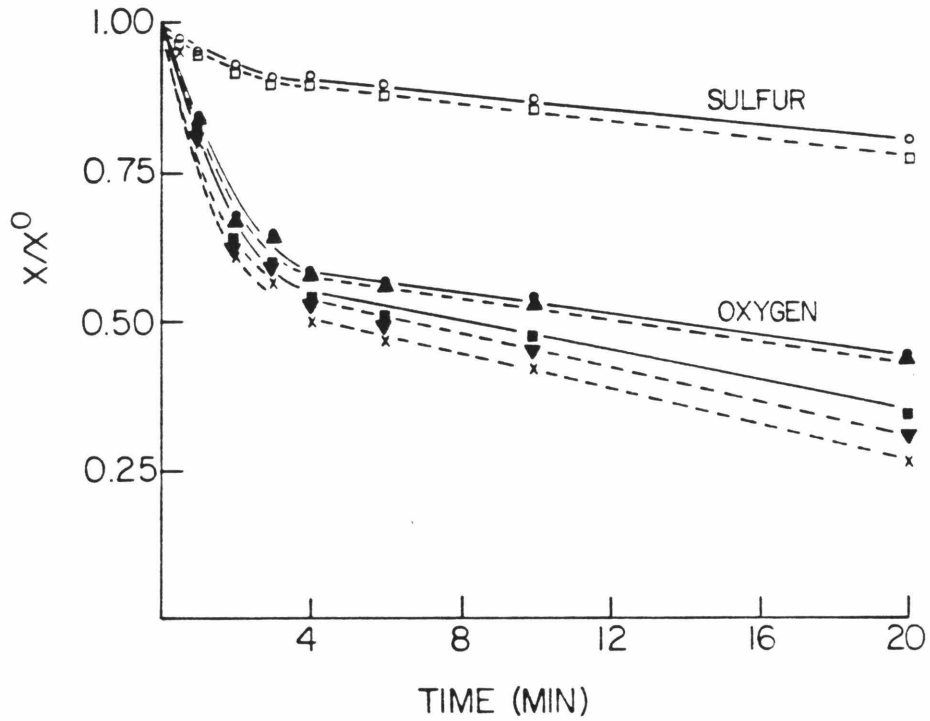
#### **4.4 Results**

##### **4.4.1. Gravimetric Results**

Sorbents which varied in both their alkali oxide components and their support were examined for their general reduction behavior at 700 and 800°C. The sorbents included Na<sub>2</sub>SO<sub>4</sub>, NaLiSO<sub>4</sub> and Li<sub>2</sub>SO<sub>4</sub> impregnated on α-alumina, and Na<sub>2</sub>SO<sub>4</sub> and NaLiSO<sub>4</sub> impregnated on γ-alumina. Measurements for sulfur and oxygen content were made for each sorbent after 20 minutes of reduction.

##### **4.4.1a. Sulfate Decomposition in N<sub>2</sub>**

The sorbents with α-alumina as a support exhibited only negligible weight loss during the heat-up period, while the sorbents with γ-alumina as a support exhibited significant decomposition. In each case, decomposition became evident at 450°C and continued with further heating. The rate of



○ no carbonate at the end of oxidation } sulfur  
 ◻ 25% carbonate at the end of oxidation }

● no carbonate at the end of reduction  
 ▲ no carbonate at the end of oxidation, 50% of aluminate formed during oxidation  
 ▼ no carbonate at the end of oxidation, all of aluminate formed during oxidation  
 ■ 25% carbonate at the end of oxidation, 50% of aluminate formed during oxidation  
 x 25% carbonate at the end of oxidation, all aluminate formed during oxidation } oxygen

Figure 4.4: Variation Due to Carbonate/Aluminate Ratio in Calculated Sorbent Composition of  $\text{Na}_2\text{SO}_4/\alpha\text{-Al}_2\text{O}_3$  Sorbents Reduced at  $700^\circ\text{C}$  (Sorbent Nα1)

decomposition greatly decreased before complete decomposition of the sulfate was achieved. The sodium-lithium sulfate continued weight loss at a higher rate than the sodium sulfate at 800°C (Fig. 4.5). This decomposition was irreversible; that is, sulfation after reduction renewed only the sulfate lost during reduction, but not that lost during N<sub>2</sub> heating prior to reduction.

#### 4.4.1.b. Reduction

The results of the reduction of each sorbent are shown in Figs. 4.6 through 4.11. In each case the weight loss is adjusted for the amounts of sodium, lithium and alumina present in the sorbents, and represents weight loss per initial weight of sulfate. The results for the  $\gamma$ -alumina sorbents is reported in terms of the sulfate present at the onset of reduction, not including the sulfate which had decomposed during the N<sub>2</sub> heat-up period. The COS and SO<sub>2</sub> production is shown in terms of moles of product gas per mole of initial sulfate per minute. Errors in the measurement of the sulfate loadings of the sorbents will therefore affect the absolute amounts of the products, but will not affect their relative amounts.

An increase in rate of weight loss with increasing temperature is seen with all the sorbents tested. The sorbents exhibited a period of slow weight loss prior to the onset of major weight loss. This initial period was most prevalent in the  $\alpha$ -alumina sorbents when lithium was present. The use of  $\gamma$ -alumina as a support shortened this initial period. This effect was more marked with sodium lithium sulfate than with sodium sulfate. The length of this initial period was significantly longer at 700°C than at 800°C. When the reduction at 700°C is carried out on a sorbent which has been reduced previously and resulfated, the temperature at which the sulfation was performed affects the length of the initial period. The sodium lithium  $\alpha$ -alumina sor-

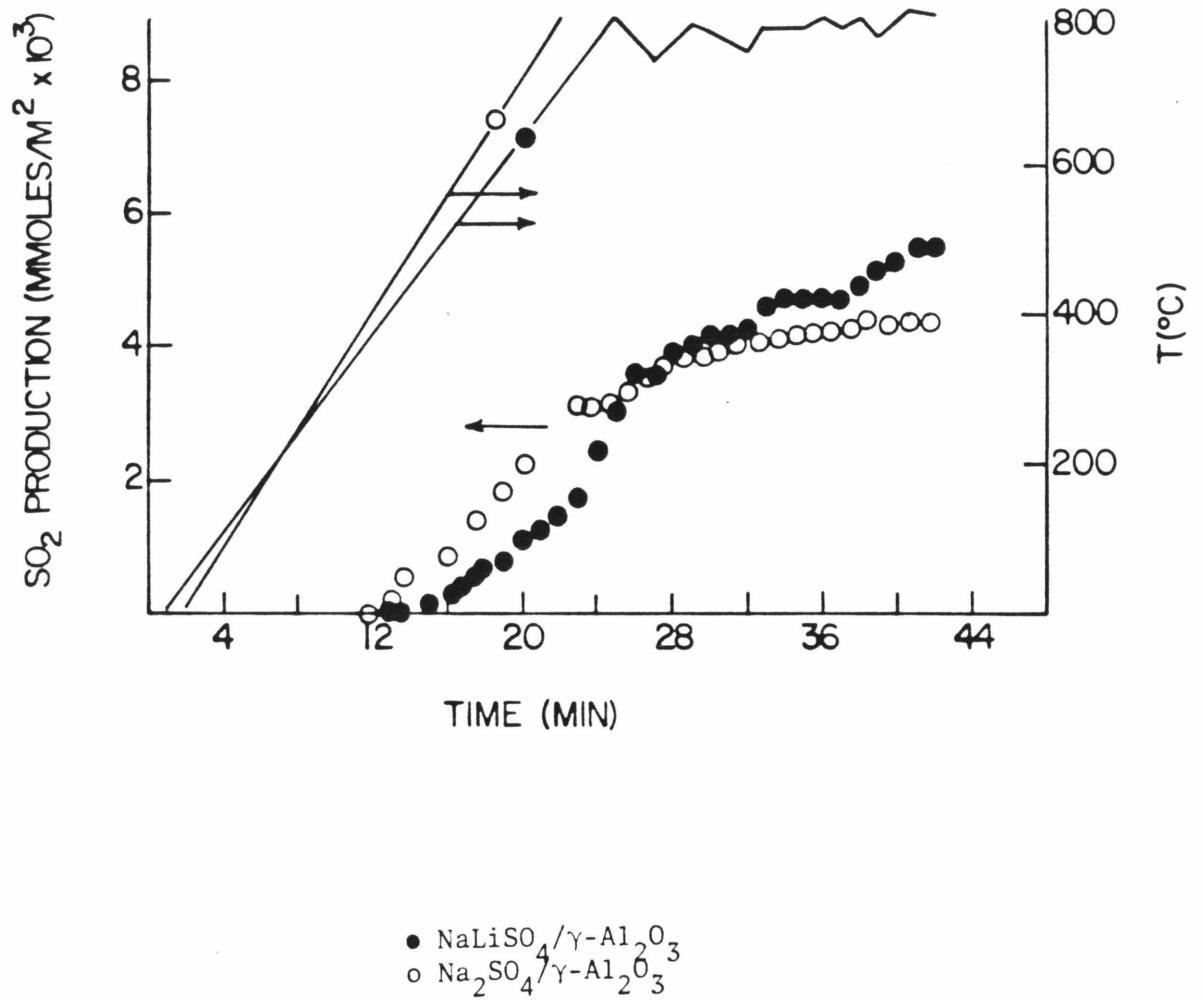


Figure 4.5: Sulfate Decomposition of  $\gamma$ -Al<sub>2</sub>O<sub>3</sub> Sorbents During Nitrogen Heating

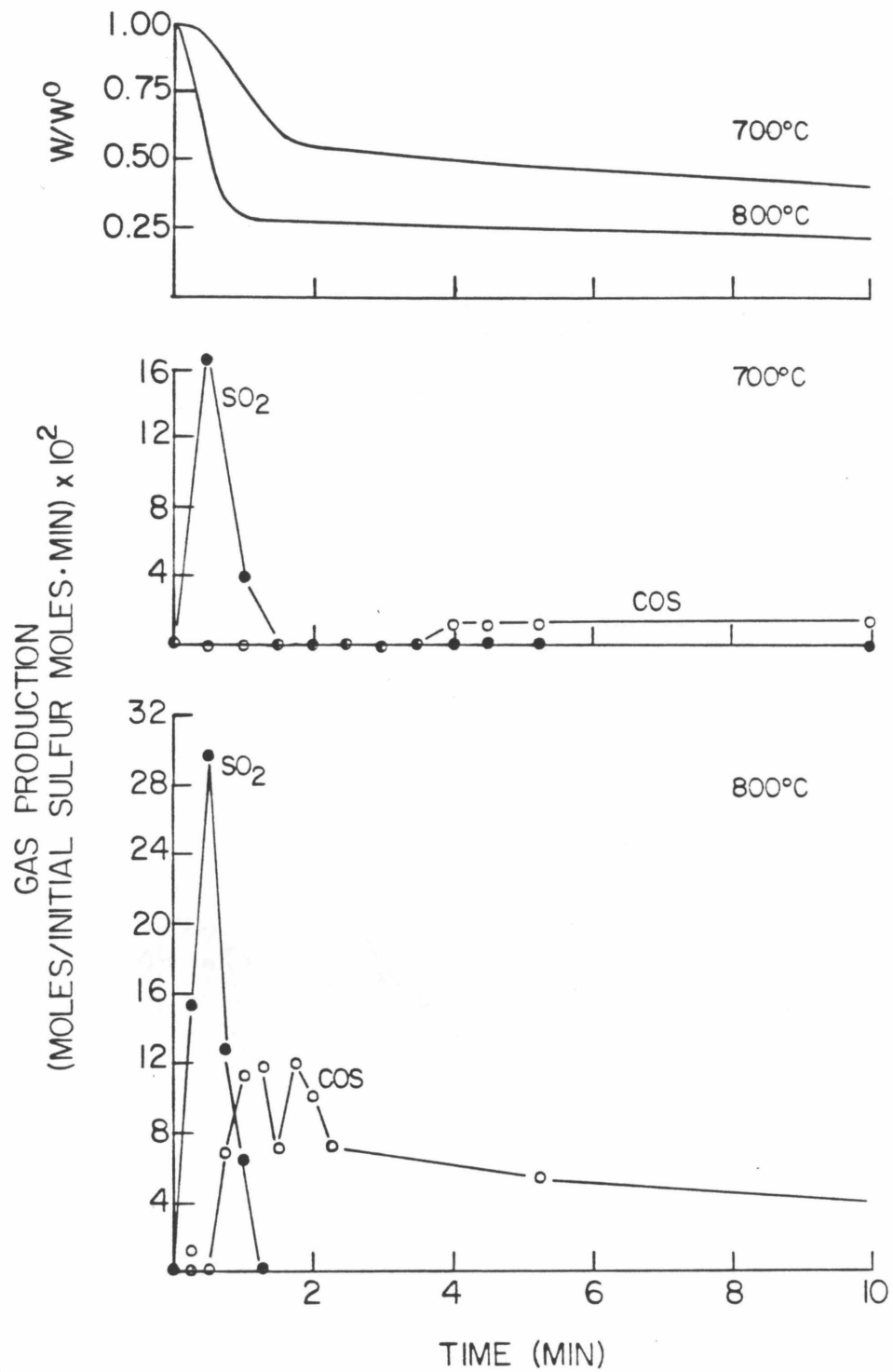


Figure 4.6: Reduction of  $\text{Na}_2\text{SO}_4/\alpha\text{-Al}_2\text{O}_3$  ( $.11 \frac{\text{m mole}}{\text{g}}$ ) at  $700^\circ\text{C}$  and  $800^\circ\text{C}$  with 10% CO Using the TGA System (Sorbent  $\text{N}\alpha 4$ )

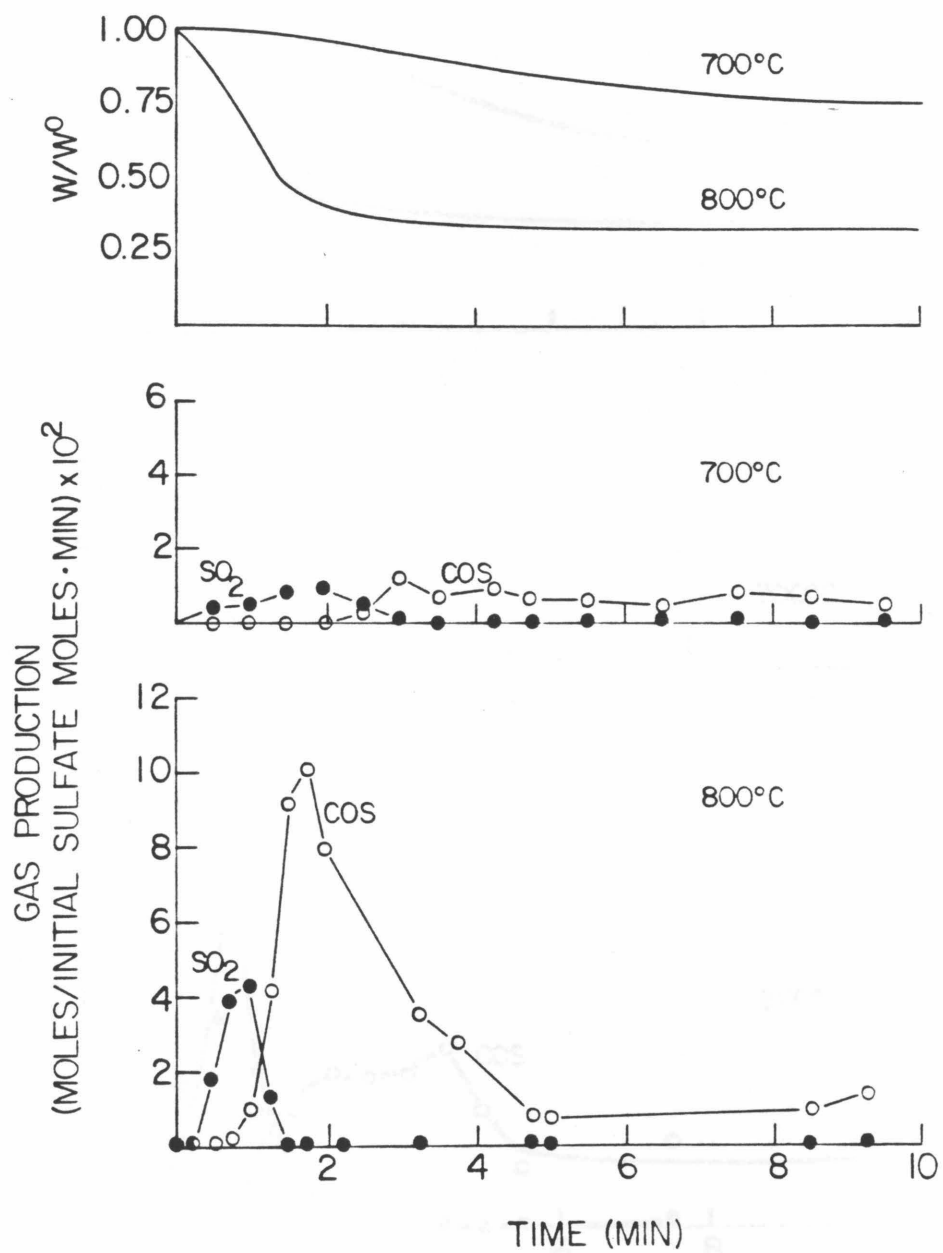


Figure 4.7: Reduction of  $\text{Na}_2\text{SO}_4/\alpha\text{-Al}_2\text{O}_3$  ( $.68 \frac{\text{m mole}}{\text{g}}$ ) at  $700^\circ\text{C}$  and  $800^\circ\text{C}$  with 10% CO Using the TGA System (Sorbent Na3)

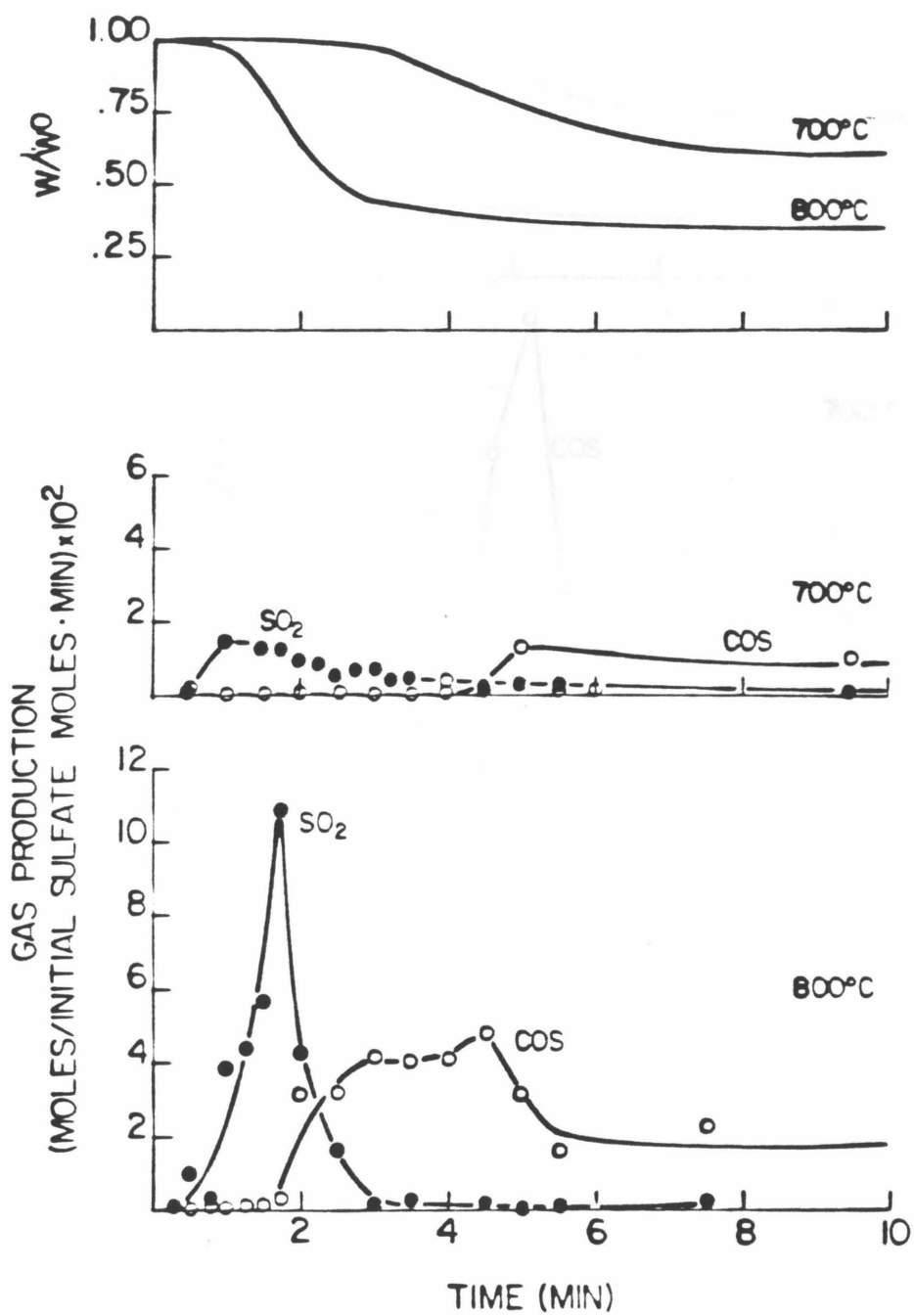


Figure 4.8: Reduction of  $\text{NaLiSO}_4/\alpha\text{-Al}_2\text{O}_3$  at 700°C and 800°C with 10% CO Using the TGA System

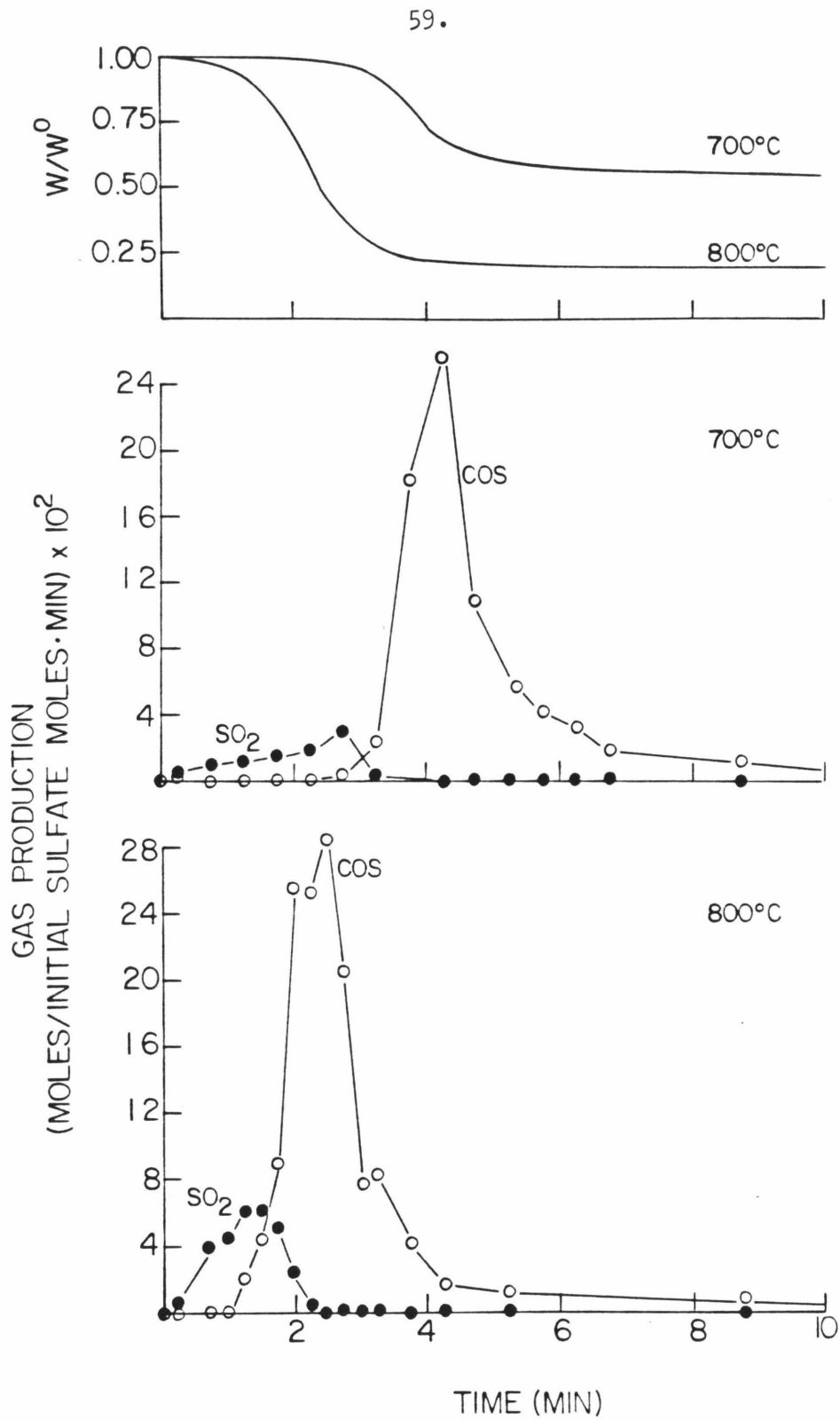


Figure 4.9: Reduction of  $\text{Li}_2\text{SO}_4/\alpha\text{-Al}_2\text{O}_3$  at 700°C and 800°C with 10% CO Using the TGA System

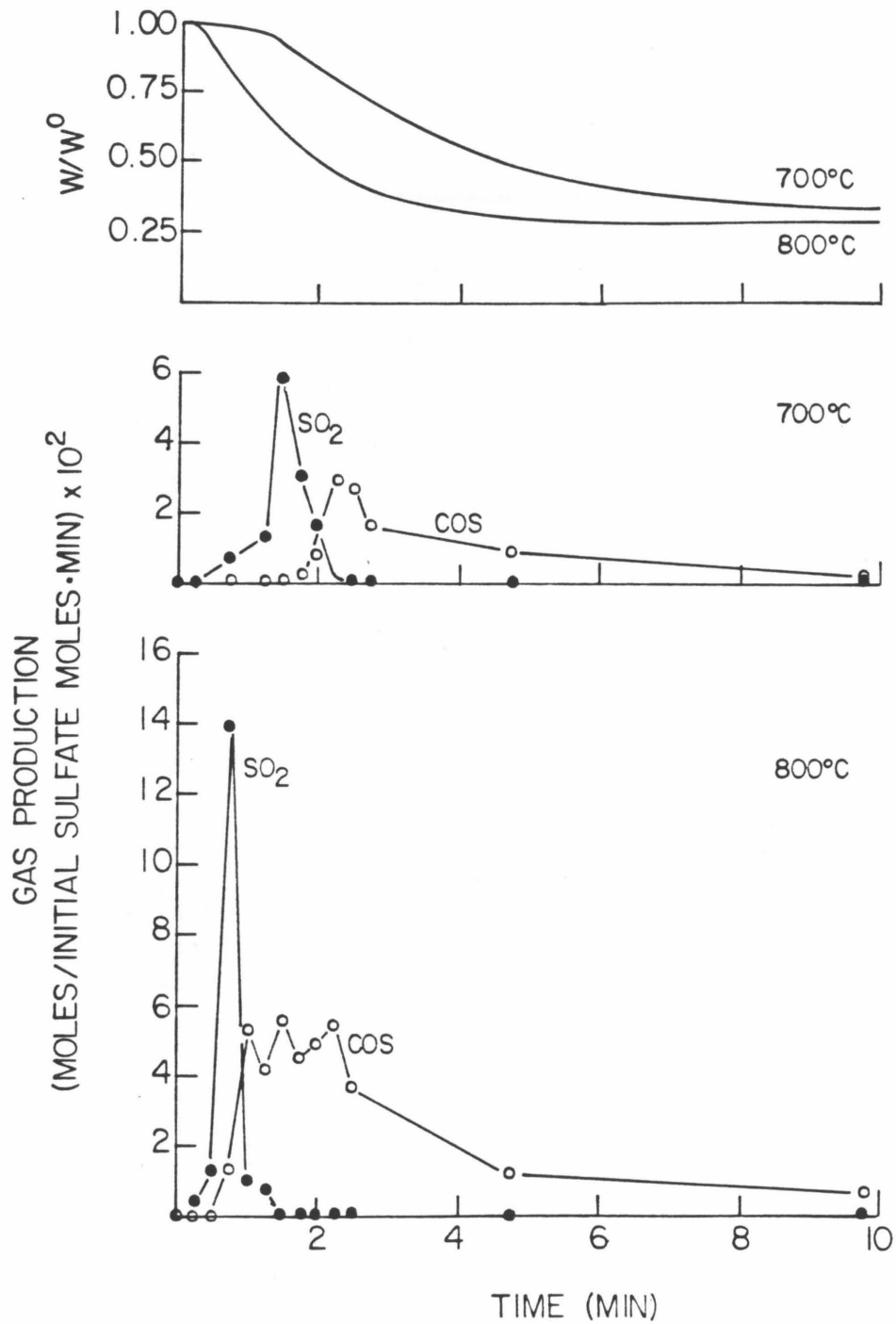


Figure 4.10: Reduction of  $\text{Na}_2\text{SO}_4/\gamma\text{-Al}_2\text{O}_3$  at 700°C and 800°C with 10% CO Using the TGA System

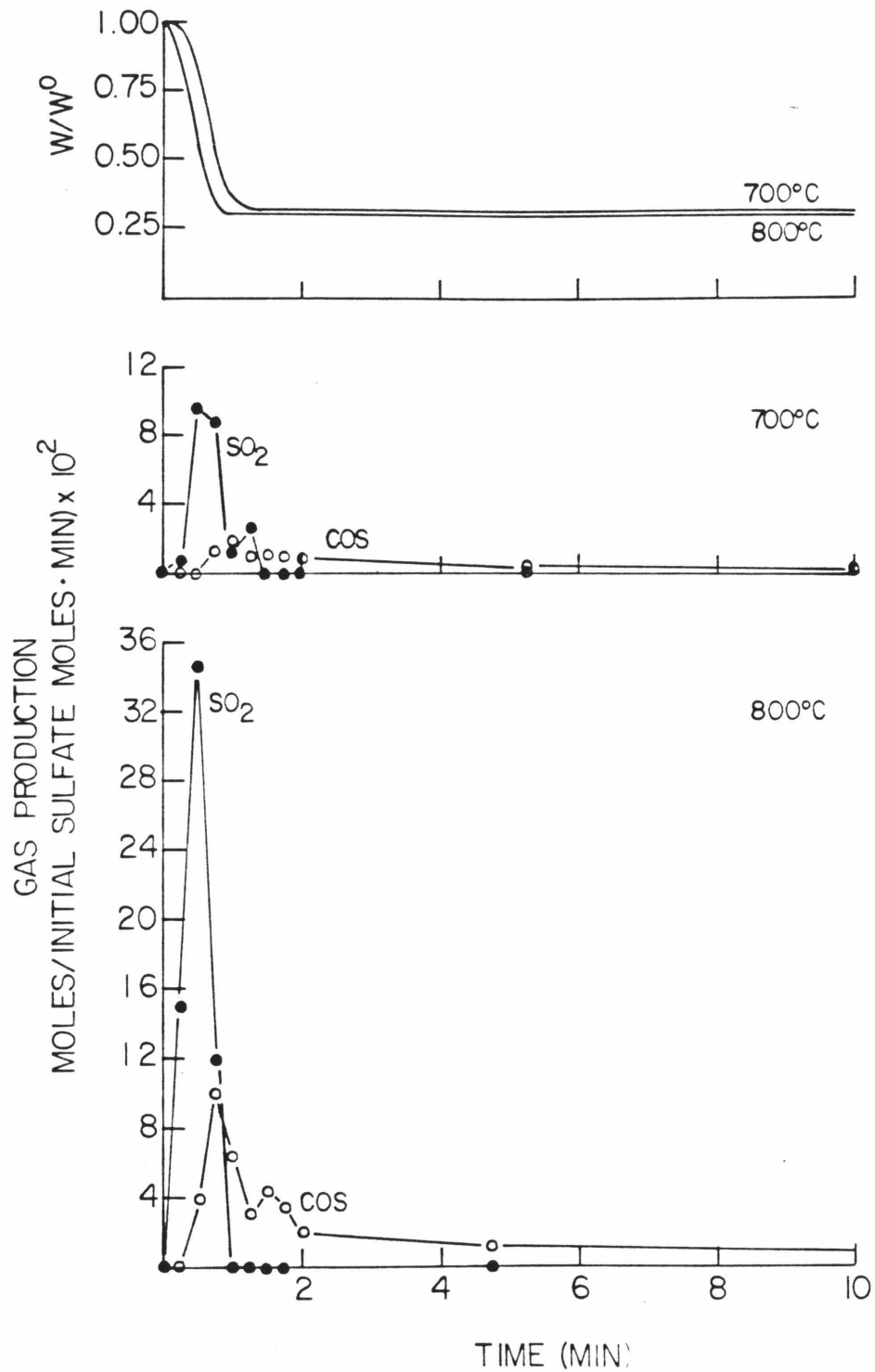


Figure 4.11: Reduction of  $NaLiSO_4/\gamma-Al_2O_3$  at 700°C and 800°C with 10% CO Using the TGA System

bent, when reduced at 700°C fresh or after 800°C sulfation, has an initial period of 3.5 minutes, while it has an initial period of 10.5 minutes after sulfation at 700°C. Similarly, the sodium  $\alpha$ -alumina sorbent's initial period increased from 3.5 minutes to 6.5 minutes when sulfation was conducted at 700°C rather than at 800°C. Separate experiments with the sodium-lithium/ $\gamma$ -alumina sorbent show that the initial period is lengthened considerably by a decrease in the CO concentration (Fig. 4.12). Increasing the CO<sub>2</sub> concentration from .55% to 5.5% increased the initial period of slow weight loss at 700°C, but had little effect at 800°C (Fig. 4.13).

The concentrations of SO<sub>2</sub> and COS in the product gas followed the same general pattern with all sorbents when reduced using 10% CO. Initially, the major gas product was SO<sub>2</sub>. After an initial period, the length of which varied with temperature, and the sorbent being reduced, the major gas product switched from SO<sub>2</sub> to COS. In all cases this switchover occurred approximately one minute after the onset of rapid weight loss. Increasing the CO<sub>2</sub> concentration increased the production of COS relative to SO<sub>2</sub>. Decreasing the CO concentration to 1% drastically reduced the COS production so that no switchover was observed.

At 800°C, the total amount of SO<sub>2</sub> does not change with sulfate loading on the sorbent. Na<sub>2</sub>SO<sub>4</sub>/ $\alpha$ -Al<sub>2</sub>O<sub>3</sub> sorbents with .68 mmole/g and .11 mmole/g sulfate loadings had the same SO<sub>2</sub> production per surface area of sorbent (Fig. 4.14). The initial rate of weight loss also does not depend on sorbent loading (Fig. 4.15). The SO<sub>2</sub> production of Na<sub>2</sub>SO<sub>4</sub>/ $\alpha$ -Al<sub>2</sub>O<sub>3</sub> sorbents differs from that of either the NaLiSO<sub>4</sub>/ $\alpha$ -Al<sub>2</sub>O<sub>3</sub> or the Li<sub>2</sub>SO<sub>4</sub>/ $\alpha$ -Al<sub>2</sub>O<sub>3</sub> sorbent. The presence of lithium increases the SO<sub>2</sub> production. The sodium lithium and the lithium sorbents have the same SO<sub>2</sub> production (Fig. 4.14). When sorbents supported on  $\gamma$ -alumina were reduced, SO<sub>2</sub> production per unit surface

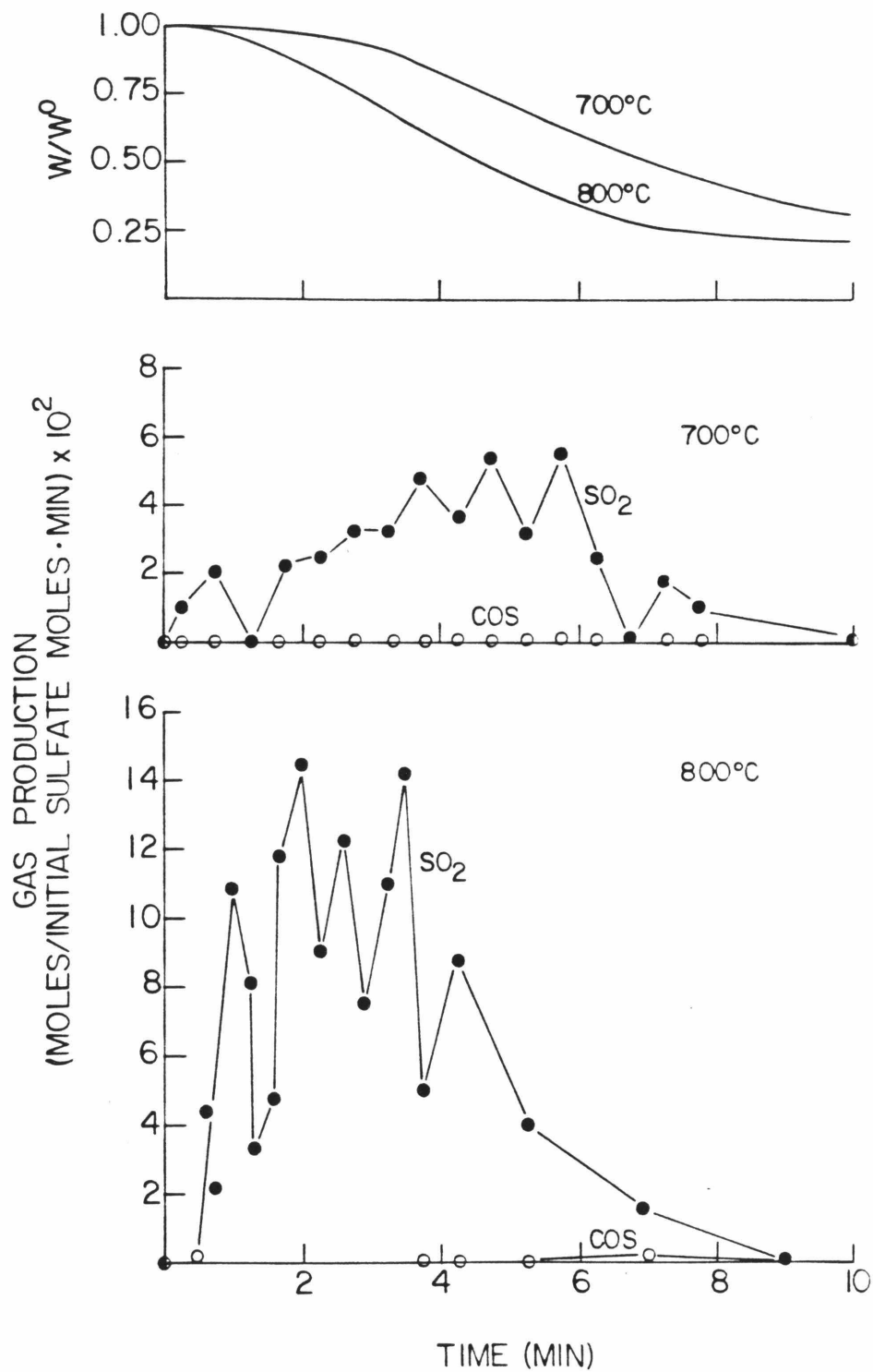


Figure 4.12: Reduction of  $\text{NaLiSO}_4/\gamma\text{-Al}_2\text{O}_3$  at 700°C and 800°C with 1% CO Using the TGA System

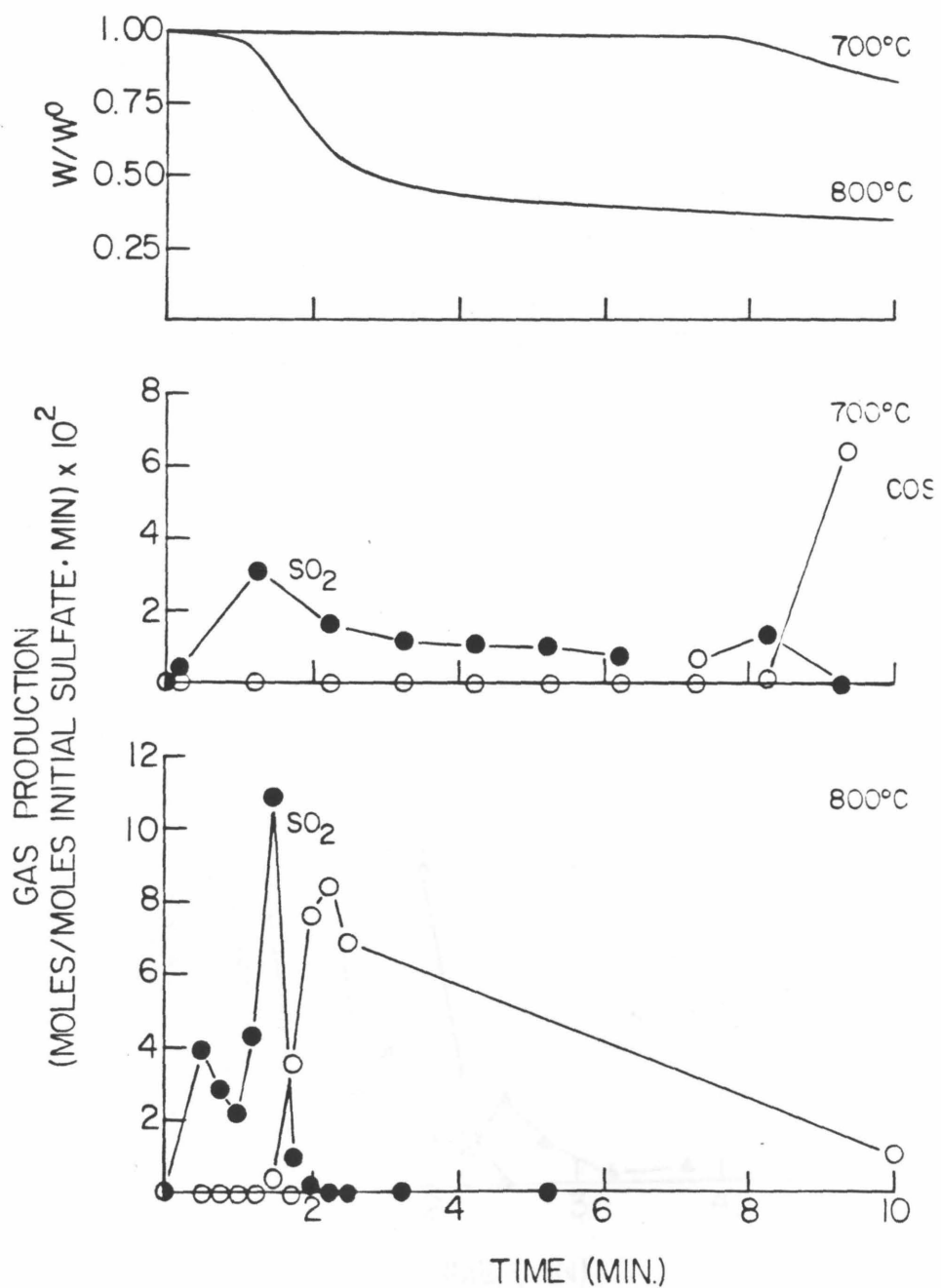


Figure 4.13: Reduction of  $\text{NaLiSO}_4/\alpha\text{-Al}_2\text{O}_3$  at 700°C and 800°C with 10% CO and 5.5% CO<sub>2</sub> Using the TGA System

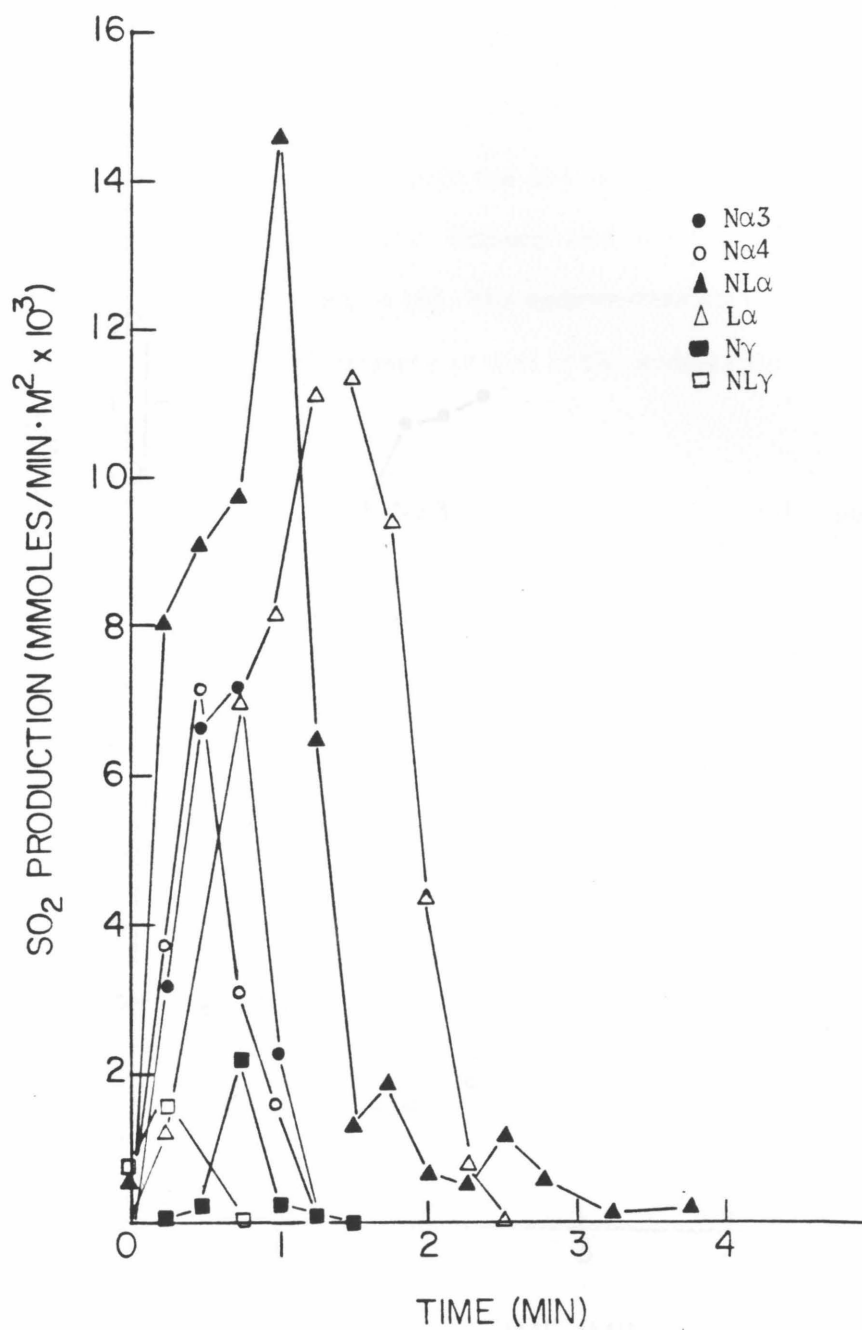


Figure 4.14: SO<sub>2</sub> Production Per Surface Area During Reduction at 800°C Using the TGA System

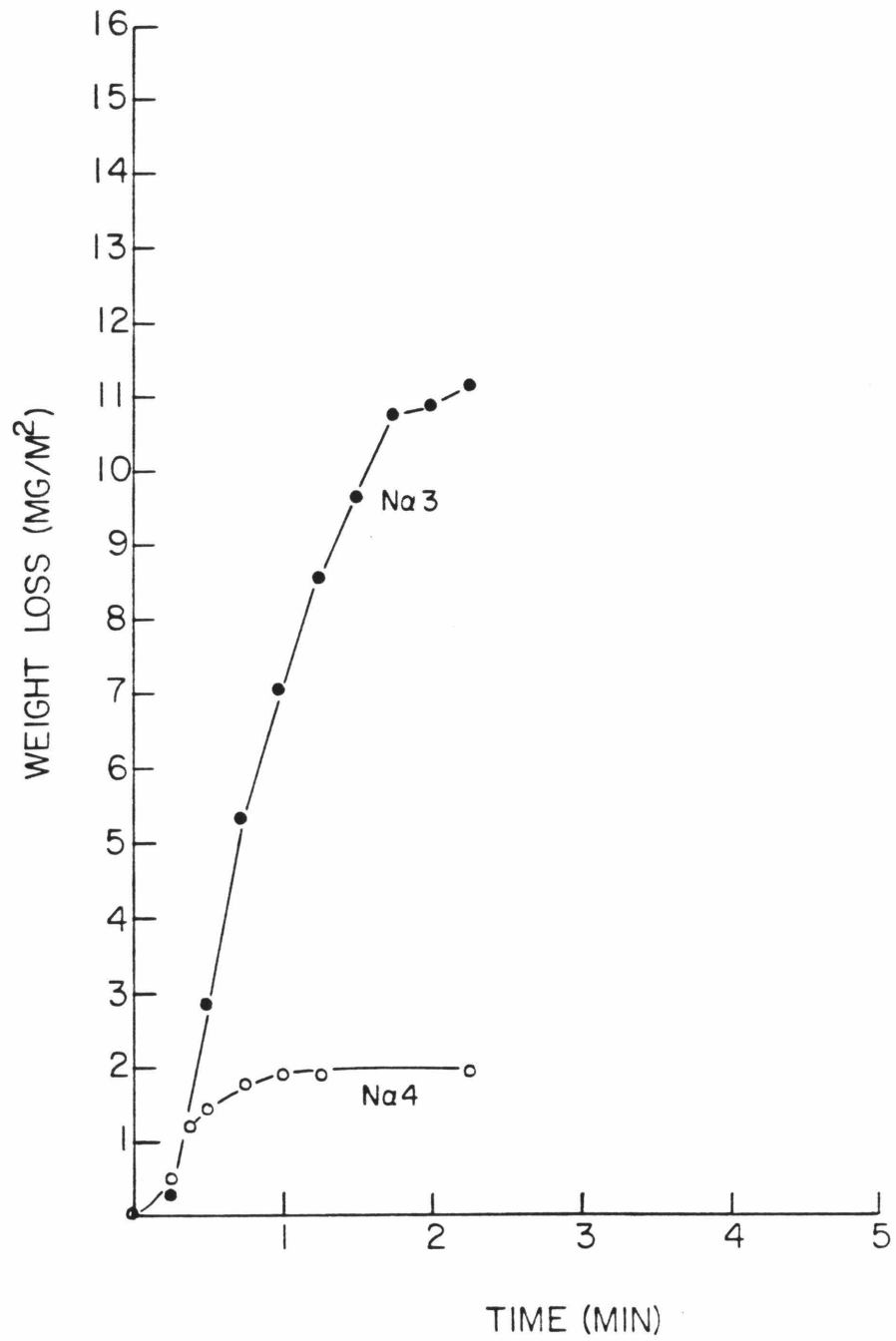


Figure 4.15: Initial Weight Loss of  $\text{Na}_2\text{SO}_4/\alpha\text{-Al}_2\text{O}_3$  Sorbents During Reduction at  $800^\circ\text{C}$

area was much less than that of sorbent supported on  $\alpha$ -alumina. Significant sulfate decomposition during the  $N_2$  heat-up period had occurred with the  $\gamma$ -alumina sorbents, however.

At 700°C, the  $SO_2$  production again did not vary with sulfate loading (Fig 4.16). At 700°C, unlike at 800°C, lithium and sodium lithium sorbents differed in  $SO_2$  production (Fig. 4.16). The sodium-lithium sorbent's  $SO_2$  production was approximately the same as that of the sodium sorbent.

#### 4.4.1.c. Product Selectivity

The overall product selectivity after 20 minutes reduction for each of the sorbents at 700 and 800°C with 10% CO is shown in Table 4.1. Sulfur removal from the sorbent is favored at the higher temperature (800°C), and when lithium is present in the alkali component of the sorbent. Less sulfur is removed when  $\gamma$ -alumina is used as a support rather than  $\alpha$ -alumina, but if the sulfur lost during heating in  $N_2$  prior to reduction is included, the final sulfur and oxygen contents of the  $\gamma$ -alumina sorbents is closer to that of the  $\alpha$ -alumina sorbents.

The selectivity for elemental sulfur rather than COS also varies with the sorbent used. The largest relative yield of elemental sulfur is obtained when both sodium and lithium are present. Elemental sulfur production is also favored by higher temperature. Elemental sulfur production is greatly decreased when  $\gamma$ -alumina is used as the support.

The CO concentration used for reduction also greatly affects the gaseous product selectivity. The sodium-lithium  $\gamma$ -alumina sorbent when reduced using 1% CO produced virtually no COS and all elemental sulfur:  $S/(S + COS)$  was .941 at 800°C and was 1.00 at 700°C. While when reduced using 10% CO it produced no elemental sulfur, and only  $SO_2$  and COS.

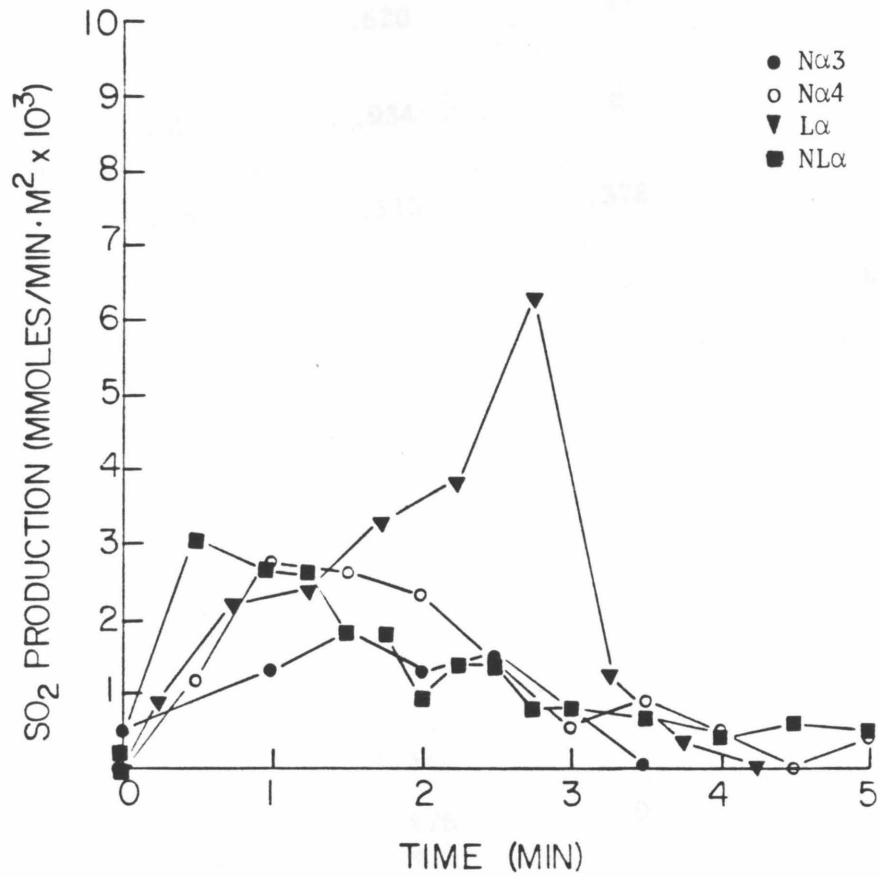


Figure 4.16: SO<sub>2</sub> Production Per Surface Area During Reduction at 700°C Using the TGA System

Table 4.1: Product Selectivity of Sorbents Reduced at 700 and 800°C, with 10% CO on the TGA System. (t=20 min.)

Sorbent	T(°C)	$S_{in\ sorbent}$	$S/(S + COS)$	$SO_2$ (mol/mol $SO_4^{--}$ )
$Na_2SO_4/\alpha Al_2O_3$ (high loading)	800	.620	.243	.0286
$Na_2SO_4/\alpha Al_2O_3$ (high loading)	700	.934	0	.0181
$Na_2SO_4/\alpha Al_2O_3$ (low loading)	800	.115	.378	.171
$Na_2SO_4/\alpha Al_2O_3$ (low loading)	700	.802	0	.054
$Na_2SO_4/\gamma Al_2O_3$	800	.687 (.580)	.096	.0541
$Na_2SO_4/\gamma Al_2O_3$	700	.902 (.753)	0	.0380
$NaLiSO_4/\alpha Al_2O_3$	800	.285	.414	.109
$NaLiSO_4/\alpha Al_2O_3$	700	.539	.573	.061
$NaLiSO_4/\gamma Al_2O_3$	800	.730 (.362)	0	.148
$NaLiSO_4/\gamma Al_2O_3$	700	.876 (.432)	0	.060
$Li_2SO_4/\alpha Al_2O_3$	800	.216	.301	.077
$Li_2SO_4/\alpha Al_2O_3$	700	.560	0	.0504

#### 4.4.1d. Carbonate Decomposition in Reduction

Aluminate formed during reduction and its physical and chemical properties may significantly impact the reduction process. To study the formation of aluminate, the decomposition of alumina impregnated with alkali carbonates was studied thermogravimetrically. Samples were heated at a constant rate, 100°C/min, until reaching 700° and then the temperature held constant at 700°C. The results are shown in Fig. 4.17. Both lithium carbonate and sodium-lithium carbonate when impregnated on  $\alpha$ -alumina decompose rapidly at temperatures above 600°C. The sodium carbonate impregnated on  $\alpha$ -alumina initially decomposes rapidly at 700°C, but then the rate of reaction slows. During the period of deceleration the conversion is proportional to the square root of time. Thus the slowing can be attributed to diffusion resistance caused a growing aluminate layer through which the sodium and carbonate ions must diffuse (Eq. 4.1).

$$\frac{n}{A} = \rho D^{1/2} t^{1/2} \quad (4.1)$$

where

$n$  = moles of carbonate reacted.

$A$  = total area of sample.

$\rho$  = molar density of  $\text{NaAlO}_2$ .

$D$  = diffusion coefficient.

Using Eq. (4.1) the diffusion coefficient is calculated to be  $7.7 \times 10^{-17} \text{ cm}^2/\text{sec}$ . Alumina impregnated with lithium containing alkali carbonate will form lithium aluminate or mixed sodium-lithium aluminate which must have less diffusion resistance for the ions than sodium aluminate.

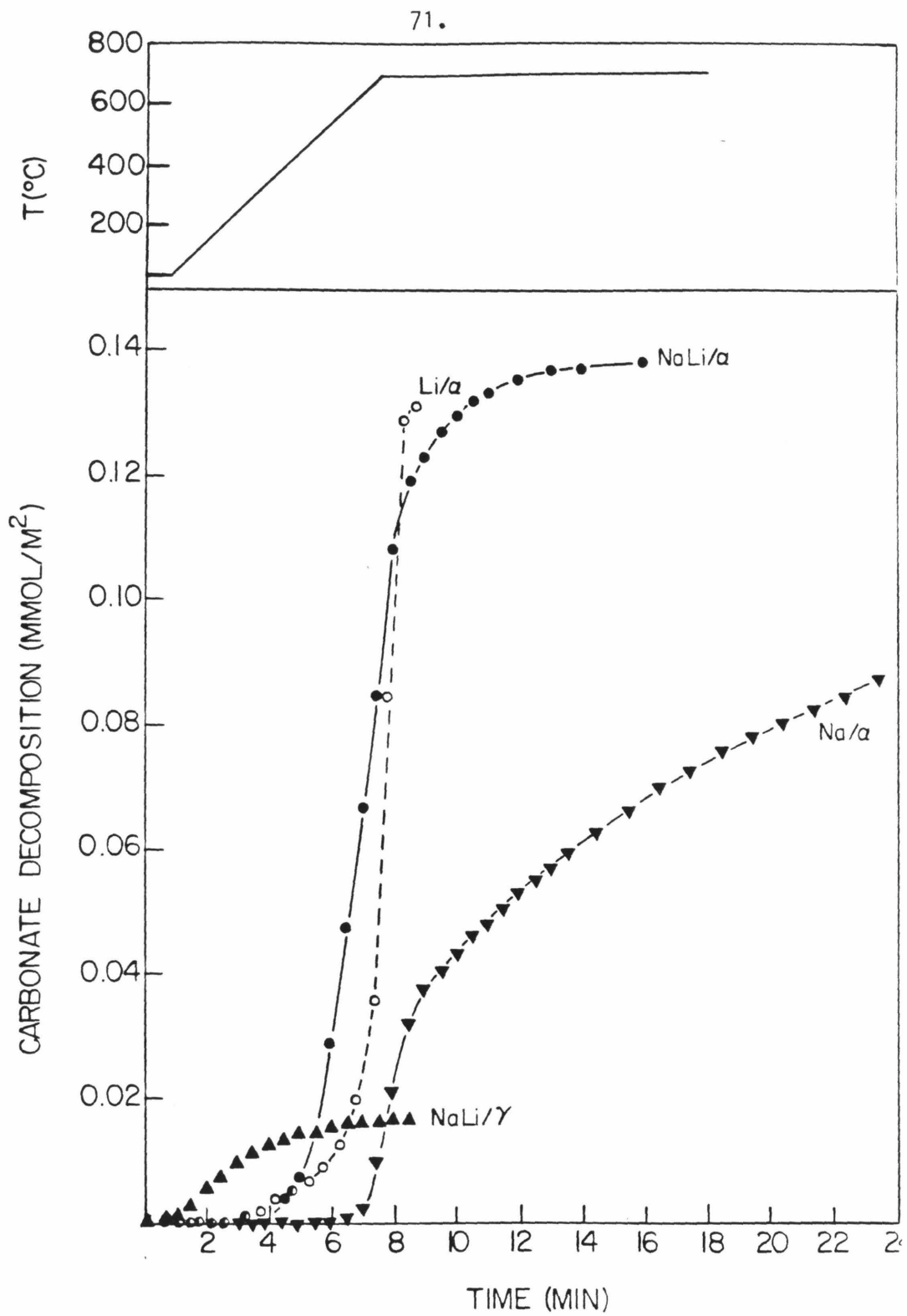


Figure 4.17: Alkali Carbonate Decomposition

When sodium-lithium carbonate impregnated  $\gamma$ -alumina was heated in  $N_2$ , decomposition began at much lower temperatures than with the  $\alpha$ -alumina, approximately  $100^\circ C$ . One other difference between the  $\alpha$ -alumina and  $\gamma$ -alumina samples was observed when completely decomposed samples were exposed to  $SO_2$  and air at  $800^\circ C$ . The  $\alpha$ -alumina samples completely sulfated, whereas the  $\gamma$ -alumina sample only showed  $\approx 50\%$  sulfation.

#### 4.4.2. Sorbent Composition Changes during Reduction

The reduction of  $Na_2SO_4/\alpha-Al_2O_3$  and  $NaLiSO_4/\alpha-Al_2O_3$  sorbents was examined in greater detail by following sorbent composition as a function of time during reduction. Results for the sodium sorbent reduced at 800 and  $700^\circ C$  are shown in Figs. 4.18 and 4.19, respectively. Results for the sodium lithium sorbent at 800, 750 and  $700^\circ C$  are shown in Figs. 4.20 through 4.22.

At  $800^\circ C$ , the reduction of both the sodium and sodium-lithium sorbents follows the same pattern and can be divided into two periods: an initial period in which the majority of oxygen is lost along with some sulfur, and a second period during which the oxygen content remains relatively constant but sulfur continues to be lost at a steady rate. Differences in the reduction of the two sorbents are most prominent in the initial period, during which the sulfur content of the sodium lithium sorbent decreases to a much greater extent than that of the sodium sorbent. The rate of sulfur loss during the second half of the reduction appears to be approximately the same for both sorbents. The change-over between these two periods in reduction corresponds to the switch-over in gas production from  $SO_2$  to  $COS$  seen in the gravimetric experiments.

At  $700^\circ C$  similar variations between the two sorbents are exhibited. Again two reduction periods are observed. Sulfur loss during the later period is,

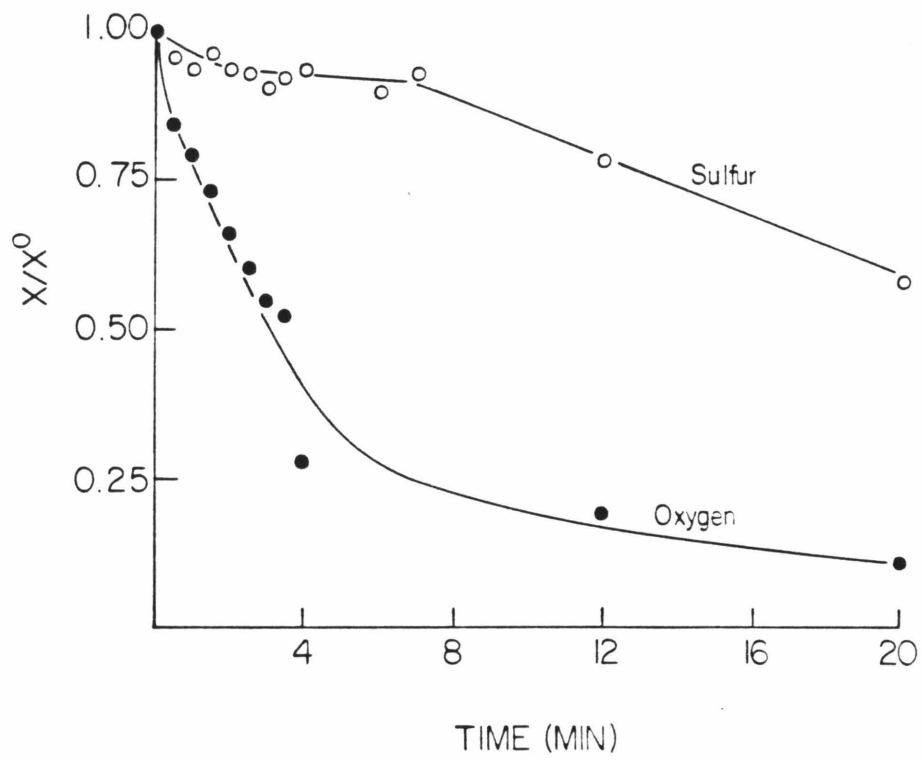


Figure 4.18: Sorbent Composition During Reduction of  $\text{Na}_2\text{SO}_4/\alpha\text{-Al}_2\text{O}_3$  at  $800^\circ\text{C}$  (Sorbent No1)

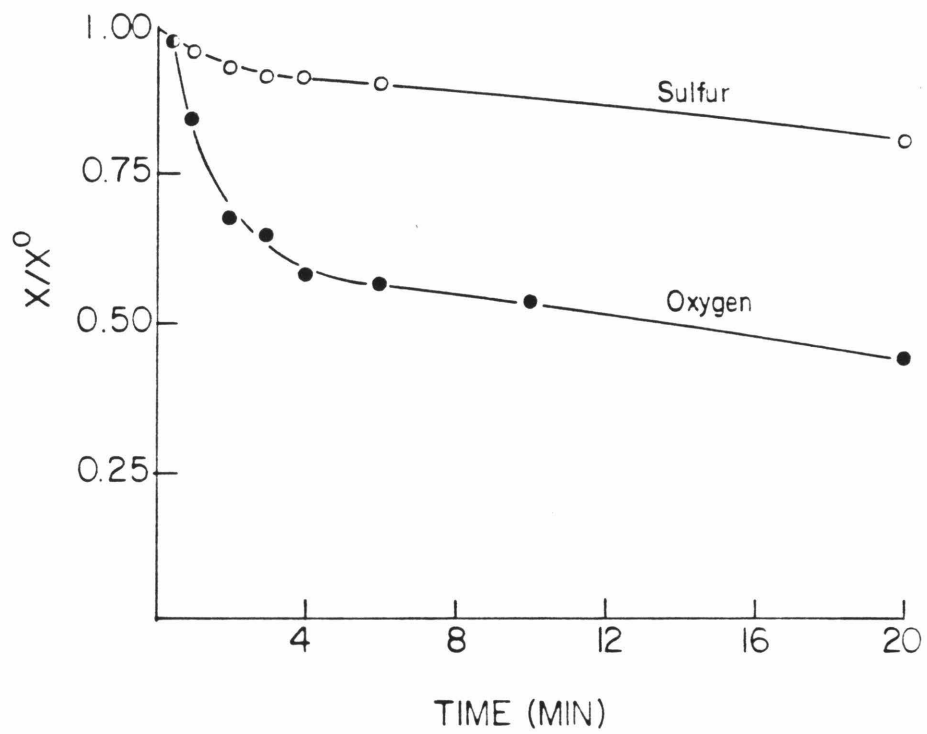


Figure 4.19: Sorbent Composition During Reduction of  $\text{Na}_2\text{SO}_4/\alpha\text{-Al}_2\text{O}_3$  at  $700^\circ\text{C}$  (Sorbent No1)

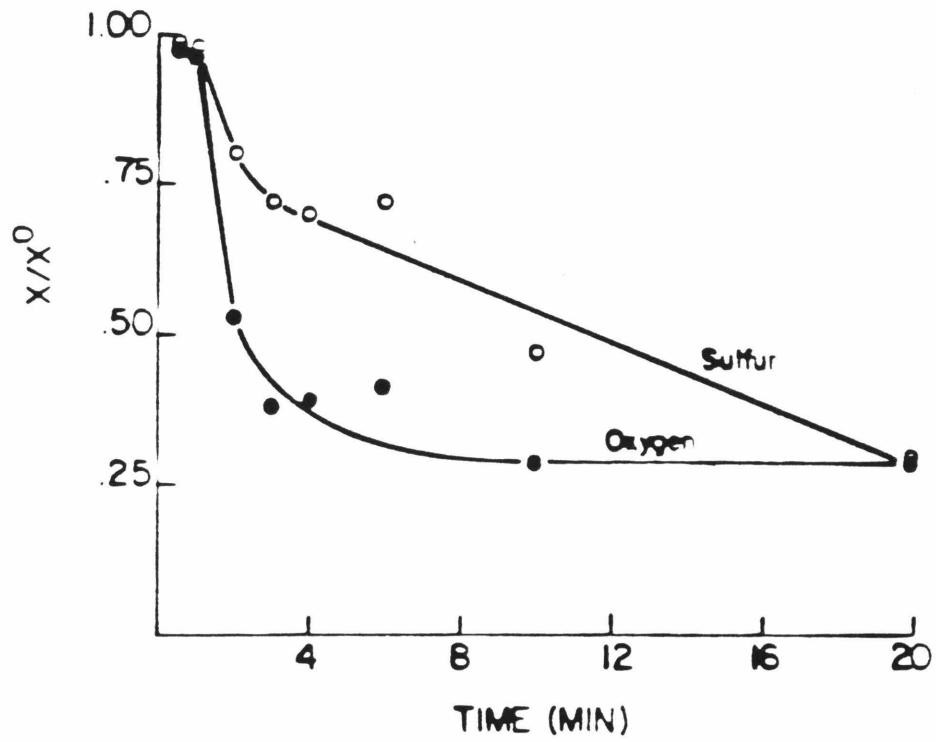


Figure 4.20: Sorbent Composition During Reduction of  $\text{NaLiSO}_4/\alpha\text{-Al}_2\text{O}_3$  at  $800^\circ\text{C}$

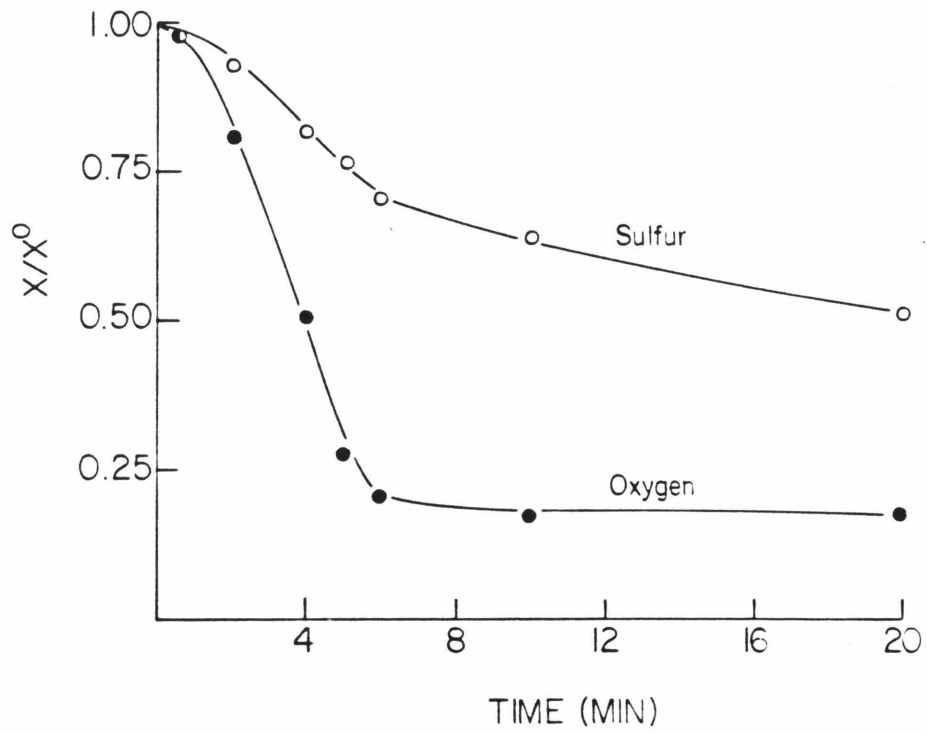


Figure 4.21: Sorbent Composition During Reduction of  $\text{NaLiSO}_4/\alpha\text{-Al}_2\text{O}_3$  at  $750^\circ\text{C}$

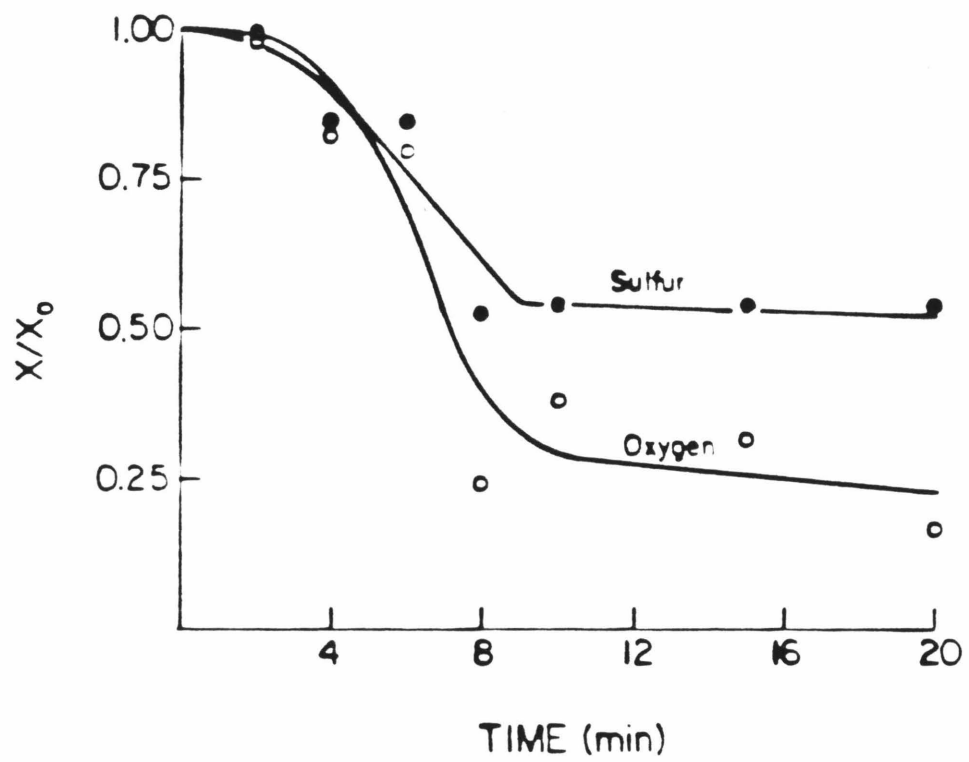


Figure 4.22: Sorbent Composition During Reduction of  $\text{NaLiSO}_4/\alpha\text{-Al}_2\text{O}_3$  at  $700^\circ\text{C}$

however, much slower than at 800°C. The behavior of the reduction of the sodium-lithium sorbent at 750°C also has two periods of reduction. The rates of sulfur and oxygen loss are intermediate between the 700°C and 800°C results.

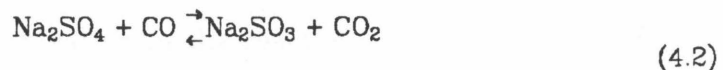
#### 4.5. Discussion

##### 4.5.1. Effect of the Nature of the Alkali Material

The nature of the alkali material present may affect the reduction process in two ways. First, different alkali materials have differing phase behavior during reduction. Second, the cations present affect the chemical and physical nature of reactants, intermediates and products.

##### 4.5.1a. Effect of the Presence of Lithium in the Alkali Material

Several differences between the reductions of the sorbents can be explained by differences in the properties of the various aluminates formed. The sulfur removal at 20 minutes (Table 4.1) for the  $\text{Na}_2\text{SO}_4/\alpha\text{-Al}_2\text{O}_3$  sorbent was much less than either the  $\text{NaLiSO}_4/\alpha\text{-Al}_2\text{O}_3$  or the  $\text{Li}_2\text{SO}_4/\alpha\text{-Al}_2\text{O}_3$  sorbent at both 700 and 800°C. Both sorbents containing lithium have approximately the same sulfur removal at 20 minutes. This difference in the sorbents is due to either the differences in relative stabilities of the sulfides and aluminates of sodium and lithium (Section 2.4.1), or differences in the formation rates of aluminate and sulfides of sodium and lithium. At the onset of reaction, sulfate is most likely quickly reduced to sulfite.



Sulfite may then react further to give either aluminate or sulfide. The rate of the aluminate formation is likely to depend on the rate of diffusion of ions, both cations and anions, through the aluminate layer. As the

aluminate layer is formed, the reaction rate of the aluminate formation reaction will decrease, while the sulfide formation reaction will continue at the same rate. The diffusional resistance of the aluminate layer will therefore determine the relative yields of aluminate and sulfide from the common sulfite precursor. This mechanism is supported by the variation in  $\text{SO}_2$  production with cation at  $800^\circ\text{C}$ . The production was higher when lithium was present, indicating a higher rate of diffusion of ions in lithium aluminate than in sodium aluminate. This higher diffusivity was also seen in the relative rates of alkali carbonate-alumina reaction. At  $700^\circ\text{C}$ , enhancement of the rate of  $\text{SO}_2$  production of the lithium sorbent over the sodium sorbent is again seen. At  $700^\circ\text{C}$  the sodium-lithium sorbent behaves like the sodium sorbent rather than the lithium sorbent, however. If the rate of  $\text{SO}_2$  production is indeed controlled by the relative rates of aluminate and sulfide formation from sulfite, the sodium-lithium  $\text{SO}_2$  production may be decreased relative to that of the lithium sorbent if the rate of sulfide formation in the sodium lithium sorbent is higher than that of the lithium sorbent. This is likely to be the case as at  $700^\circ\text{C}$  the sodium-lithium sulfate will be molten while the lithium sulfate will be solid (see Section 4.5.1b).

Sulfur removal from the sorbent at later times may be accomplished through a different mechanism than at early times. This may possibly occur through the reaction of  $\text{CO}_2$  (always present in the reaction gas stream) and sulfide to form aluminate (Eq. 2-16). This reaction would be considerably thermodynamically favored in the presence of lithium (Fig. 2.17). An increase in the  $\text{CO}_2$  concentration in the reaction gas should also increase the rate of this reaction. The rate of COS production is considerably increased for the lithium sorbent over either that of the sodium or sodium lithium sorbent, at both  $700$  and  $800^\circ\text{C}$ . Increasing the  $\text{CO}_2$  concentration

did increase the rate of COS production at both 700 and 800°C during reduction of the sodium lithium  $\alpha$ -alumina sorbent. The sulfur loss as a function of time observed in the sorbent composition experiments shows two periods of sulfur loss, and also supports two mechanisms for sulfur loss.

#### 4.5.1.b. Effect of the Phase Behavior of the Alkali Material

The phase behavior, i.e. the amount of solid or melt present, varies with the sorbent, the degree of reduction and the temperature (Section 3.1.1). The sulfate being molten may affect the relative yields of sulfide and oxide. Sulfide may be formed by the disproportionation of sulfite. This disproportionation is likely to proceed through ion-ion reactions, which would be accelerated if the ions were in a melt rather than a solid. At 800°C all the sorbents will become molten during the reduction and the rate of sulfite disproportionation should be approximately the same for all sorbents. At 700°C only the sodium-lithium sorbent will be appreciably molten. Differences in the SO<sub>2</sub> production between the sodium-lithium and lithium sorbents at 700°C can be explained by the sodium-lithium sorbent having a higher sulfide formation rate relative to that of the lithium sorbent.

The presence of melt in the alkali material appears to increase the production of elemental sulfur during reduction. Elemental sulfur production is greater for sodium-lithium sorbents than for either of the other alkali materials. Among the sorbents only the sodium-lithium sorbent remains entirely molten throughout the reaction period. Elemental sulfur production also increased with increasing temperature, which increases the extent of the molten phase. No sulfur was produced at 700°C for either the lithium or sodium sorbents, both of which would be solid at this temperature.

#### 4.5.2. Effect of the Support

The major difference between the two support materials,  $\alpha$ - $\text{Al}_2\text{O}_3$  and  $\gamma$ - $\text{Al}_2\text{O}_3$ , is the decomposition of sulfates during heating in  $\text{N}_2$  observed with the  $\gamma$ - $\text{Al}_2\text{O}_3$  support.  $\gamma$ - $\text{Al}_2\text{O}_3$  is less stable than  $\alpha$ - $\text{Al}_2\text{O}_3$  and therefore more reactive towards formation of aluminates. It is of major importance that sulfate decomposition to form aluminates is irreversible; that is, upon re-sulfation only the aluminate formed during reduction reacted to form sulfate. The aluminate formed during sulfate decomposition, therefore, must "remember" the type of alumina from which it was formed. Two aluminates, with different structures, may form: Kovalenko and Bukin (1978), in studying the reaction of sodium carbonate with  $\alpha$ -alumina and  $\gamma$ -alumina, found that monoaluminate was formed initially, but that further reaction between monoaluminate and alumina to form polyaluminates followed further heating. Polyaluminate formation proceeded faster in the presence of  $\gamma$ -alumina. Takahashi and Kuwabara (1979) studied the solid state reaction between  $\text{NaAlO}_2$  and  $\gamma$ - $\text{Al}_2\text{O}_3$  to form various polyaluminates, between 700 and 1200°C. The reaction rate appeared to depend on the  $\text{NaAlO}_2$  diffusion into the  $\gamma$ - $\text{Al}_2\text{O}_3$ . Similar reactions between  $\alpha$ -alumina and aluminate have been studied but at higher temperatures 1900-2000 K (Szymanski and Wlosinski, 1979). During heating in  $\text{N}_2$  and subsequent reduction, therefore, polyaluminates stable to sulfation may form when  $\gamma$ -alumina is present.

The reduction process itself was affected by the nature of the support. In general,  $\gamma$ -alumina sorbents reacted more quickly than  $\alpha$ -alumina sorbents (per unit mass of alkali sulfate) and this difference was more pronounced for the sodium lithium sorbents. When  $\text{SO}_2$  production, as a measure of the initial rate, is compared on a per surface area basis, the reaction rate of the  $\gamma$ -alumina sorbents actually was slower than that of the  $\alpha$ -alumina sorbents. If, as previously discussed, this rate depends on the diffusion of ions through

an aluminate layer, the rate should be suppressed by the presence of an aluminate layer formed during the preceding heating in  $N_2$ . The effect of the presence of an aluminate layer at the onset of reduction is also evident in the extent of sulfur removal, after 20 minutes of reduction. Sulfur removal is less for  $\gamma$ -alumina sorbent than for  $\alpha$ -alumina sorbents but the difference is diminished when the sulfur lost during the  $N_2$  heat-up of the  $\gamma$ -alumina sorbents is also considered with that lost during reduction. This evidence supports the hypothesis that sulfur removal depends upon the rate of aluminate formation in comparison to the rate of sulfide formation, the aluminate formation rate being controlled by diffusional resistance in the aluminate layer formed.

The production of COS from sulfur and CO appears to be catalyzed by  $\gamma$ -alumina. Elemental sulfur was not found as a product when  $\gamma$ -alumina was the support, as predicted by equilibrium calculations.  $\gamma$ -alumina is most likely a better catalyst than  $\alpha$ -alumina due to its larger surface area, as in the literature the nature of the active surface was not found to be important at high temperatures (Section 2.3.2).

#### **4.5.3. Interpretation of the Sorbent Composition Changes during Reaction**

The results of the sorbent composition experiments can be interpreted in a number of different ways. The simplest interpretation is to assume only sulfate, sulfide and oxide, in the form of aluminate, are present at any given time. Another interpretation allows for the reduction of sulfate to sulfite followed by reaction of sulfite to sulfide and aluminate. Sulfate, sulfite, sulfide and oxide (aluminate) as fractions of the initial sulfate based on the sorbent composition experiment have been calculated and are shown for the

$\text{Na}_2\text{SO}_4/\alpha\text{-Al}_2\text{O}_3$  and  $\text{NaLiSO}_4/\alpha\text{-Al}_2\text{O}_3$  sorbents in Figs. 4.23 and 4.24, respectively. Calculations used mass balances on sulfur and oxygen and balances on the total number of anions. The sulfate-sulfite-sulfide-aluminate curves are a combination of calculations assuming sulfate, sulfite and aluminate presence, and calculations assuming sulfite, sulfide and aluminate presence. The assumption of only sulfate, sulfite and aluminate being present leads to impossible mole fractions at all but early times. The assumption of only sulfite, sulfide and aluminate being present leads to impossible mole fractions at early times. The crossover times between these two assumptions coincide. The sulfite content can be interpreted to mean either the sulfite ion ( $\text{SO}_3^-$ ) or an oxide (aluminate) ion and adsorbed  $\text{SO}_2$ . This model for the reaction ignores any elemental sulfur which might be adsorbed on the surface or present in the alkali material as dissolved elemental sulfur or polysulfide.

Interpreting the sorbent composition in this way brings to light differences between the sodium and sodium-lithium sorbent. Reduction of sodium sulfate to sulfite is very rapid at both  $700^\circ\text{C}$  and  $800^\circ\text{C}$  with the sodium sorbent. Reduction of the sodium-lithium sulfate occurs at a comparable rate to that of the sodium sorbent only at  $800^\circ\text{C}$ . The initial period of slow weight loss seen with the sodium-lithium sorbent appears to be due to the slow rate of sulfate reduction to sulfite. Although the sodium sulfate reduction to sulfite is faster than that of sodium lithium sulfate at  $700^\circ\text{C}$ , the sodium sulfite reacts more slowly than the sodium-lithium sulfite.

Increasing the temperature increased the initial rate of both aluminate and sulfide formation. However, for the sodium sorbent the increase in sulfide formation was much more pronounced than the increase in aluminate formation. The rate of aluminate was only slightly increased. If

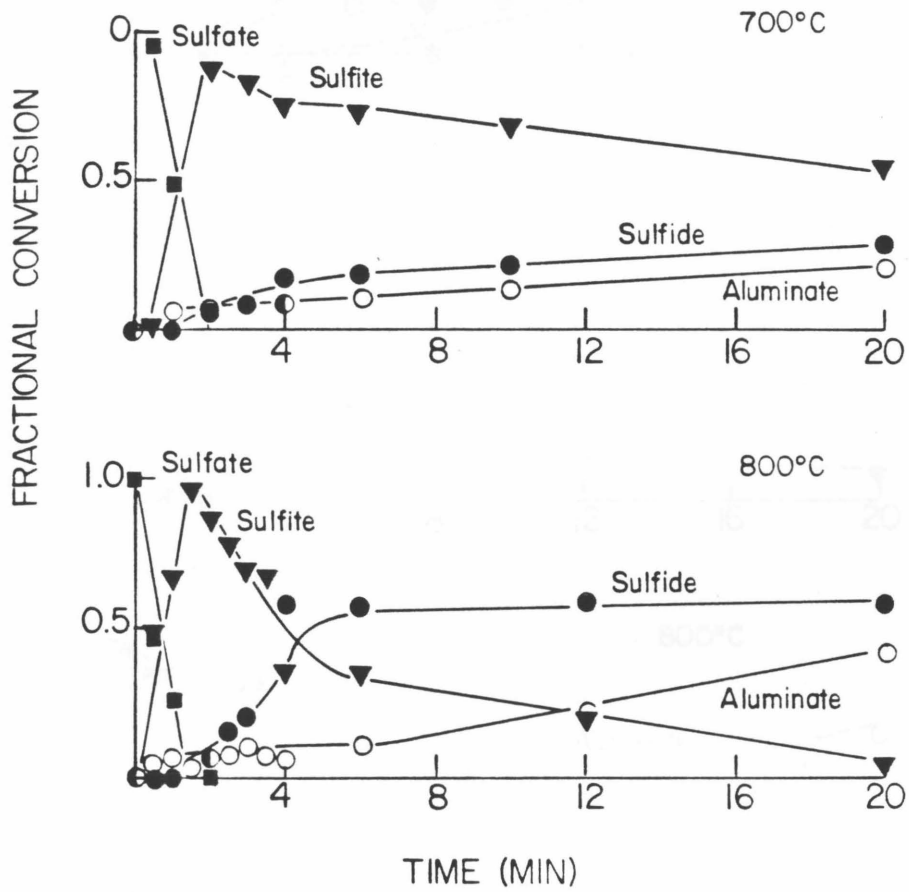


Figure 4.23: Sulfate-Sulfite-Sulfide-Aluminate Contents During Reduction of  $\text{Na}_2\text{SO}_4/\alpha\text{-Al}_2\text{O}_3$

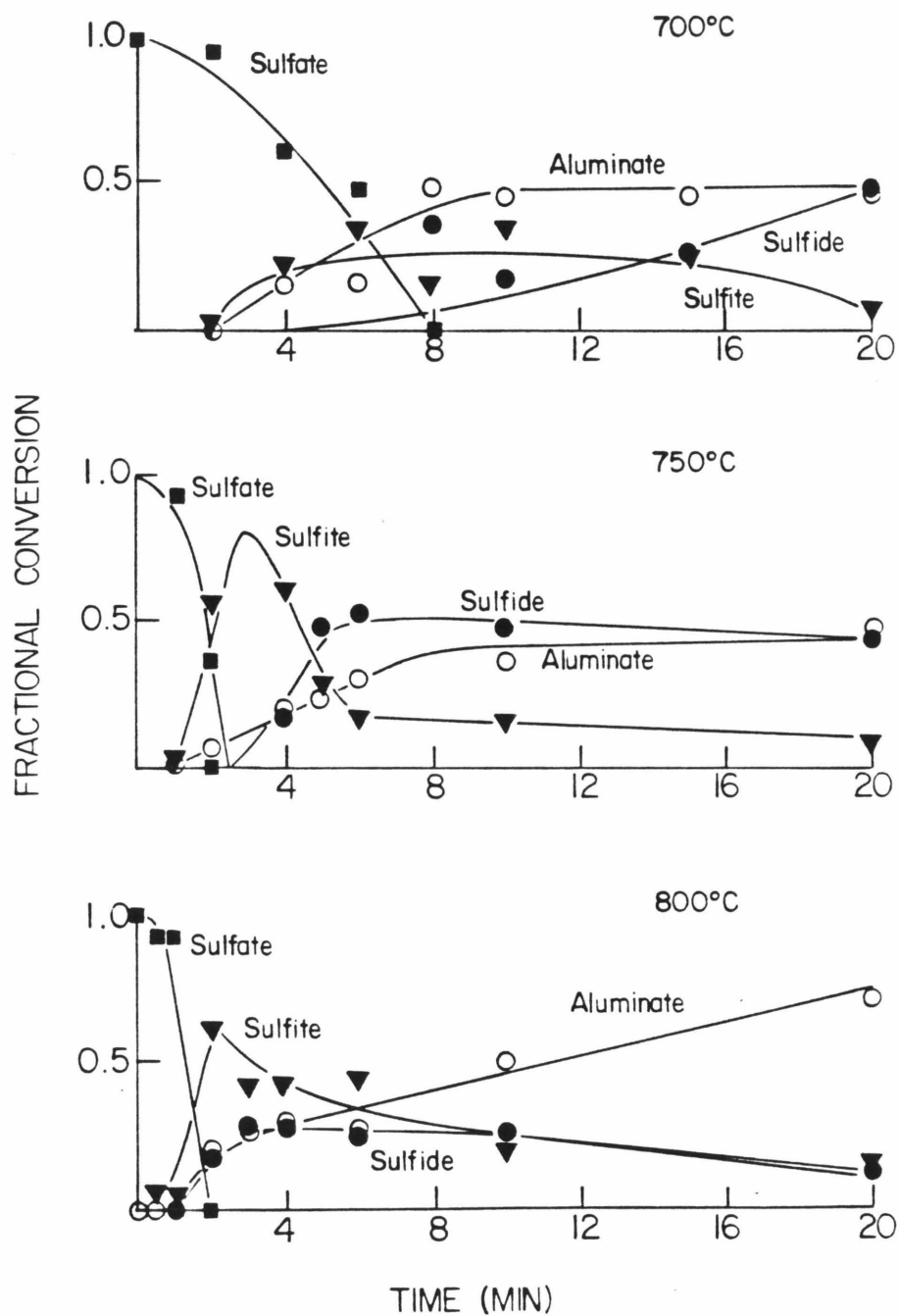


Figure 4.24: Sulfate-Sulfite-Sulfide-Aluminate Contents During Reduction of  $\text{NaLiSO}_4/\alpha\text{-Al}_2\text{O}_3$

as is suggested in Section 4.5.2.b the rate of aluminate formation depends on the rate of diffusion through an aluminate layer, these results would imply that the diffusivity of ions in sodium aluminate is not a strong function of temperature. The sodium-lithium sorbent shows significant increase in the rate of aluminate formation when the temperature is increased from 750 to 800°C, but hardly any increase when the temperature is increased from 700 to 750°C. The sulfide formation rate, on the other hand, shows a large increase when the temperature is increased from 700°C to 750°C, but stays approximately the same between 750 and 800°C. Sulfide may be formed by the disproportionation of sulfite, the sulfate which is formed again being reduced to sulfite. The disproportionation depends on ion-ion reactions in the alkali material. These ion-ion reactions should be faster in the molten state. Thus, the sodium sorbent which is solid at 700°C shows sulfite to be very stable in relation to the formation of sulfide, and the rate of sulfide formation greatly increased at 800°C when the material is at least partially molten.

**References**

1. Christie, J. R., A. J. Darnell and D. F. Dustin, "Reaction of Molten Carbonate with Aluminum Oxide," *J. Phys. Chem.* **82**(1), 33 (1978).
2. Kovalenko, V. I. and H. G. Bukin, "Reaction of Sodium Carbonate with Different Forms of Aluminum Oxide," *Russ. J. Inorg. Chem.* **23**(2), 158 (1978).
3. Szymanski, A. and W. K. Wlosinski, "Diffusional Changes of Ceramic Bodies Composition and Structure During the Second Step of Sintering Process," *Mater. Sci. Monographs*, **4**, 196 (1979).
4. Takahashi, T. and K. Kuwabara, "Formation of  $\beta$  and  $\beta'$ - $\text{Al}_2\text{O}_3$  by the Solid State Reaction between  $\text{NaAlO}_2$  and  $\gamma$ - $\text{Al}_2\text{O}_3$ ," *J. Solid State Chem.*, **30**, 321 (1979).

CHAPTER 5

FOURIER TRANSFORM INFRARED SPECTROSCOPY

## 5.1. Introduction

Fourier transform infrared spectroscopy (FTIR) was used to obtain direct information about species present during the reduction of  $\alpha$ -alumina supported sodium lithium sulfate (sorbent NL $\alpha$ ). This information is useful interpreting and corroborating reaction data from the thermogravimetric analyzer and microreactor studies.

### 5.1.1. Inorganic Infrared Spectroscopy

Qualitative analysis of inorganic ions by infrared spectroscopy was demonstrated as early as 1952 by Miller and Wilkins. Since that time several compilations of spectra of inorganic compounds have been published (Nyquist and Kagel, 1971; Brügel, 1962; Bentley et al., 1968). The useful region for identification of inorganic ionic species is 1500 to 300  $\text{cm}^{-1}$ . Absorption in this region results from the stretching and bending vibrations of bonds in the individual ions. Ionic groups such as sulfate, sulfite or carbonate exhibit characteristic frequency ranges at which they absorb, the actual frequency being somewhat affected by the cations present. Quantitative analysis of inorganic species is limited by methods of sample preparation. The main complications arising from the samples being solid and for the most part insoluble in nonaqueous solvents. The characteristic absorption wavelengths for species which may occur during reduction of sulfates are shown in Fig. 5.1.

### 5.1.2. Fourier Transform Infrared Spectroscopy

A complete description of the theory of FTIR and its advantages over other infrared spectroscopy is given elsewhere (Griffiths, 1978). Briefly, FTIR's use of an interferometer with polychromatic radiation instead of a grating which selects wavelengths allows for faster scanning of the sample with equal

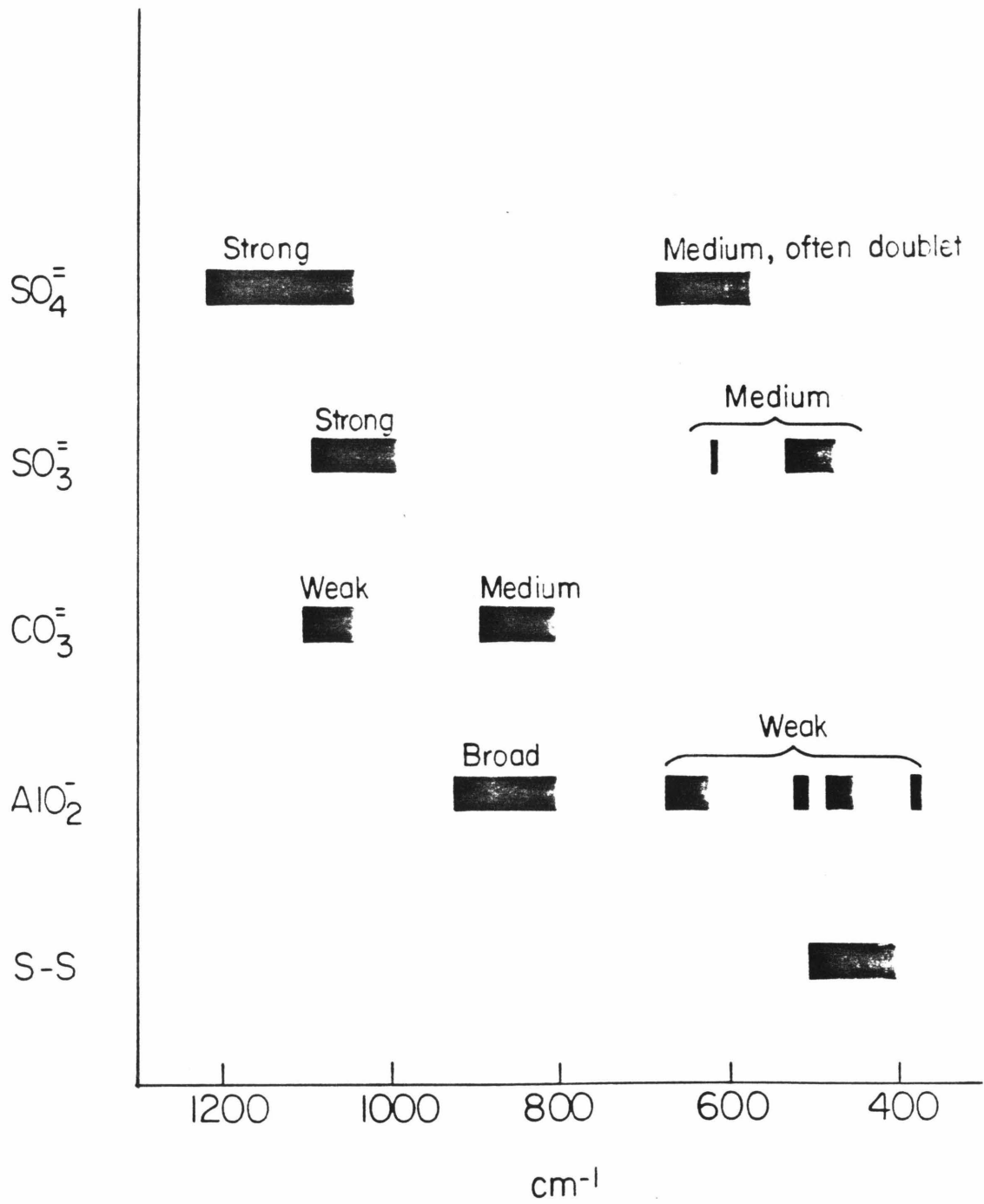


Figure 5.1: Characteristic Wavelengths of Absorption

resolution. In addition, the FTIR has a dedicated computer system associated with it so that signal averaging over several runs can be accomplished, allowing for an increased signal-to-noise ratio. Moreover, the computer allows for addition or subtraction of absorption spectra. This is valuable in analyses of complicated mixed samples.

## **5.2. Experimental Conditions and Sample Preparation**

Samples of resulfated, reduced and partially reduced  $\text{NaLiSO}_4/\alpha$ -alumina sorbent were analyzed by FTIR. The reductions were carried out in 10%  $\text{CO}$ , .55%  $\text{CO}_2$  at either 700 or 800°C. Sulfations were carried out using 1%  $\text{SO}_2$  and air at 700 and 800°C, after reduction for 20 minutes at the same temperature.

### **5.2.1. Sample Preparation**

Samples were prepared by exposure to the appropriate conditions in the TGA system. The samples were then cooled in  $\text{N}_2$  flow to room temperature. The cooling in  $\text{N}_2$  prevented oxidation of the species, which would have occurred if exposed to air at high temperatures. The cooling time under  $\text{N}_2$  was sufficient for removal of absorbed species. After preparation and cooling to ambient temperatures, the samples were ground and made into a mull with nujol. This mull was then pressed between KBr windows.

### **5.2.2. Spectrometry**

The spectrometry was carried out on a Mattson Sirius 100 FTIR using a TGS detector. Signal averaging was used with 512 scans. The scans were taken over a range of 4000-400  $\text{cm}^{-1}$ . With the aid of the computer the spectra of each of the samples was normalized by subtracting the spectra of  $\alpha$ -alumina. All spectra are reported in terms of absorbance vs. wavelength

instead of the more common transmittance vs. wavelength, as these subtractions are carried out on absorbance spectra. The normalized spectra were compared to known absorption bands (Fig. 5.1). The spectra are somewhat difficult to decipher because of shifting baselines. Variation in the sample mull preparation also caused difficulty in comparing spectra. Only qualitative analysis was performed.

### 5.3. Results and Discussion

#### 5.3.1. Resultated Samples

The fresh unreacted sulfate was compared to samples which had been reduced and resultated at either 700 or 800°C (Fig. 5.2). Both of the resultated samples show absorption at  $1150\text{ cm}^{-1}$ , indicating sulfate is reformed on sulfation after reduction. There is also, however, slight absorption at  $\approx 980\text{ cm}^{-1}$ , indicating some sulfite may have been formed. No significant difference is seen between the sample resultated at 700°C and the sample resultated at 800°C.

#### 5.3.2. Reduction at 800°C

The spectra of samples partially reduced at 800°C are shown in Fig. 5.3. Disappearance of the band due to sulfate ( $1150\text{ cm}^{-1}$ ) occurs between one and four minutes of reduction. A band at  $\approx 980\text{ cm}^{-1}$ , which would correspond to sulfite, is evident at one minute reduction. Aluminate formation would be evidenced by a broad band from  $800\text{--}920\text{ cm}^{-1}$ , and several weak bands ( $\approx 650$ ,  $\approx 510$ ,  $\approx 460\text{ cm}^{-2}$ ). No broad peak is observed but a peak does appear at  $510\text{ cm}^{-1}$  and many split peaks appear between  $450$  and  $500\text{ cm}^{-1}$ . There is, therefore, some evidence of aluminate formation. A very sharp peak at  $420\text{ cm}^{-1}$  develops between 4 and 10 minutes reduction. This band is difficult to assign but may be due to S-S stretching. Bands which

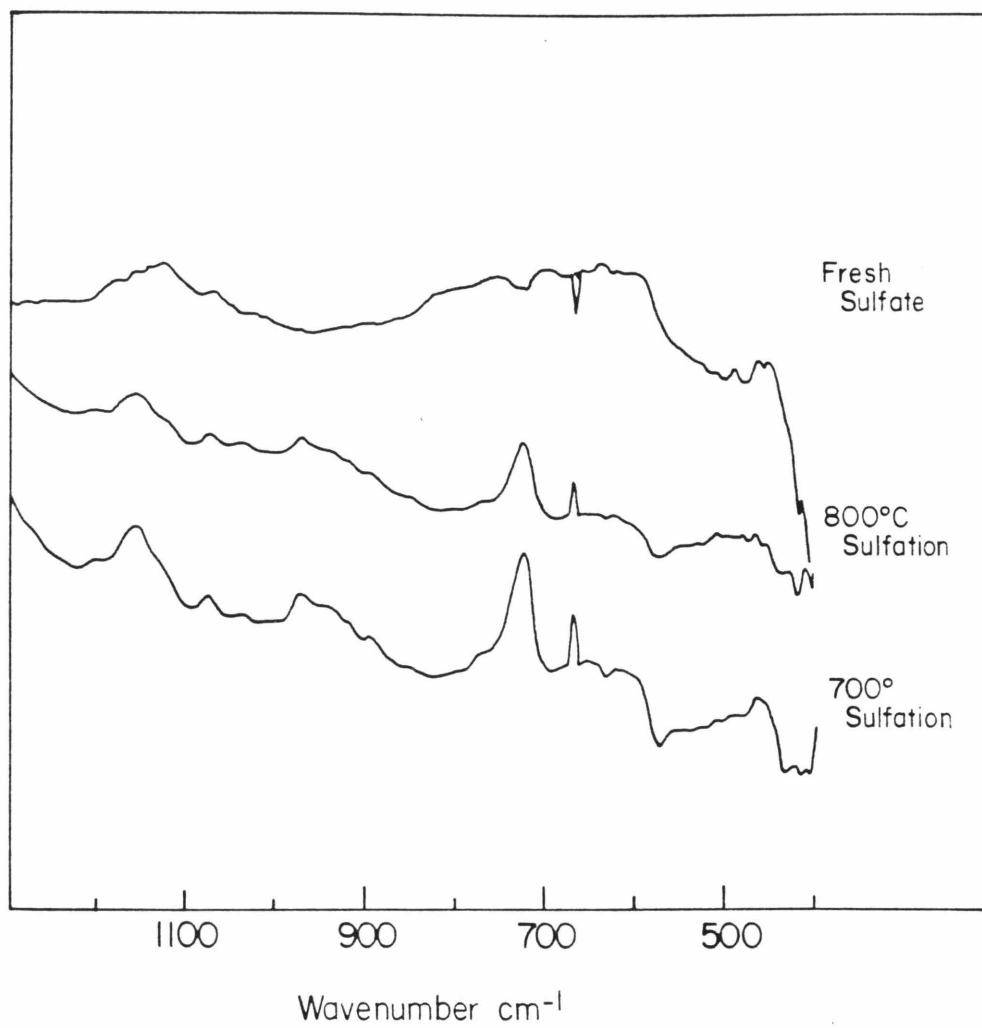


Figure 5.2: Spectra of Sulfated Samples

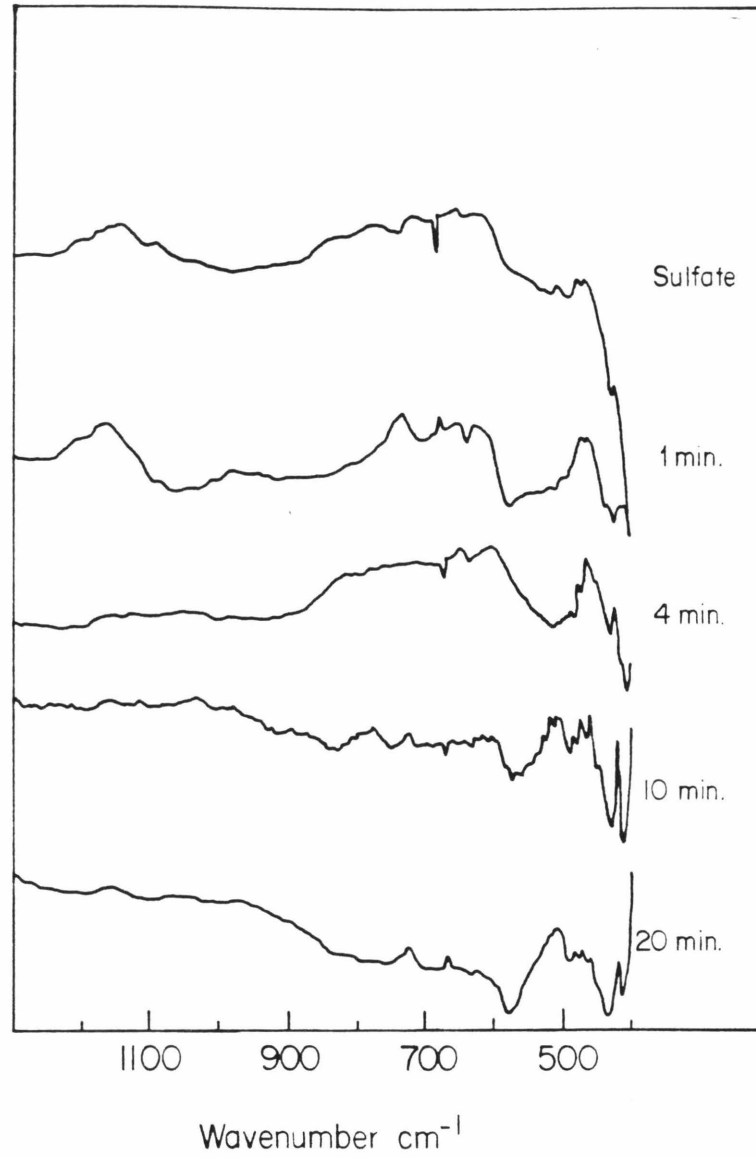


Figure 5.3: Spectra of Samples Reduced and Partially Reduced at  $800^{\circ}\text{C}$

would be produced by carbonate are not seen in any of the spectra. Carbonate may, however, have decomposed during the sample treatment after reduction.

### 5.3.3. Reduction at 700°C

The spectra of samples partially reduced at 700°C are shown in Fig. 5.4. Results are similar to those of the samples reduced at 800°C. The sulfate band ( $1150\text{ cm}^{-1}$ ) is observable at 2 minutes reduction. Absorbance due to sulfite is also observable at 2 minutes reduction. These bands diminish through further reduction. The time at which they completely disappear is difficult to determine because of the variance between the baselines of spectra and the subtracted alumina sample. Slight absorbance due to aluminate formation is observable, but is not as prominent as with reduction at 800°C. Again, no absorption due to carbonate is observed at any time.

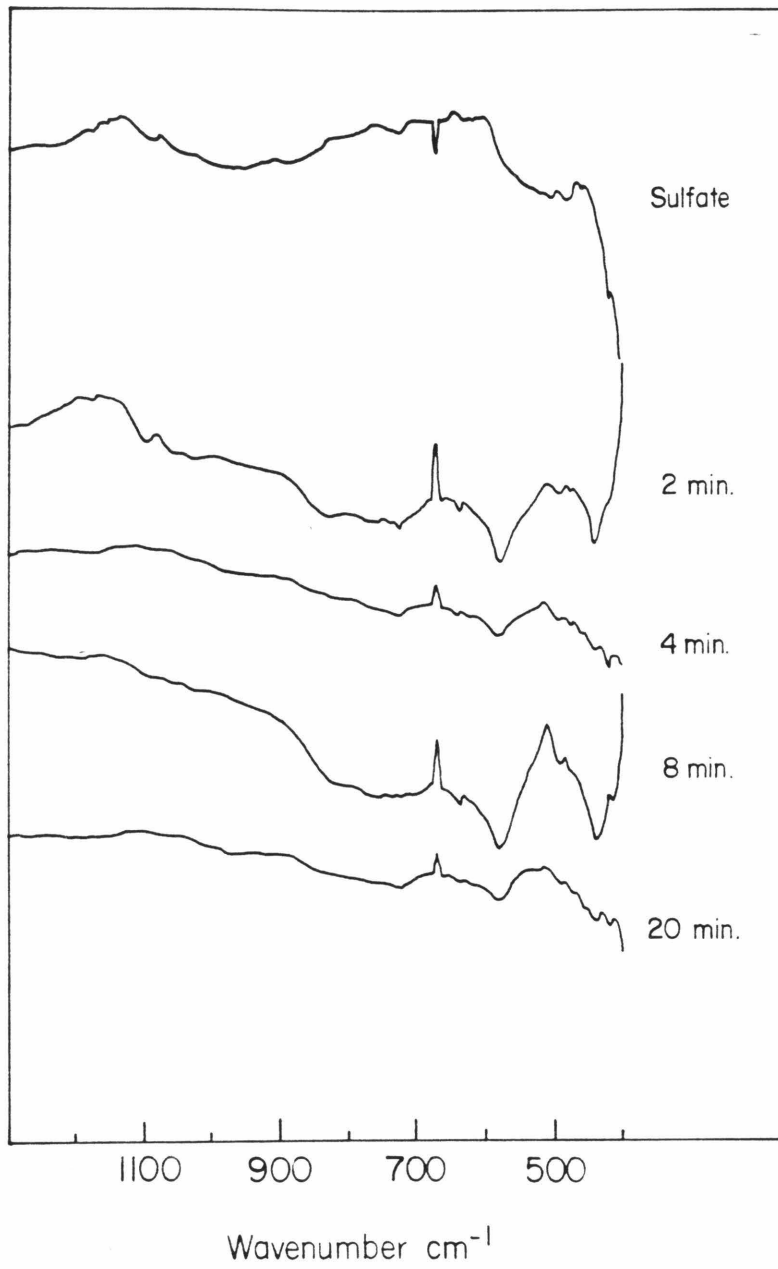


Figure 5.4: Spectra of Samples Reduced and Partially Reduced at  $700^{\circ}\text{C}$

**References**

1. Bentley, F. F., L. D. Smithson and A. L. Rozek, *Infrared Spectra and Characteristic Frequencies ~700-300 cm<sup>-1</sup>*, Interscience Publishers, John Wiley and Sons, 1968.
2. Brugel, W., *An Introduction to Infrared Spectroscopy*, John Wiley and Sons, New York, 1962.
3. Griffiths, P. R., ed., *Transform Techniques in Chemistry*, Plenum Press, New York, 1978.
4. Kolesova, V. A., "Infrared Absorption Spectra of Synthetic Aluminates of the Alkali and Alkaline-Earth Metals," *Spek. Akad. Nauk. SSSR* **10**, 209 (1961).
5. Miller, F. A. and C. H. Wilkins, "Infrared Spectra and Characteristic Frequencies of Inorganic Ions," *Anal. Chem.* **24**(8), 1253 (1952).
6. Nyquist, R. A. and R. O. Kagel, *Infrared Spectra of Inorganic Compounds*, Academic Press, New York, 1971.

CHAPTER 6

MICROREACTOR EXPERIMENTS

### 6.1. Introduction

Parallel experiments to those conducted in the thermogravimetric analyzer system were conducted using a small packed bed reactor. The results from this system show the effect of secondary reactions between sorbent materials and gaseous products moving through the bed. This system, therefore, is an attempt to study how secondary reactions might affect the sorbent regeneration in a real process. This system was also used to study the interaction of gaseous products with the support materials alone.

### 6.2. Experimental System

The flow microreactor system, shown in Fig. 6.1, was composed of a vertical fixed bed reactor and a Hewlett Packard 5750 gas chromatograph with a flame photometric detector. The flow microreactor system consisted of a .8 cm ID quartz tube mounted vertically in an electric tube furnace (Fig. 6.2). The bed of 1.5 to 2 grams of sample was held in place in the center of the tube by a quartz frit and quartz wool. The temperature of the bed was monitored using a type K (chromel/alumel) thermocouple inserted within a .3 cm OD quartz thermal well which was imbedded in the solid sample. The thermal well arrangement enabled the temperature to be read at different points in the bed. A typical temperature profile at reaction temperature is shown in Fig. 6.3. Temperatures varied  $\pm 10^{\circ}\text{C}$  over the bed length.

The flow of reactant gases was measured using calibrated gas flow meters. The reactant stream could bypass the reactor so that the concentration of the stream's sulfur components could be measured by the gas chromatograph.

Elemental sulfur produced during reactions was collected in traps immersed in an ice bath. All lines between the reactor and the sulfur trap

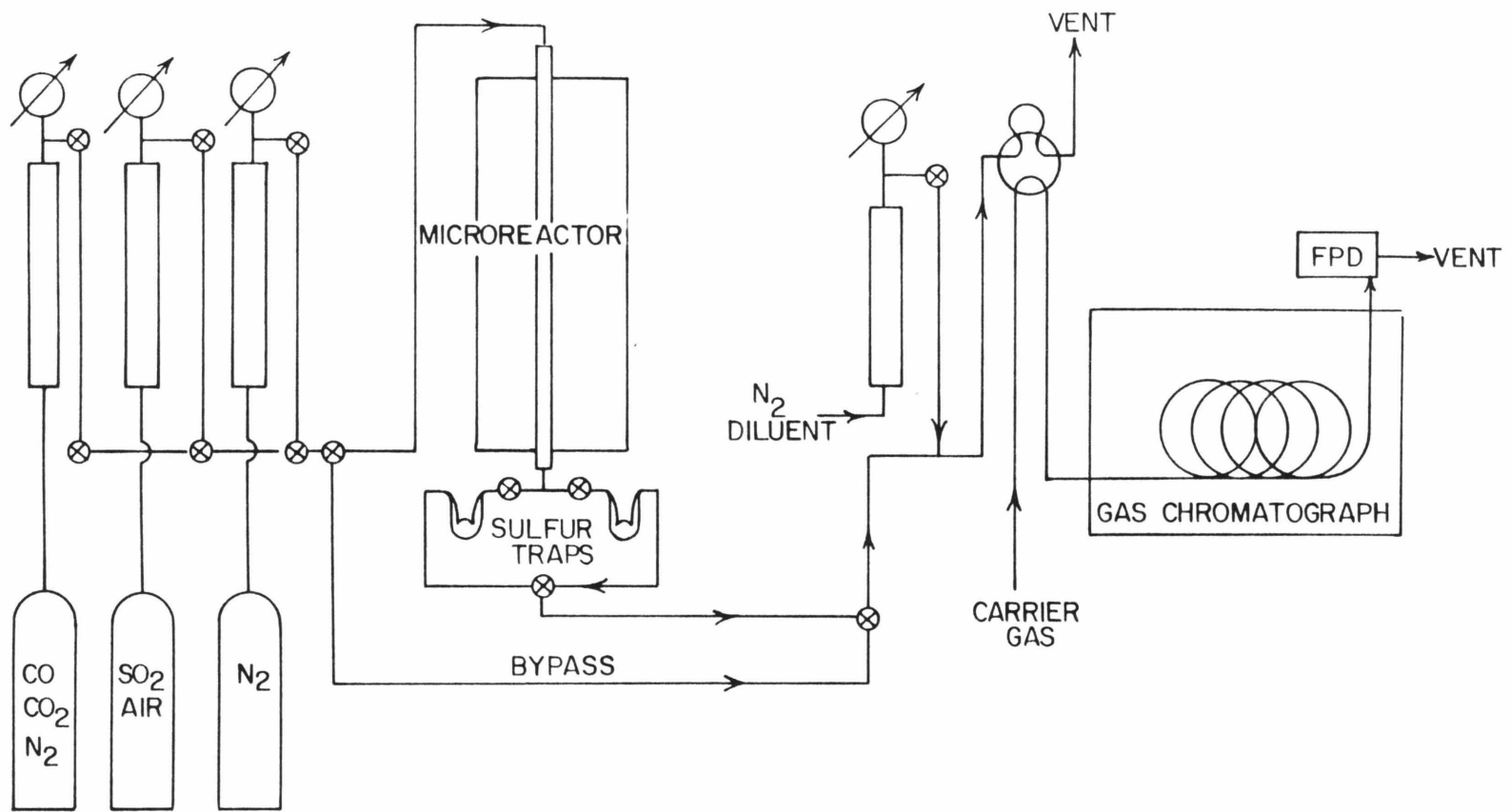


Figure 6.1: Microreactor System

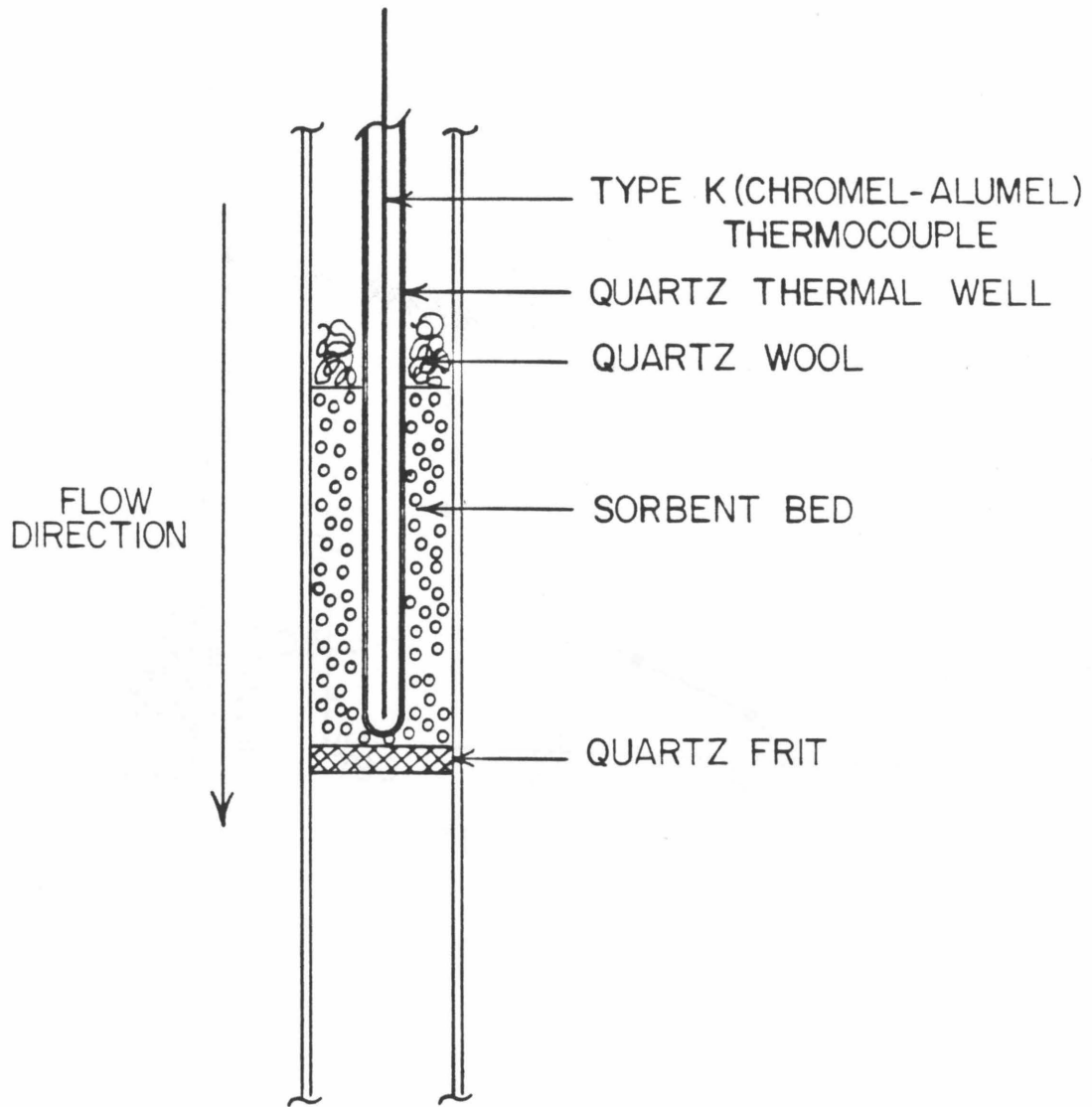


Figure 6.2: Detail of Microreactor

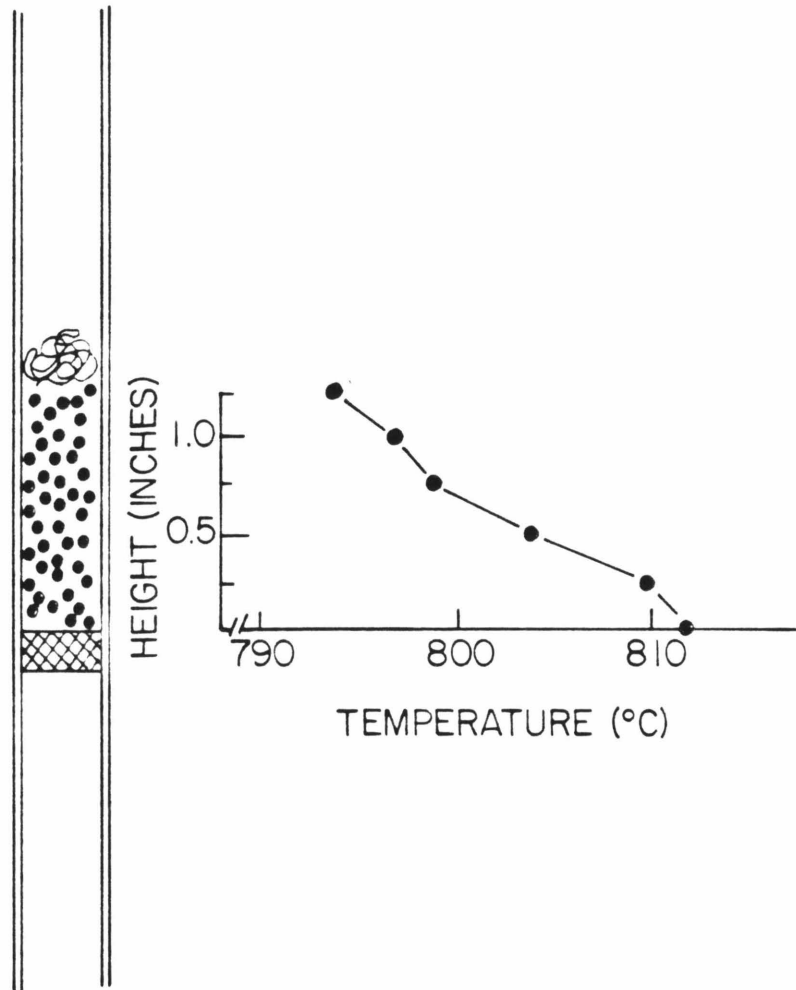


Figure 6.3: Temperature Profile of Reactor Bed

were heated to prevent condensation of sulfur before the trap. An alternate trap arrangement was used so traps could be switched during experimental runs. Sulfur collected in the traps was measured by weighing the traps before and after each experiment.

COS and SO<sub>2</sub> were determined using gas chromatography. As concentrations of product gas exiting the reactor were at times in excess of those the detector was able to handle, the exit stream was diluted with N<sub>2</sub> prior to injection into the chromatograph. The column used was a Supelco 6 ft. x 1/8 in. Chromosil 310 column. The column was used isothermally at 60°C with a helium carrier gas flow of 60 ml/min. Each analysis required 2 to 3 minutes depending on the concentration of SO<sub>2</sub> which elutes last.

### **6.3. Experimental Conditions**

#### **6.3.1. Sorbent Reduction**

Experiments were run by cycling the sorbents first through reduction and then through sulfation. A N<sub>2</sub> purge was run between reduction and sulfation. Elemental sulfur was collected during reduction and during the N<sub>2</sub> purge following reduction. SO<sub>2</sub> and COS production measured by the gas chromatograph were integrated to determine the total amount of SO<sub>2</sub> and COS produced during a reduction period. The elemental sulfur, SO<sub>2</sub> and COS produced during reduction and the sulfur produced during the nitrogen purge were totaled, and this total subtracted from the initial amount of sulfur on the sorbent to determine the amount of sulfur remaining on the sorbent at the conclusion of a reduction-N<sub>2</sub> purge period. Two reduction gases were used routinely: 10% CO, .55% CO<sub>2</sub> in N<sub>2</sub>, and 1% CO, .17% CO<sub>2</sub> in N<sub>2</sub>. Sulfation was accomplished using 3% SO<sub>2</sub> in air.

### 6.3.2. Support Catalysis

Experiments to determine the catalytic activity of the supports were conducted. Gas containing CO, at 12 or 1%, and SO<sub>2</sub>, at approximately 2000 ppm, was passed through a bed of support material. The products, SO<sub>2</sub> and COS, were measured continuously and elemental sulfur was measured at the end of the run.

## 6.4. Reduction Results and Discussion

### 6.4.1. Results

#### 6.4.1a. $\alpha$ -Alumina Supported Sorbents

The microreactor was used to examine the effect of temperature and CO concentration on the reduction process. The Na<sub>2</sub>SO<sub>4</sub>/ $\alpha$ -Al<sub>2</sub>O<sub>3</sub> sorbent was reduced at 800°C with 1 and 10% CO. The NaLiSO<sub>4</sub>/ $\alpha$ -Al<sub>2</sub>O<sub>3</sub> sorbent was reduced at both 700 and 800°C with 1 and 10% CO. The production of SO<sub>2</sub> and COS under each of these reduction conditions is shown in Figs. 6.4 through 6.9. For the purpose of presentation, the cumulative amount of sulfur measured at the end of the experiment is reported in the form of an average rate, constant throughout the reduction period. The gas production is reported in terms of moles per mole of initial sulfate per minute. Table 6.1 shows the total amount of SO<sub>2</sub>, COS and sulfur produced. Table 6.1 also shows the amount of sulfur produced during the nitrogen purge immediately following the reduction period. Significant amounts of sulfur were produced during this nitrogen purge. Although the rate of product generation is slower, the time dependence of gas production is similar to that in the thermogravimetric experiments. The major gas product switches from SO<sub>2</sub> to COS and the switch-over time varies greatly with CO concentration at 800°C. During the reduction of the sodium sorbent at 800°C, the switch-over time is

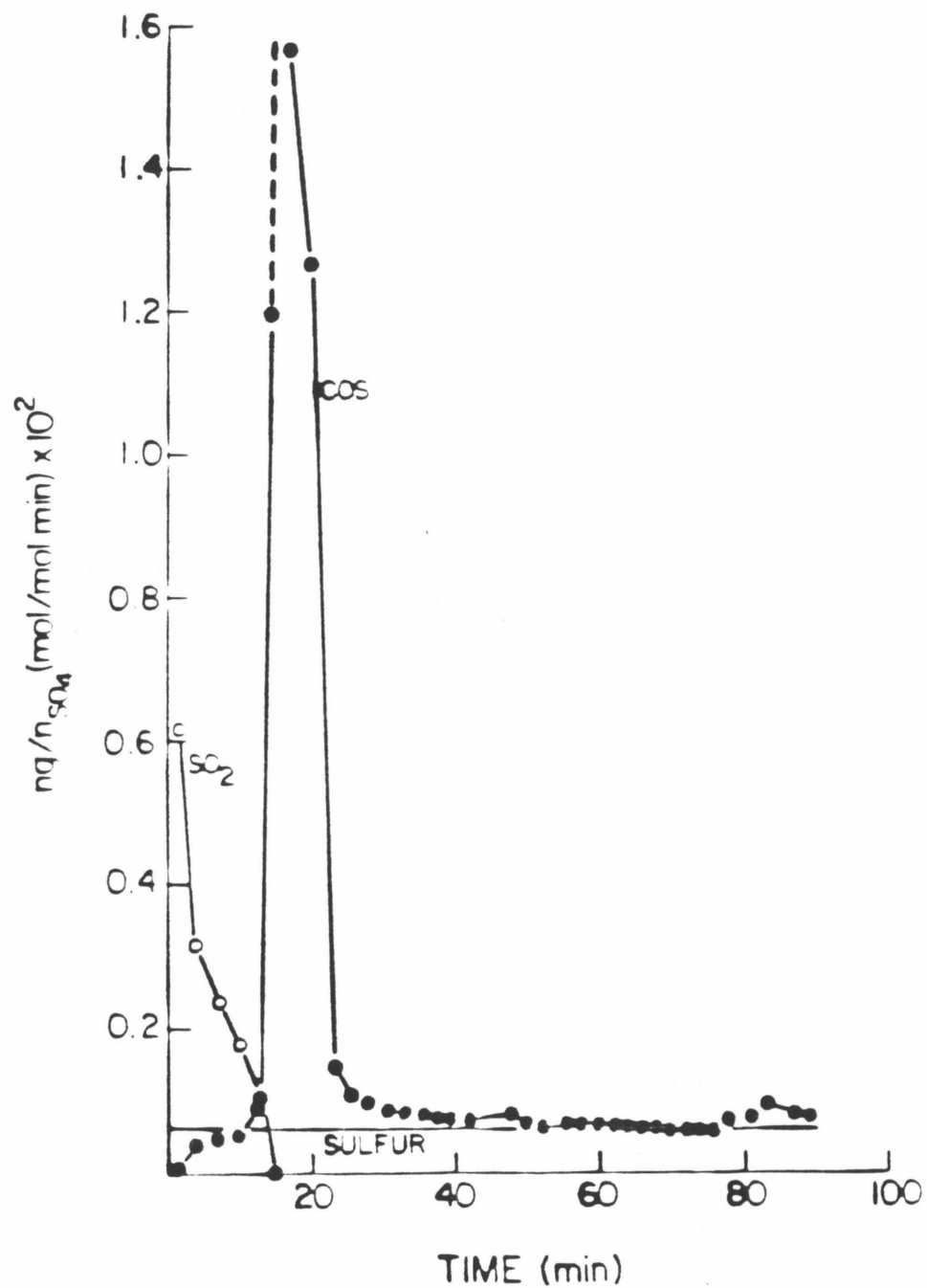


Figure 6.4: Reduction of  $\text{Na}_2\text{SO}_4/\alpha\text{-Al}_2\text{O}_3$  with 10% CO at  $800^\circ\text{C}$  Using the Microreactor System

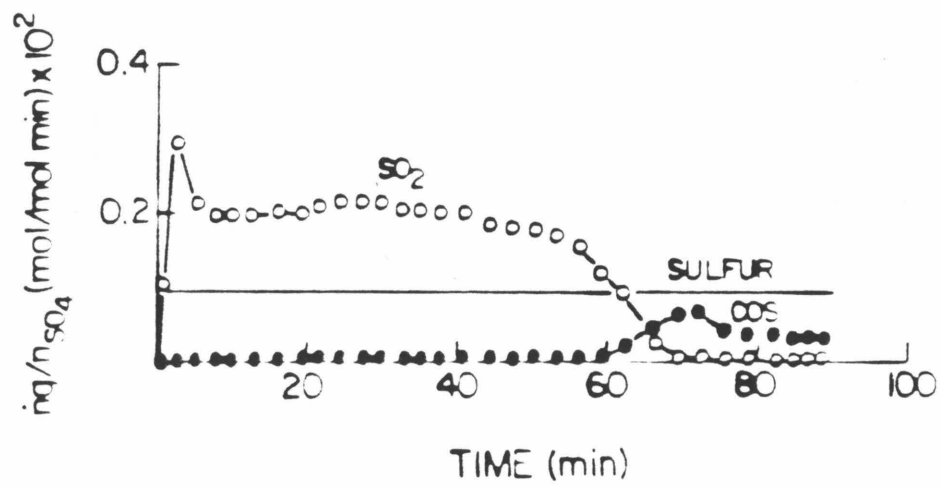


Figure 6.5: Reduction of  $\text{Na}_2\text{SO}_4/\gamma\text{-Al}_2\text{O}_3$  with 1% CO at  $800^\circ\text{C}$  Using the Microreactor System

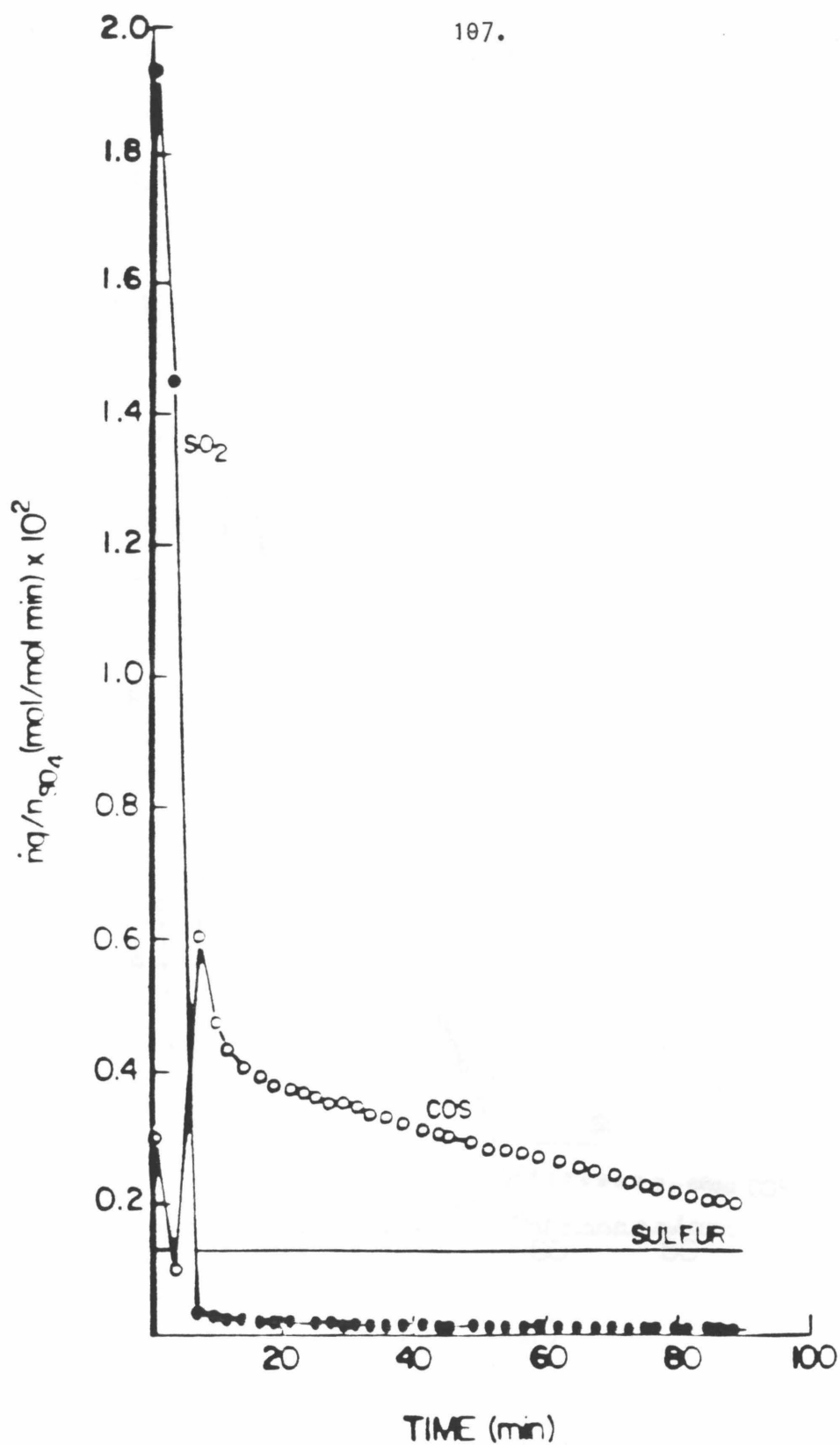


Figure 6.6: Reduction of  $NaLiSO_4/\alpha-Al_2O_3$  with 10% CO at 800°C Using the Microreactor System

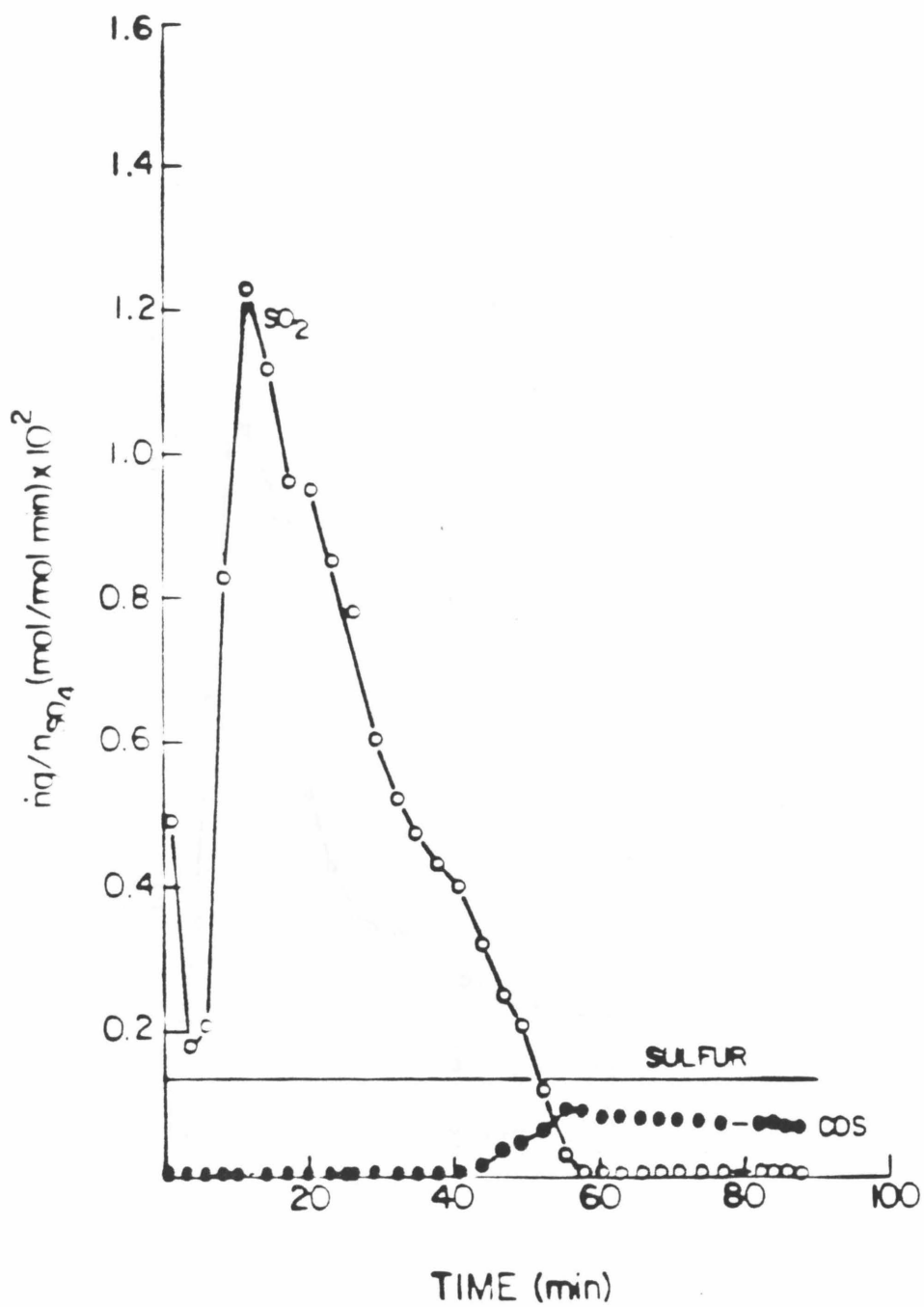


Figure 6.7: Reduction of  $\text{NaLiSO}_4/\alpha\text{-Al}_2\text{O}_3$  with 1% CO at  $800^\circ\text{C}$  Using the Microreactor System

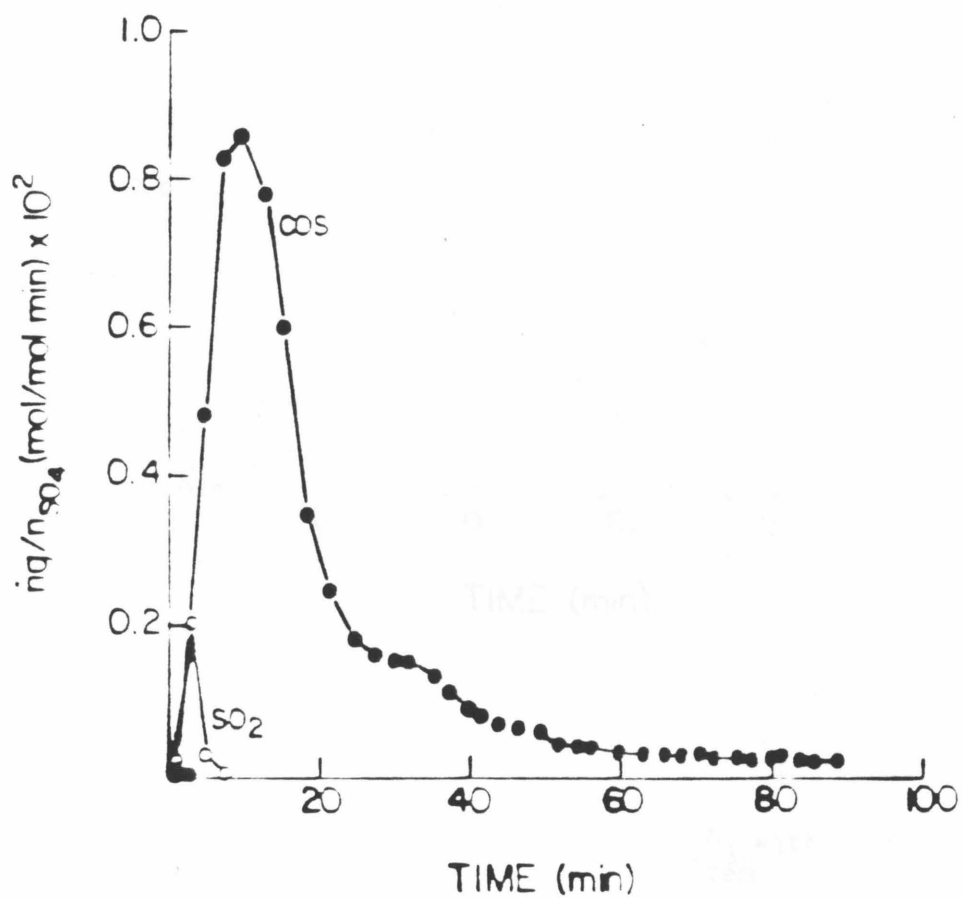


Figure 6.8: Reduction of  $NaHSO_4/\alpha-Al_2O_3$  with 10% CO at 700°C Using the Microreactor System

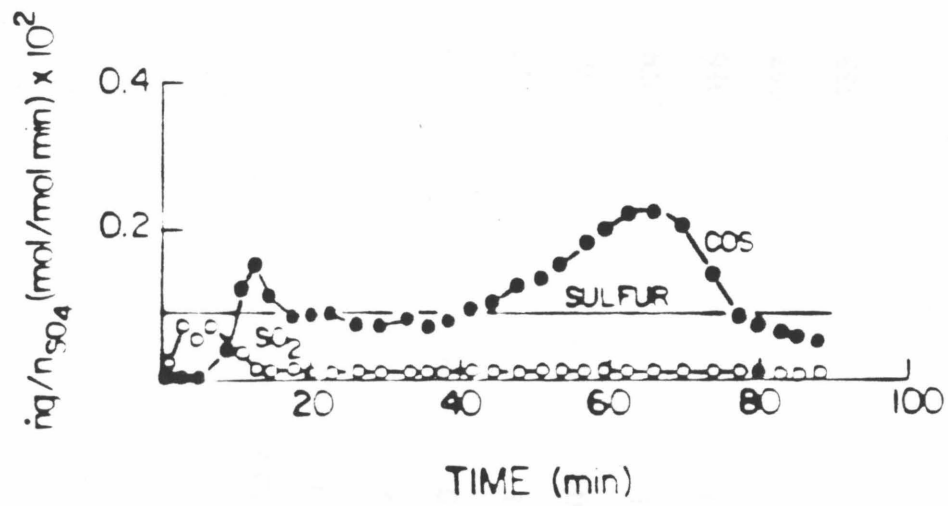


Figure 6.9: Reduction of  $\text{NaLiSO}_4/\alpha\text{-Al}_2\text{O}_3$  with 1% CO at 700°C Using the Microreactor System

Table 6.1: Product Selectivity of Sorbents Reduced Using the Microreactor System (t = 90 min)

<u>Sorbent</u>	<u>T(°C)</u>	<u>CO(%)</u>	<u>Products (mol/mol SO<sub>4</sub>)</u>				
			<u>SO<sub>2</sub></u>	<u>COS</u>	<u>S</u>	<u>S<sub>purge</sub></u>	<u>S<sub>in sorbent</sub></u>
Na <sub>2</sub> SO <sub>4</sub> /αAl <sub>2</sub> O <sub>3</sub>	800	10	.0356	.177	.054	.146	.59
Na <sub>2</sub> SO <sub>4</sub> /αAl <sub>2</sub> O <sub>3</sub>	800	1	.122	.016	.085	.060	.72
NaLiSO <sub>4</sub> /αAl <sub>2</sub> O <sub>3</sub>	800	10	.097	.269	.113	.132	.39
NaLiSO <sub>4</sub> /αAl <sub>2</sub> O <sub>3</sub>	800	1	.316	.034	.122	.080	.45
NaLiSO <sub>4</sub> /αAl <sub>2</sub> O <sub>3</sub>	700	10	.011	.279	0	.332	.38
NaLiSO <sub>4</sub> /αAl <sub>2</sub> O <sub>3</sub>	700	1	.014	.097	.079	.241	.57
NaLiSO <sub>4</sub> /ZrO <sub>2</sub>	800	10	.177	.045	.016	.252	.51
NaLiSO <sub>4</sub> /ZrO <sub>2</sub>	700	10	.003	.267	.057	.040	.63
NaLiSO <sub>4</sub> /SiO <sub>2</sub>	800	10	.156	.006	.035	.014	.79

13 minutes and 62 minutes for 10% and 1% CO, respectively. The sodium-lithium sorbent shows the same trend at 800°C. At 700°C the switch-over time is much less sensitive to the CO concentration. At 800°C the initial SO<sub>2</sub> production is much higher for the NaLiSO<sub>4</sub> sorbent than for the Na<sub>2</sub>SO<sub>4</sub> sorbent.

Reducing the CO concentration drastically altered the product distribution between SO<sub>2</sub>, COS and elemental sulfur, increasing both the SO<sub>2</sub> and elemental sulfur formed. Reducing the CO concentration also reduced the overall sulfur removal from the sorbent.

Temperature effects were observed in experiments with the sodium lithium sorbent. Reducing the temperature to 700°C greatly decreased the elemental sulfur and SO<sub>2</sub> produced.

Sulfur was also produced during the nitrogen purge following reduction. The amount of sulfur produced during this purge varied with the reduction conditions, but did not appear to be affected by the sorbent material reduced. The sulfur production during the nitrogen purge increased with increasing CO concentration, and with decreasing temperature.

#### **6.4.1b. Silica and Zirconia Supported Sorbents**

To investigate the effect of the support material on the reduction porous silica and zirconia impregnated with sodium-lithium sulfate were reduced using 10% CO, .5% CO<sub>2</sub> in N<sub>2</sub> at 800°C (Figs. 6.10, 6.11). The NaLiSO<sub>4</sub>/ZrO<sub>2</sub> sorbent was also reduced with 10% CO at 700°C (Fig. 6.12).

The reduction of the NaLiSO<sub>4</sub>/SiO<sub>2</sub> sorbent differed greatly from that of the NaLiSO<sub>4</sub>/α-Al<sub>2</sub>O<sub>3</sub> sorbent. SO<sub>2</sub> was the major product throughout the entire reduction of the silica sorbent and no switchover to COS as the major product was observed. Very little sulfur was produced during the nitrogen

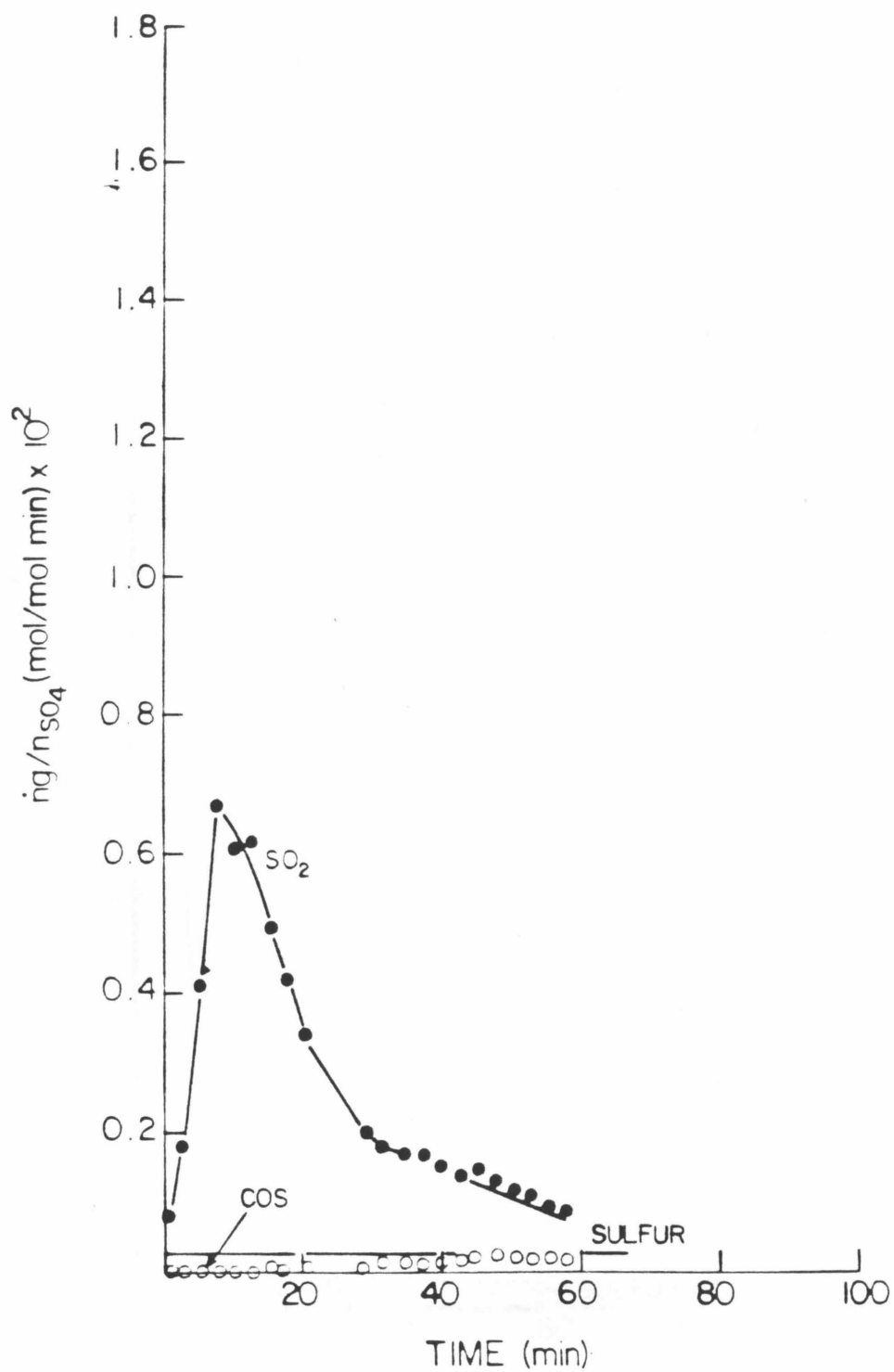


Figure 6.10: Reduction of  $NaHSO_4/SiO_2$  with 10% CO at 800°C Using the Microreactor System

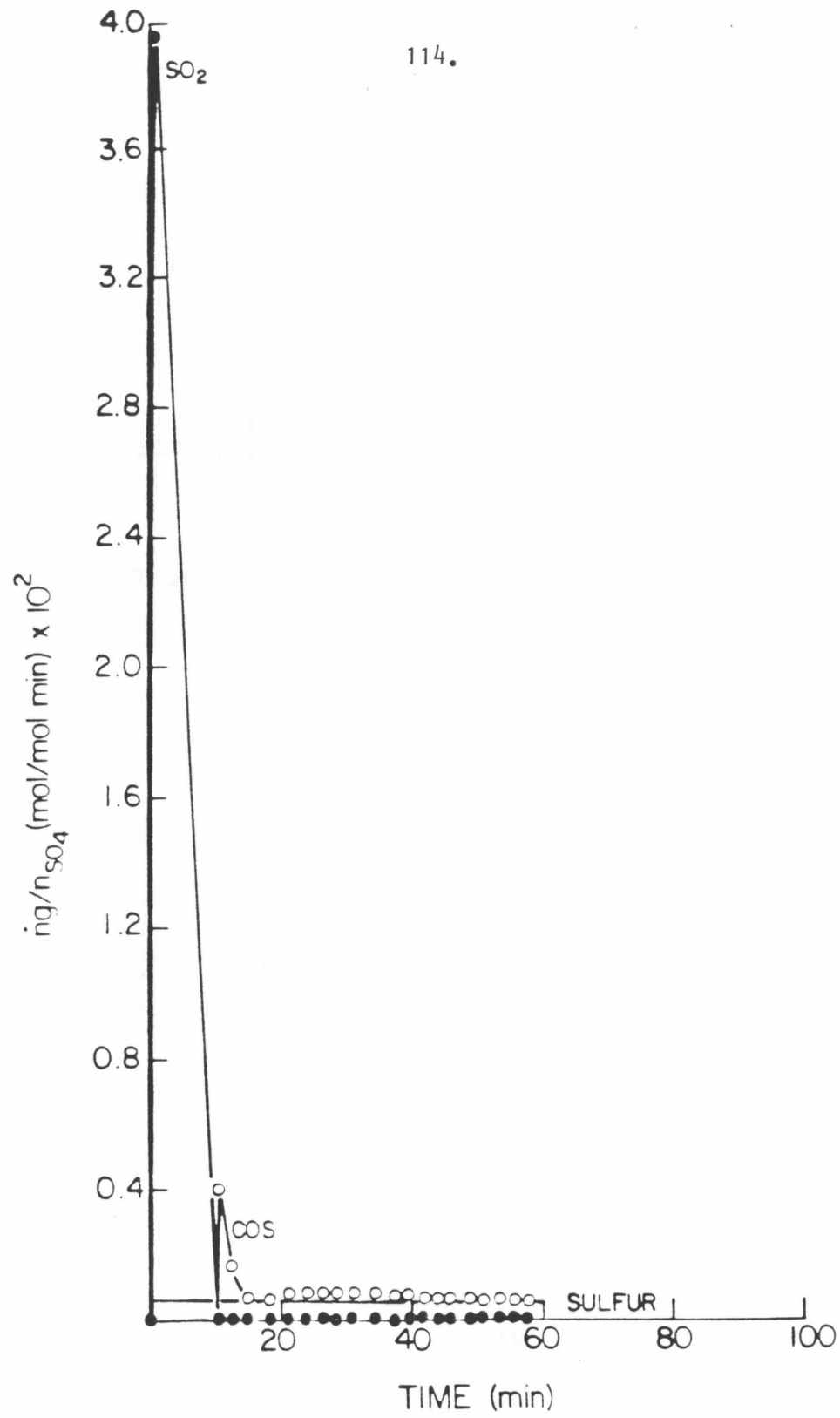


Figure 6.11: Reduction of NaLiSO<sub>4</sub>/ZrO<sub>2</sub> with 10% CO at 800°C Using the Microreactor System

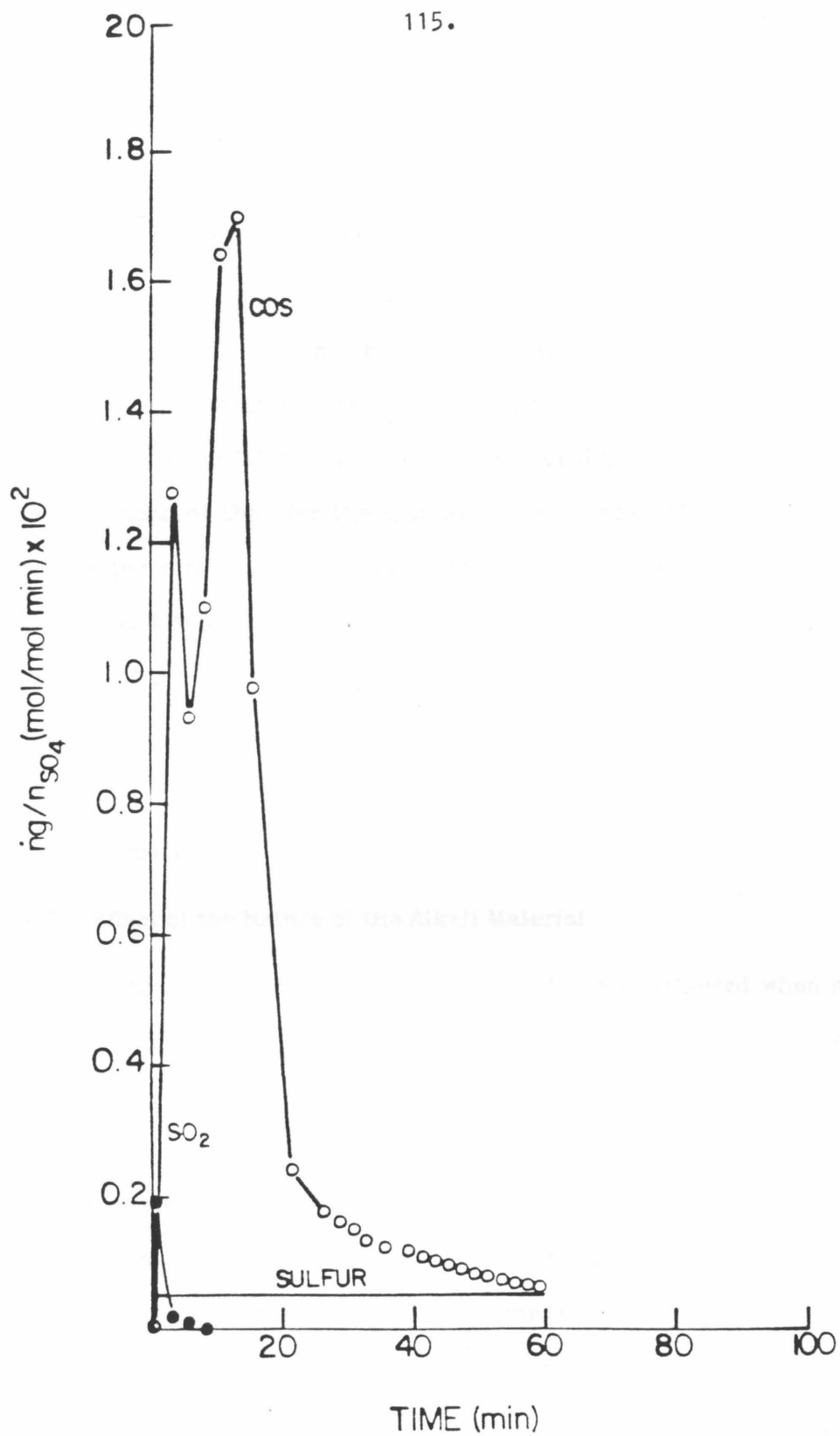


Figure 6.12: Reduction of NaLiSO<sub>4</sub>/ZrO<sub>2</sub> with 10% CO at 700°C Using the Microreactor System

purge following reduction (Table 6.1). A more significant difference between these two sorbents was the inability of the reduced silica sorbent to readsorb  $\text{SO}_2$  and  $\text{O}_2$ . This inability eliminates silica as a possible support for regenerable sorbent.

The  $\text{NaLiSO}_4/\text{ZrO}_2$  sorbent behaved in a similar manner to the  $\text{NaLiSO}_4/\alpha\text{-Al}_2\text{O}_3$  sorbent at both 700 and 800°C, although some differences were observed. At 800°C the initial production of  $\text{SO}_2$  was much higher for the zirconia sorbent than for the alumina sorbent, when the two are compared on a per mole basis. The initial production of  $\text{SO}_2$  is higher for the alumina sorbent when compared on a surface area basis (Fig. 6.13). Both COS and sulfur production were lower for the zirconia sorbent. At 700°C, the zirconia sorbent produced more sulfur than the alumina sorbent during the reduction period, but much less sulfur during the nitrogen purge.

#### **6.4.2. Discussion**

##### **6.4.2a. Effect of the Nature of the Alkali Material**

Higher sulfur removal during reduction at 800°C was achieved when sorbents contained sodium and lithium rather than just sodium. This trend is observed with reduction with either 1% or 10% CO. This may be caused by the higher relative stability of the lithium aluminate over the sodium aluminate relative to their sulfides. The relative rates of sulfide formation and aluminate formation, as controlled by diffusion through the aluminate layer, differ for the two materials, and control the initial partition between sulfide and aluminate (see Section 4.5.1).

The nature of the alkali material does not appear to affect the distribution between COS and elemental sulfur. This distribution must then be determined by another property of the sorbent material

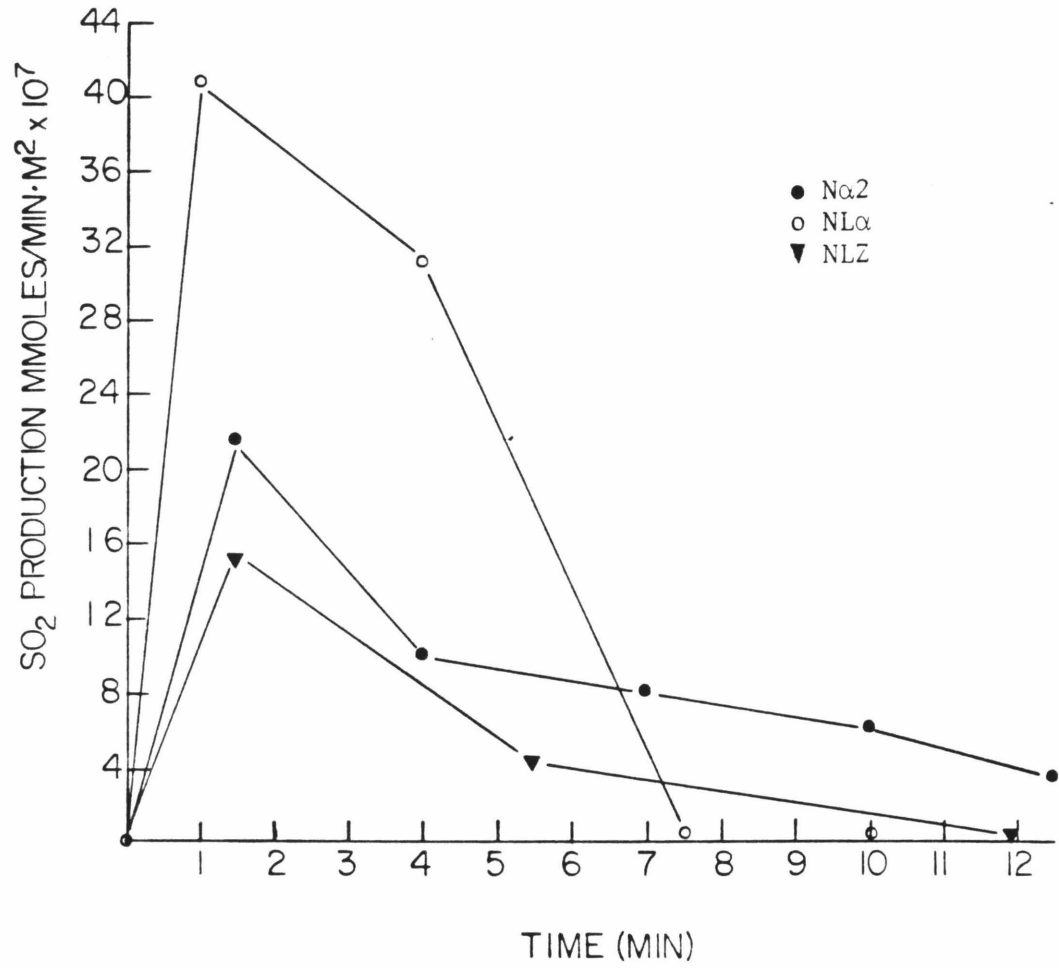


Figure 6.13: SO<sub>2</sub> Production Per Surface Area During Reduction at 800°C Using the Microreactor System

#### 6.4.2b. Effect of Support

The support used with an alkali phase of  $\text{NaLiSO}_4$  is significant. Silica, when used as a support, produced a nonregenerable sorbent. Silica in combination with oxide produced during the reduction forms a silicate which is stable to  $\text{SO}_2$  and air. Such a silicate was observed to form from sodium carbonate and silica at temperatures above  $700^\circ\text{C}$  (Cobb, 1910).

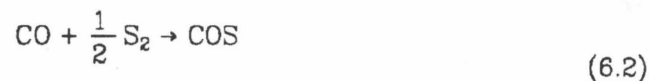
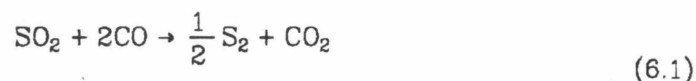
Zirconia and  $\alpha$ -alumina showed the same general behavior. Zirconia and oxide formed during reduction will combine to form "zirconates". When zirconia impregnated with sodium-lithium carbonate was heated and the weight monitored using the thermogravimetric analyzer, weight loss due to "zirconate" formation was observed. Zirconate formation must play the same role in the reduction of zirconia supported sorbents that aluminate plays in the reduction of alumina sorbents. Diffusion in the zirconate may be slower than in the aluminate as the  $\text{SO}_2$  production of the zirconia sorbent is lower.

Zirconia and  $\alpha$ -alumina differ in their catalytic and adsorptive properties. These differences seem to have little effect on the reduction at  $800^\circ\text{C}$ . The distribution between COS and elemental sulfur is approximately the same for both sorbents. The COS-elemental sulfur distribution is also approximately the same for both sorbents at  $700^\circ\text{C}$ . This is not surprising as the  $\text{CO-S}_2\text{-CO}$  reaction was found to be catalyzed by any surface at high temperatures (Haas and Khalafalla, 1973). Differences in the adsorptive properties of the two materials affect the reduction product selectivity. The sulfur produced during the nitrogen purge, although approximately the same for the two sorbents at  $800^\circ\text{C}$ , was much higher for the alumina sorbent than for the zirconia sorbent at  $700^\circ\text{C}$ . The source of this sulfur may be elemental sulfur absorbed or absorbed by the support material during reduction. At  $700^\circ\text{C}$   $\alpha$ -

alumina may be significantly more absorptive for sulfur than zirconia.

#### 6.4.2c. Effect of CO Concentration

Lowering the CO concentration being used to reduce the sulfates drastically alters the COS-elemental sulfur selectivity. Lowering the CO concentration favors the production of elemental sulfur at the expense of COS. SO<sub>2</sub> production is also greatly increased. This effect on the selectivity of the gaseous products is not surprising as they are chemically related by sequential reactions involving CO.



The most significant effect of lowering the CO concentration from 10 to 1% is the extension of the SO<sub>2</sub> production period prior to the switch-over in major gas product to COS. At 800°C this period is greatly lengthened for both sodium and sodium lithium sorbents. The sodium lithium α-alumina sorbent when reduced at 700°C did not show the same extension of SO<sub>2</sub> production. In this case, however, there is a major increase in the production of COS at approximately 40 minutes. High SO<sub>2</sub> production early in the reduction may be masked by high absorption of SO<sub>2</sub> at 700°C.

One possible explanation for the switch-over in the major gas product from SO<sub>2</sub> to COS is that a change occurs in the catalytic activity of the support during reduction. A change in activity could be caused by the accumulation of a reaction product on the surface of the support or by the disappearance of an inhibitor from the surface. Elemental sulfur has been suggested in connection with the activation of alumina for the reduction of SO<sub>2</sub> by CO (Khalafalla and Haas, 1972); sulfate removed during reduction is a

poison for Claus catalysts (Pearson, 1973).

The incorporation of alkali hydroxide into alumina Claus catalysts has been found to increase the activities of these catalysts (George, 1975). Reducing the CO concentration could decrease the rate of sulfate reduction and lengthen the period during which sulfate is in contact with the alumina surface. Both sulfur and aluminate are reduction products, and possible catalyst activators. The formation of either of these compounds would be retarded by a slower reduction rate.

#### **6.4.2d. Effect of Temperature**

Decreasing the temperature decreases the overall reaction rate of  $\alpha$ -alumina. Decreasing the temperature from 800 to 700°C increases the adsorption of SO<sub>2</sub> on  $\alpha$ -alumina, as seen in the breakthrough curves for 200 ppm SO<sub>2</sub> in N<sub>2</sub> shown in Fig. 6.14. The adsorption of sulfur may also increase significantly with decreasing temperature. The results of increased adsorption of sulfur (or of SO<sub>2</sub> which is reduced by CO to form adsorbed sulfur) can be seen in the decrease or lack of sulfur production during reaction at 700°C, and the large amount of sulfur produced during the N<sub>2</sub> purge following reduction at 700°C.

### **6.5. Support Catalysis Results and Discussion**

When COS and SO<sub>2</sub> were passed over  $\alpha$ -alumina, reaction forming COS and elemental sulfur was observed. The support material first adsorbed either SO<sub>2</sub>, or its reduction products, and as a result the SO<sub>2</sub> or COS production as measured by the gas chromatograph changed with time. After this initial break-in period, a steady state conversion was reached. When CO and SO<sub>2</sub> were passed over aluminate, a similar pattern was seen, although the break-in period was longer for the aluminate than for the alumina at 800°C. The

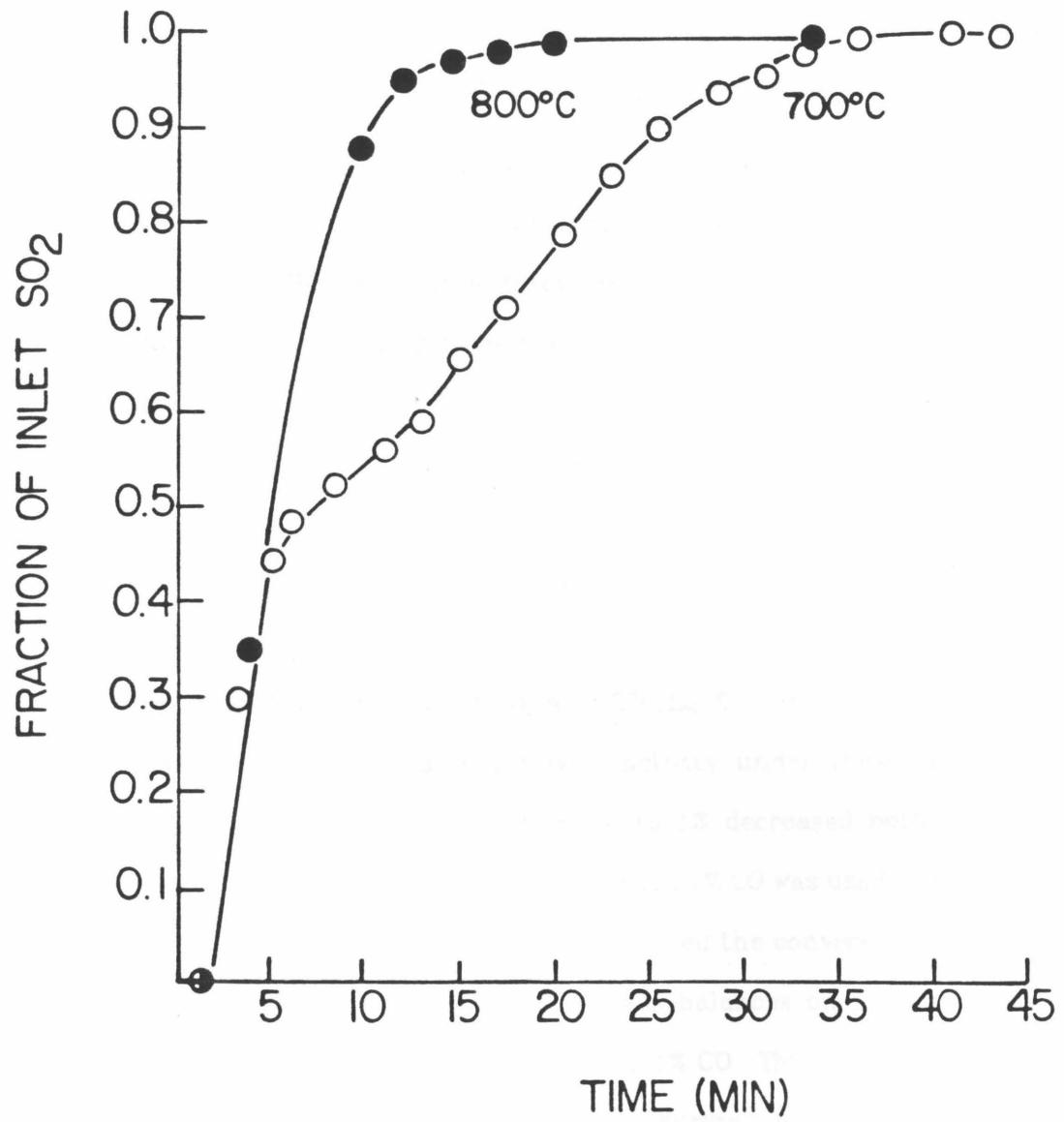


Figure 6.14: SO<sub>2</sub> Absorption by  $\alpha$ -Alumina

conversion to COS as a function of time at different temperatures and CO concentrations is shown in Figs. 6.15 through 6.18. For purposes of presentation, sulfur production is represented by an average conversion constant throughout the entire reaction period. This is probably not accurate as sulfur production most likely goes through a break-in period.

Final steady-state COS and SO<sub>2</sub> conversion and the average sulfur conversion are shown for each reaction condition in Table 6.2. Also shown are the equilibrium COS, SO<sub>2</sub> and sulfur fractions expected under reaction conditions. No SO<sub>2</sub> was predicted to be present at equilibrium under any of the reaction conditions used. Equilibrium was achieved only when 12% CO was used as the reducing gas at 800°C. Lowering the temperature from 800 to 700°C while using 12% CO increased the yield of elemental sulfur at the expense of COS, but did not decrease the total conversion of SO<sub>2</sub>. The rate of the COS formation reaction (Eq. 6.2) must therefore be more temperature dependent than the reduction of SO<sub>2</sub> with CO (Eq. 6.1) at 12% CO.  $\alpha$ -alumina and aluminate have the same catalytic activity under these conditions. Decreasing the CO concentration from 12 to 1% decreased both the total conversion of SO<sub>2</sub> and the COS formation. When 1% CO was used, lowering the temperature from 800 to 700°C greatly decreased the conversion of SO<sub>2</sub>. No COS was formed at 700°C with 1% CO. Mass balances on sulfur were not satisfied under all conditions, notably 800°C 1% CO. This is probably due to adsorption of elemental sulfur by the surface during a break-in period, which is not included in the calculation of the average conversion to sulfur.

These experiments indicate that significant reaction may occur under certain reaction conditions when gaseous products are eluting through the fixed bed reactor. These reactions may be important to the overall product selectivity. Although a break-in period prior to steady state conversion was

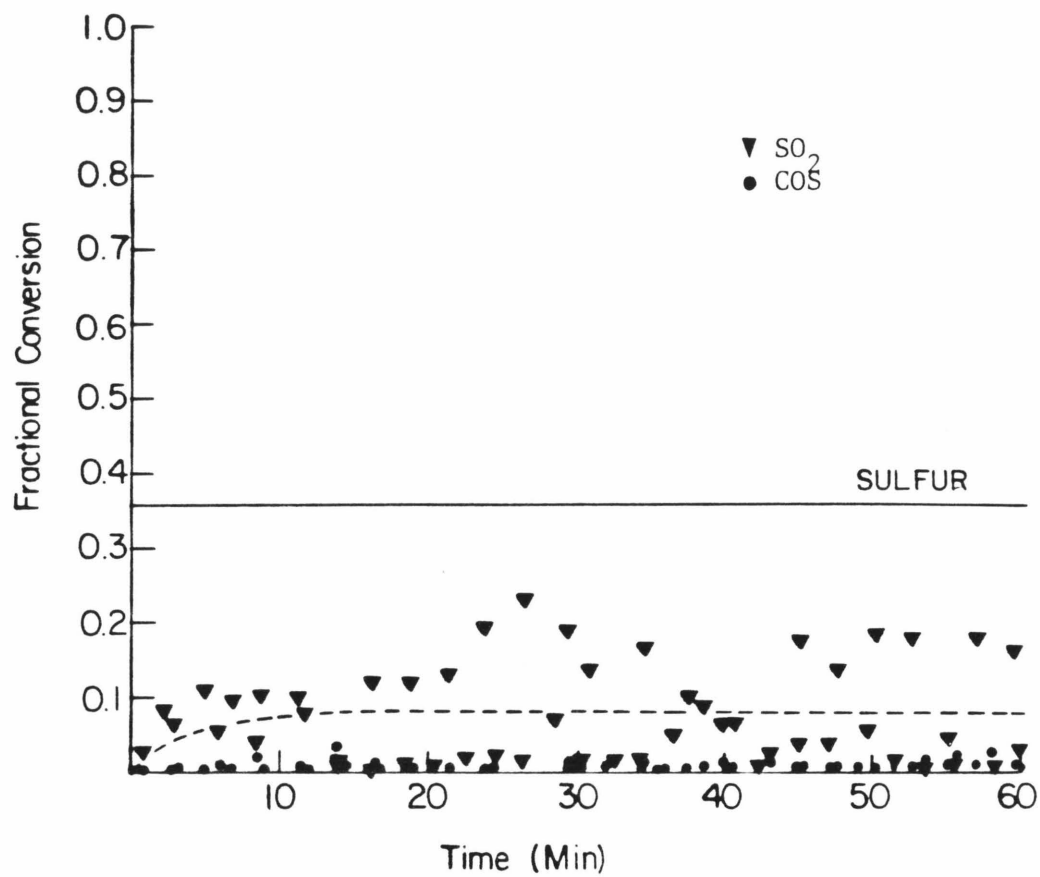


Figure 6.15: Conversion of 1% CO/2000 ppm SO<sub>2</sub> at 800°C

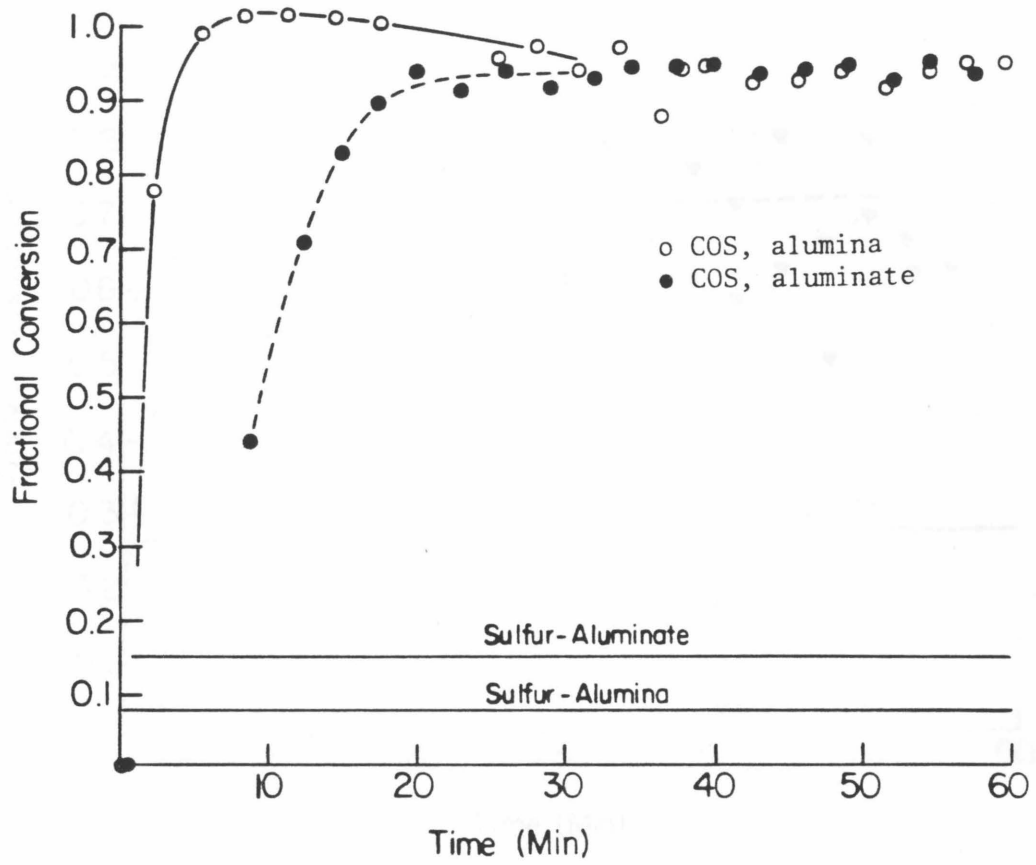


Figure 6.16: Conversion of 12% CO/2000 ppm SO<sub>2</sub> at 800°C

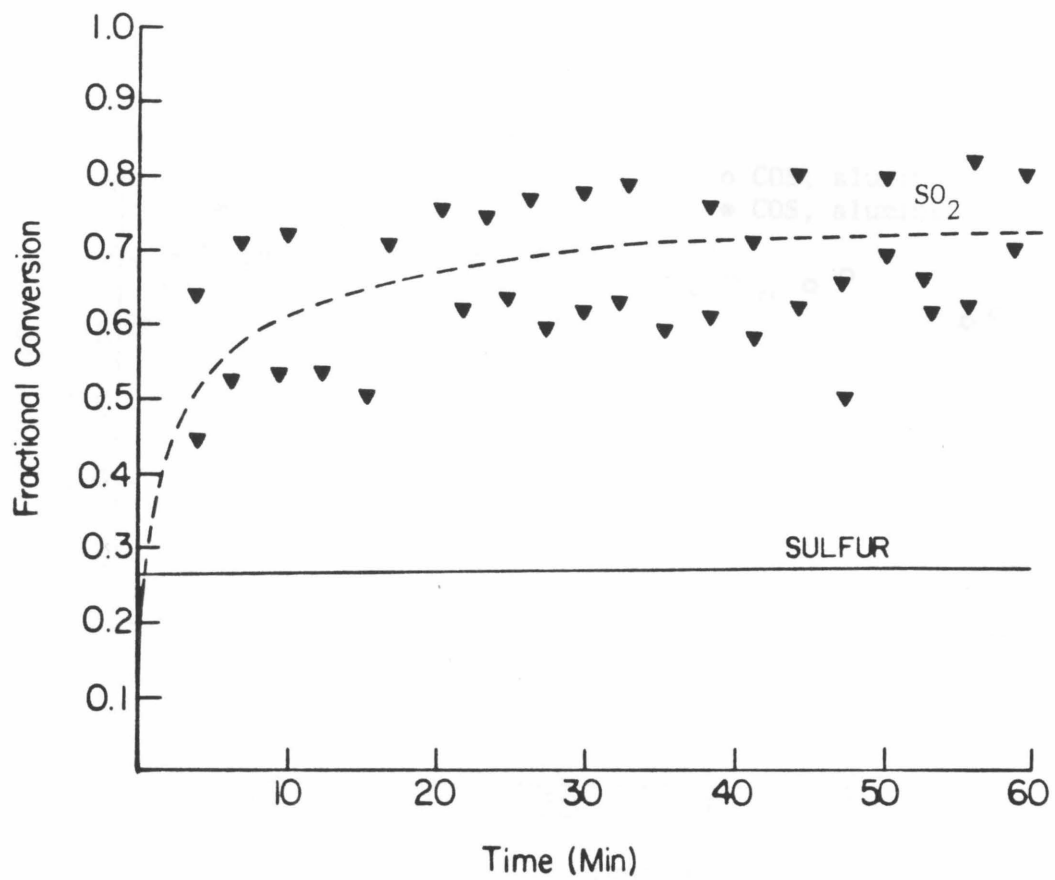


Figure 6.17: Conversion of 1% CO/2000 ppm SO<sub>2</sub> at 700°C

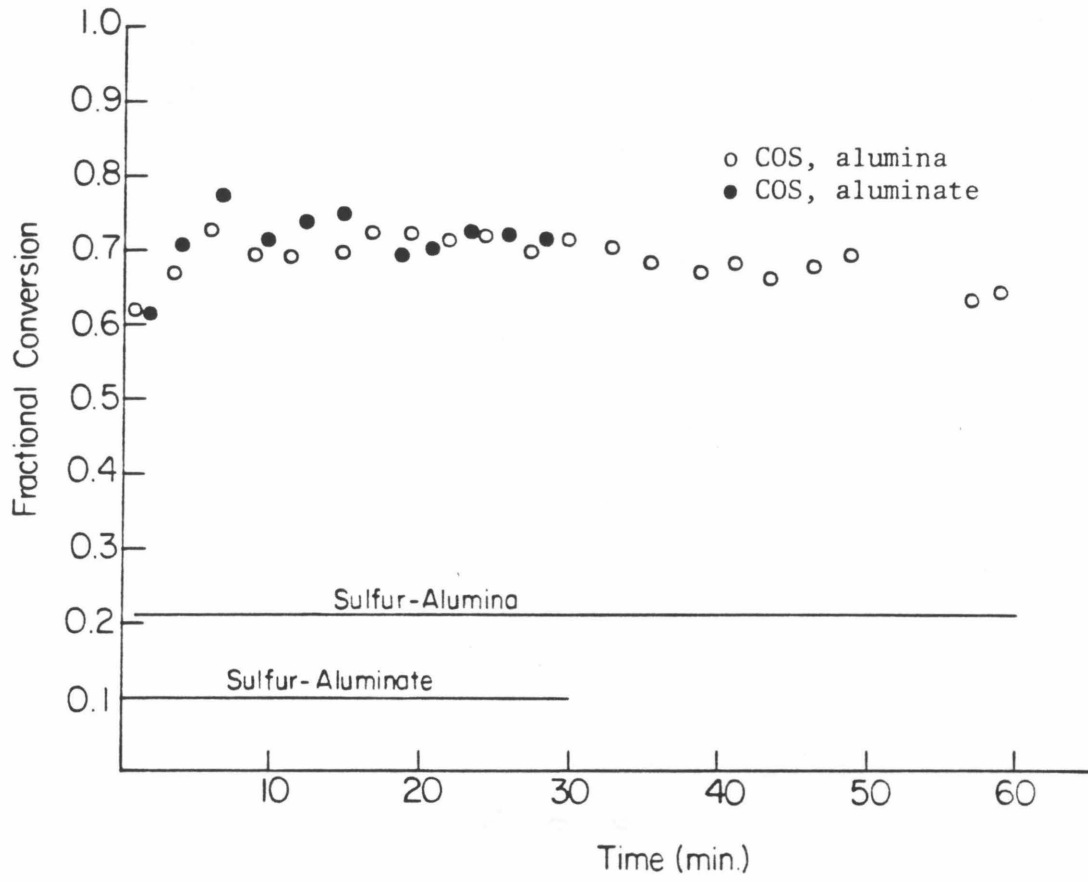


Figure 6.18: Conversion of 12% CO/2000 ppm SO<sub>2</sub> at 700°C

Table 6.2: Steady-State Conversion of and CO Over Support Materials

<u>Material</u>	<u>T(°C)</u>	<u>Inlet Concentration</u>		<u>Steady State Mole Fraction</u>			<u>Equilibrium Mole Fraction</u>		
		<u>CO(%)</u>	<u>SO<sub>2</sub>(ppm)</u>	<u>SO<sub>2</sub></u>	<u>COS</u>	<u>S<sub>2</sub></u>	<u>SO<sub>2</sub></u>	<u>COS</u>	<u>S<sub>2</sub></u>
α-alumina	800	12	2000	0	.93	.08	0	.94	.06
α-alumina	800	1	2000	.09	.02	.36	0	.21	.79
α-alumina	700	12	2000	0	.67	.21	0	.99	.01
α-alumina	700	1	2000	.72	0	.26	0	.48	.52
aluminate	800	12	2000	0	.94	.15	0	.94	.06
aluminate	700	12	2000	0	.71	.10	0	.99	.01

observed, no switchover between products, as occurred during reduction experiments, was observed either with  $\alpha$ -alumina or aluminate. If a change in the catalytic activity of the support was responsible for the switchover it is a change which does not occur when the support is not in contact with the alkali sulfate.

**References**

1. Cobb, J. W., "The Synthesis of a Glaze, Glass or Other Complex Silicate," *J. Soc. Chem. Ind.*, **29**, 399 (1910).
2. George, Z. M., "Effect of Basicity of the Catalyst on Claus Reaction," *Adv. in Chemistry Ser.*, **139**, 75 (1975).
3. Haas, L. A. and S. E. Khalafalla, "Catalytic Thermal Decomposition of Carbonyl Sulfide and Its Reactions with Sulfur Dioxide," *J. Catal.*, **30**, 451 (1973).
4. Khalafalla, S. E. and L. A. Haas, "The Role of Metallic Component in the Iron-Alumina Bifunctional Catalyst for Reduction of SO<sub>2</sub> with CO," *J. Catal.*, **24**, 121 (1972).
5. Pearson, M. J., "Developments in Claus Catalysts," *Hydrocarbon Processing*, 81 (1973).

CHAPTER 7

CONCLUSIONS AND RECOMMENDATIONS

### 7.1. Comparison of TGA and FTIR Results

The results obtained by FTIR analysis are consistent with the sorbent composition results obtained with the thermogravimetric system for the  $\text{NaLiSO}_4/\alpha\text{-Al}_2\text{O}_3$  sorbent. Difference between the two sets of data occurs only in the time of the disappearance of sulfite from the sorbent. The FTIR results predict disappearance of sulfite between one and four minutes at  $800^\circ\text{C}$ . The sorbent composition data show sulfite persisting throughout the entire 20 minutes of reduction, although it is greatly decreased in the first four minutes. The sulfite which is observed as persisting may, however, be aluminate and surface adsorbed  $\text{SO}_2$  (see Section 4.5.3). This  $\text{SO}_2$  would have desorbed during FTIR sample preparation and would not show up in the FTIR results.

### 7.2. Comparison of TGA and Microreactor Results

The same major reaction trends are exhibited in both the TGA and microreactor systems. Both systems exhibit a switchover from  $\text{SO}_2$  to COS as the major gas product. The  $\text{SO}_2$  production period is extended by lowering the CO concentrations in both cases. One difference between trends in the reductions carried out on the two systems appears when the data for reduction of  $\text{NaLiSO}_4/\alpha\text{-Al}_2\text{O}_3$  at  $700^\circ\text{C}$  are examined. On the TGA system, decreasing the temperature increases the length of the  $\text{SO}_2$  production period. On the microreactor the length of the period is unaffected by temperature when 10% CO is present and actually decreased with decreasing temperature when 1% CO is used. The microreactor  $\text{SO}_2$  production may be masked by large  $\text{SO}_2$  adsorption at  $700^\circ\text{C}$ . An increase in COS is seen at the point where the later switchover would be expected at  $700^\circ\text{C}$  with 1% CO.

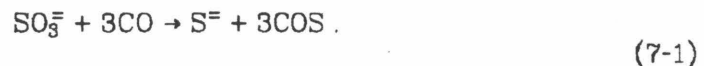
The trend for higher overall sulfur removal from sorbents containing lithium rather than just sodium is seen in reduction results from both systems.

### 7.3. Possible Reaction Mechanism

The experimental results can be qualitatively explained by the reaction network pictured in Fig. 7.1. The first step is the reduction of sulfate to sulfite. The sulfite may then go through a number of possible reactions: it may decompose to form oxide, and dissolved or adsorbed sulfur dioxide; it may react with  $\text{CO}_2$  to form carbonate; it may react with alumina to form aluminate; or it may disproportionate to form sulfide and reproduce sulfate. The first three possibilities all lead to dissolved or adsorbed sulfur dioxide. Any oxide or carbonate formed is rapidly converted to aluminate.

Dissolved or adsorbed  $\text{SO}_2$  will either desorb to the gas phase or react further in the melt or at the melt-solid interface to produce elemental sulfur. Sulfur may desorb from the melt unreacted or may remain dissolved to react further. Dissolved sulfur may react with CO to form COS. Reaction of sulfur with sulfide to produce polysulfides is also possible.

The above scheme attributes sulfide formation to the disproportionation of sulfite. Another possible route to sulfide is the sequential reduction of sulfite with carbon monoxide



Sulfide may react with  $\text{CO}_2$  under certain circumstances to produce COS directly.



This reaction would explain the two periods of sulfur loss observed in the



sorbent composition experiments. Another explanation may be decomposition at later times of initially formed polysulfides, formed from elemental sulfur and sulfide.

The proposed mechanism and its relation to the composition will be commented upon further in the conclusions following.

#### **7.4. Conclusions**

Several conclusions can be made about the importance of the various elements which constitute the sorbent.

1. The formation and stability of alkali-support compounds, such as aluminate, provide part of the driving force for regeneration by reduction. Without the formation of these compounds, sulfur removal during reduction would depend on the stability of the alkali carbonate relative to that of the alkali sulfide.
2. The partition between alkali-support compounds, i.e. aluminate, and sulfide, depends at least initially on the relative rates of formation of these two compounds. The rate of aluminate formation is determined by the rate of diffusion through the aluminate product layer and will slow as aluminate is formed. Selectivity initially favoring aluminate, may later switch to favor sulfide.
3. The rate of diffusion through the aluminate layer is controlled by the nature of the aluminate and the ions diffusing. Lithium ions could have higher diffusivities than sodium atoms because of their smaller size.
4. The phase behavior of the alkali material in the sorbent may effect the rate of reaction and the product selectivity between sulfide and oxide, and, hence, the regenerability of the sorbent. The phase behavior will

affect the rate of ion-ion reactions such as are involved in the disproportionation of sulfite.

5. The support materials used may greatly affect the reduction through the formation of compounds such as aluminates. Some of these materials are deleterious, as they will not decompose to form sulfate upon resulfation. Silica and  $\gamma$ -alumina when used as supports suffer these deleterious effects.
6. The selectivity of gaseous product is controlled by the extent to which CO reduces  $\text{SO}_2$  to elemental sulfur and by the extent to which this elemental sulfur reacts with CO to form COS. The CO concentration during reduction is therefore an important process variable. Some COS may be produced directly from the reaction of  $\text{CO}_2$  and sulfide, however.
7. The change in catalytic activity of the support through removal of poisons or by the production of activators during reduction is important to the overall gas selectivity.

## 7.5 Recommendations

This is the beginning of a research program to investigate the use of alkali oxide-supported sorbents for  $\text{SO}_2$  removal. Although conclusions have been drawn about the importance of various aspects of the composition of the sorbents, the study has raised more questions than it has answered. The following is a list of experimental problems the study of which would further extend our understanding of these sorbents.

1. The partition between oxide and sulfide and, therefore, the regenerability of the sorbent depends, in part at least, on the diffusion of various ions through lithium, sodium or mixed lithium-sodium aluminate. This

diffusion must be further investigated, and diffusion coefficients be determined in order to carry out kinetic modeling.

2. The production of sulfide during reduction is a prevalent but unwanted reaction. The source of sulfide and the factors which influence its production need to be investigated. Other important reactions which occur in the alkali material need to be investigated in the absence of reaction with the support. The corrosiveness of these materials makes them difficult to investigate as bulk melts. Melt reactions might be studied by supporting the materials on aluminates. In this way no further reaction to form aluminate would occur.
3. The catalytic nature of the support surface significantly affects the gas phase product selectivity. Further study into the adsorption and catalysis by various supports is needed. The effect of compounds which may be present during reaction on the adsorption and catalysis must also be investigated.
4. Further work with *in situ* FTIR may help in identifying reaction intermediates.
5. The effect on the reduction of sorbents of possible promoting materials such as iron should be investigated. This may lead to the discovery of sorbent better suited for particular applications. It is also important to know what effects the presence of impurities in the sorbents might have on the reduction.
6. The effect of H<sub>2</sub>O and NO<sub>x</sub> in the gas phase on the reduction reactions should be investigated, as these compounds are likely to be present in real-life applications.